FORSCHUNGSZENTRUM ROSSENDORF FZR

FZR-220
Juli 1998

B. Böhmer, G. I. Borodkin, E. B. Brodkin, V. P. Gorbunov, G. N. Manturov, A. M. Tsiboulia, S. M. Zaritsky

Erhöhung der Zuverlässigkeit der Bestimmung der Neutronenbelastung von WWER-Reaktorkomponenten zwecks Ableitung von Vorschlägen für eine sicherere Betriebsführung von WWER-Reaktoren

Abschlußbericht zum BMBF-Forschungsvorhaben
Förderkennzeichen 1501021

Das diesem Bericht zugrundeliegende Vorhaben wurde mit Mitteln des Förderkonzepts Reaktorsicherheitsforschung im 4. Programm Energieforschung und Energietechnologien des Bundesministers für Bildung und Forschung (BMBF) unter dem Förderkennzeichen 1501021 gefördert. Die Verantwortung für den Inhalt dieses Abschlußberichtes liegt bei den Autoren.

Herausgeber:
FORSCHUNGSZENTRUM ROSSENDORF
Postfach 51 01 19
D-01314 Dresden
Telefon +49 351 26 00
Telefax +49 351 2 69 04 61
http://www.fz-rossendorf.de/

Als Manuskript gedruckt

FZR-220
Juli 1998

B. Böhmer, G. I. Borodkin, E. B. Brodkin, V. P. Gorbunov,
G. N. Manturov, A. M. Tsiboulia, S. M. Zaritsky

Erhöhung der Zuverlässigkeit der Bestimmung der Neutronenbelastung von WWER-Reaktorkomponenten zwecks Ableitung von Vorschlägen für eine sicherere Betriebsführung von WWER-Reaktoren

Abschlußbericht zum BMBF-Forschungsvorhaben
Förderkennzeichen 1501021

Berichtsblatt

1. ISBN	2. Berichtsart	3.
	Abschlußbericht	

4 Titel des Berichtes

Erhöhung der Zuverlässigkeit der Bestimmung der Neutronenbelastung von WWER-Reaktorkomponenten zwecks Ableitung von Vorschlägen für eine sicherere Betriebsführung von WWER-Reaktoren

5. Autor(en) (Name, Vorname(n))	6. Abschlußdatum des Vorhabens
Böhmer, Bertram; Borodkin, Gennady I.; Brodkin, Ernst B.; Gorbunov, Victor P.; Manturov, Gennadie N.; Tsiboulia, Anatoli M.; Zaritsky, Sergei M.;	31. Oktober 1997
	7. Veröffentlichungsdatum: Juli 1998
8. Durchführende Institution (Name, Adresse): Forschungszentrum Rossendorf e. V. Institut für Sicherheitsforschung Postfach 51 01 19 01314 Dresden	9. Ber.Nr. Durchführende Institution
	10. Förderkennzeichen: 1501021
	11. Seitenzahl: 122
	12. Literaturangaben: 71
13. Fördernde Institution (Name, Adresse): Bundesministerium für Bildung, Wissenschaft, Forschung und Technologie (BMBF) 53175 Bonn	14. Tabellen: 61
	15. Abbildungen: 51

16. Zusätzliche Angaben

17. Vorgelegt bei (Titel, Ort, Datum)

18. Kurzfassung

Das Vorhaben zielte auf die Erhöhung der Sprödbruchsicherheit von Reaktoren des Typs WWER-1000 durch Beiträge zur zuverlässigeren und genaueren Bestimmung der Neutronenbelastung der Reaktordruckbehälter. Dazu wurden sechs Wissenschaftler aus 3 russischen Forschungseinrichtungen gefördert, die mit ihren Arbeiten ein weiteres, dem gleichen Ziel dienendes, BMBF-Vorhaben des FZR unterstützten.

Durch Sammlung und Aufbereitung von Ausgangsdaten zur Nachrechnung von Aktivierungsexperimenten an zwei WWER-1000 und durch Formulierung entsprechender Reaktormodelle wurden die Voraussetzungen für weitergehende Untersuchungen sowohl im FZR als auch in mehreren russischen und westlichen Forschungseinrichtungen geschaffen.

Die führende russische Kerndatenbibliothek für Reaktorberechnungen ABBN/MULTIC wurde weiterentwickelt und getestet. Die in die Berechnung des Fluenzspektrums am Druckbehälteraußenrand eingehenden Fehler wurden analysiert. Davon wurde eine Spektrumskovarianzmatrix abgeleitet.

Die Methoden zur experimentellen Bestimmung von Aktivierungsraten und zur transporttheoretischen Berechnung von Fluenzen und Aktivierungsraten im Druckbehälterbereich wurden weiterentwickelt und durch Interlaborvergleiche überprüft. Diese erfolgten unter Beteiligung weiterer russischer sowie tschechischer und westlicher Institute und wurden durch den "International Workshop on the Balakovo-3 Interlaboratory Dosimetry Experiment" im September 1997 in Rossendorf ausgewertet. Verglichen wurden Messungen untereinander, Rechnungen untereinander sowie Rechnungen mit Messungen. Im Ergebnis der Arbeiten konnten die erreichten Genauigkeiten eingeschätzt und Vorschläge zur Verbesserung der eingesetzten Methoden abgeleitet werden.

19. Schlagwörter

Schlagwörter: Neutronenversprödung, Reaktordruckbehälter, Neutronentransport, Neutronendaten, Monte-Carlo-Methode, S_N-Methode, Unsicherheitsanalyse, Spektrumskovarianzen, Spektrumsjustierung

20. Verlag	21. Preis
Forschungszentrum Rossendorf e. V. Postfach 51 01 19, 01314 Dresden	

Document Control Sheet

1 ISBN	2 Type of Report	3
	Final Report	

4 Report Title	Increasing the accuracy of the determination of the neutron load of VVER reactor components to get additional information for a safer operation of VVER reactors

5 Author(s) (Family Name, First Name)	6 End of Project
Boehmer, Bertram; Borodkin, Gennady I.; Brodkin, Ernst B.; Gorbunov, Victor P.; Manturov, Gennadie N.; Tsiboulia, Anatoli M.; Zaritsky Sergei M.;	31.October 1997
	7 Publication Date: July 1998

8 Performing Organization(s) (Name, Address)	9 Originator's Report No
Research Center Rossendorf, Inc. Institute for Safety Research PF 510119, D-01314 Dresden/Germany	10 Reference No: 1501021
	11 No Of Pages: 122
	12 No Of References: 71

13 Sponsoring Agency (Name, Address)	14 No Of Tables
Bundesministerium für Bildung, Wissenschaft, Forschung und Technologie (BMBF) 53175 Bonn	61
	15 No of Figures: 51

16 Supplementary Notes

17 Presented at (Title, Place, Date)

18. Abstract

The Project aims to improve the safety against embrittlement of VVER-1000 type reactors by a more reliable and accurate determination of the neutron load of reactor pressure vessels. Therefore, six scientist from three Russian research institutions were sponsored to support with their work another BMBF project of the FZR aimed at the same goal.

By providing reliable data for the evaluation of ex-vessel neutron activation experiments at two VVER-1000 and formulating the corresponding reactor models a basis has been established for further investigations as well in the FZR as well as in several Russian and Western research institutions.

The leading Russian nuclear data library ABBN/MULTIC has been improved and tested. The uncertainties affecting the calculations of the fluence spectrum at the outer boundary of the pressure vessel have been analysed and a spectrum covariance matrix has been derived.

The methodologies for the experimental determination of activation rates and for calculations of fluence spectra and activation rates have been further developed and tested by interlaboratoy comparisons. Measurements of different laboratories were compared with each other, as well as the corresponding calculations. Moreover, measurements and calculations were compared against each other, partly with participation of further Russian, Czech and Western institutes. The results of the Intercomparisons have been evaluated by the "International Workshop on the Balakovo-3 Interlaboratory Dosimetry Experiment" in September 1997 in Rossendorf. As a result of these works a better evaluation of the reached accuracies was possible and proposals for an improvement of the used methods could be derived.

19 Keywords

Neutron embrittlement, reactor pressure vessel, neutron transport, neutron data, monte carlo method, S_N-method, uncertainty analysis, spectrum covariances, spectrum adjustment

20 Publisher	21. Price
Forschungszentrum Rossendorf e.V. Postfach 510119, D-01314 Dresden	

Abschlußbericht

Förderkennzeichen: 1501021

Berichtszeitraum: 1. 11. 1995 bis 31.10.1997

Vorhabenstitel:

Erhöhung der Zuverlässigkeit der Bestimmung der Neutronenbelastung von WWER-Reaktorkomponenten zwecks Ableitung von Vorschlägen für eine sicherere Betriebsführung von WWER-Reaktoren

Project Title:

Increasing the accuracy of the determination of the neutron load of VVER reactor components to get additional information for a safer operation of VVER reactors

Kurztitel: Neutronenbelastung

Projektleiter: B. Böhmer

Gemeinsames Vorhaben von

Forschungszentrum Rossendorf e.V., Deutschland
und
Russian Research Centre "Kurchatov Institute" (RRC), Moskau, Rußland
Scientific and Engineering Centre of Russian GOSATOMNADZOR (SEC), Moskau, Rußland,
Institute of Physics and Power Engineering (IPPE), Obninsk, Rußland

Autoren:

B. Böhmer (FZR)
G. I. Borodkin, V. P. Gorbunov (SEC)
E. B. Brodkin, S. M. Zaritsky (RRC)
G. N. Manturov, A. M. Tsiboulia (IPPE)

Inhalt:

Anhang:

1. Übergeordnete Zielsetzung

Der durch Neutronenbelastung initiierte Sprödbruch eines WWER-Reaktordruckbehälters muß mit größter Sicherheit verhindert werden. Obwohl beim WWER-1000 der Druckbehälter einer deutlich geringeren Neutronenbelastung als beim WWER-440 ausgesetzt ist, führt der höhere Nickelgehalt des Stahls zu einer schnelleren Versprödung, weshalb auch beim WWER-1000 die Neutronenversprödung des Druckbehälters einer sorgfältigen Überwachung bedarf. Weiterhin kann die durch hohe Neutronenbelastung verursachte Verschlechterung der Materialeigenschaften von Konstruktionselementen innerhalb des Druckbehälters und die nach neueren Erkenntnissen selbst bei geringen Neutronenfluenzen mögliche vorzeitige Alterung von Bauteilen (z.B. Aufhängung des Druckbehälters) zu Störfällen führen.
Voraussetzung für alle Maßnahmen zur Verringerung diesbezüglicher Risiken ist eine genaue Kenntnis der auftretenden Neutronenbelastungen.
Durch das Vorhaben sollte im Rahmen der Reaktorsicherheitsforschung des BMBF, Forschungsschwerpunkt "Komponentensicherheit und Qualitätssicherung" ein Beitrag zur Erhöhung der Zuverlässigkeit der Bestimmung der Neutronenbelastung von Reaktordruckbehältern (RDB) und anderen WWER-Reaktorkomponenten im Bereich außerhalb des Reaktorkernes geleistet werden. Das sollte erreicht werden durch Unterstützung von Aktivierungsexperimenten und deren Nachrechnung mit in Rußland üblichen Methoden sowie durch Vergleich mit alternativen Berechnungsmethoden. Ausgehend davon sollten Schlußfolgerungen für eine zuverlässige Überwachung der Neutronenbelastung gezogen werden. Das Vorhaben diente der Unterstützung von leistungsfähigen Forschergruppen auf dem Gebiet der Reaktorsicherheitsforschung in Rußland und trug zur Vertiefung bestehender Kooperationen bei. Es unterstützte die im Rahmen des BMBF-Projekts 1501022 "Entwicklung einer fortgeschrittenen Methodik zur Bestimmung der Neutronenbelastung des Druckbehältermaterials vom Reaktor des Typs WWER-1000" (1/1996-12/1997) im Institut für Sicherheitsforschung des FZR durchgeführten Arbeiten.
Gefördert wurden 3 Forschergruppen zu je 2 Mitarbeitern aus den folgenden russischen Forschungseinrichtungen:

- Sientific and Engineering Center for Nuclear and Radiation Safety of Russian GOZATOMNADZOR, Moskau (SEC),
- Institute of Nuclear Reactors of the Russian Research Center "Kurchatov Institute", Moskau (RRC KI),
- Institute of Physical and Power Engineering, Obninsk (IPPE).

2. Einzelzielsetzungen

Insbesondere wurden folgende Einzelzielsetzungen verfolgt:

- Weiterentwicklung und Überprüfung der Datenbasis für Neutronenfluenzberechnungen,
- Sammlung zuverlässiger Daten für die Nachrechnungen von Experimenten an WWER-Reaktoren und Formulierung entsprechender Reaktormodelle,
- Einschätzung und Weiterentwicklung der experimentellen Methoden zur Überprüfung der Berechnungen,
- Einschätzung und Weiterentwicklung der transporttheoretischen Berechnungen mit russischen Daten und Programmen,
- Vorschläge zu einer sichereren Betriebsführung.

Daraus ergaben sich folgende Aufgaben:

- Überprüfung und Weiterentwicklung des ABBN/MULTIC Gruppensatzes für Abschirmberechnungen,
- Validierung der Gruppenkovarianzmatrizen von Neutronenwirkungsquerschnitten und Bestimmung von Kovarianzen berechneter Neutronenspektren für den WWER-1000,
- Entwicklung und Bereitstellung von Reaktormodellen für Präzisionsberechnungen der Neutronenfluenz an den Druckbehältern von zwei WWER-1000 Reaktoren (Rovno-3, Balakovo-3),
- Aktivierungsmessungen an den Druckbehältern der Reaktoren Balakovo-3 und Rovno-3,
- Neutronentransportrechnungen für den Druckbehälterbereich von Balakovo-3 und Rovno-3 mit Hilfe russischer Berechnungsprogramme,
- Vergleich der Ergebnisse verschiedener Berechnungen und der Experimente
- Ableitung von Vorschlägen für eine genauere Überwachung der Neutronenbelastung des RDB.

Im vorliegenden Bericht werden die zu den einzelnen Punkten der Aufgabenstellung durchgeführten Arbeiten und die erzielten Ergebnisse kurz dargestellt. Ausführlichere Darstellungen (in Englisch) sind in dem als Anhang beigelegten Berichten der russischen Bearbeiter /A1-A6/ zu finden.

3. Ablauf der Arbeiten

Zunächst wurden vom FZR mit den russischen Teilnehmern Verträge über die Zusammenarbeit zum Vorhaben mit Festlegungen zu den wichtigsten Arbeitszielen abgeschlossen. Etwa ein Jahr nach Beginn der Arbeiten im Oktober 1996 wurden auf einem Arbeitstreffen in Rossendorf die erreichten Ergebnisse diskutiert und der erfolgreiche Abschluß der ersten beiden Etappen des Projekts festgestellt. Im Mittelpunkt der Diskussionen standen dabei Messungen und Rechnungen im Rahmen des vom SEC GOSATOMNADZOR organisierten Interlabor vergleichs "Interlaboratory VVER-1000 Ex-Vessel Experiment at the Balakovo-3 NPP" /1/, an dem neben 5 russischen Forschungsinstituten und dem FZR auch Forschungseinrichtungen aus Tschechien, Frankreich und den Niederlanden teilnahmen. Dieser teilweise vom Vorhaben unterstützte Interlaborvergleich umfaßte

- die Bestrahlung von Detektoren der verschiedenen beteiligten Einrichtungen während des 5. Brennstoffzyklus des Reaktors Balakovo-3,
- die unabhängige Bestimmung der Aktivitäten und mittleren Reaktionsraten in verschiedenen Laboratorien sowie deren Vergleich untereinander und
- die unabhängige Berechnung von Aktivitäten und zugehörigen Fluenzen durch mehrere Forschungseinrichtungen und deren Vergleich untereinander sowie mit Meßgrößen.

Ein erster Vergleich der erhaltenen Ergebnisse erfolgte während des "International Workshop on the Balakovo-3 Interlaboratory Dosimetry Experiment" vom 2. - 5. September 1997 in Rossendorf /A7/.

4. Weiterentwicklung und Validierung der Neutronendatenbasis /A1/

4.1 Aufgabenstellung

Aufgrund der Fortschritte in den Berechnungsmethoden, die vor allem mit der rasanten Entwicklung der Kapazitäten moderner Computer zusammenhängen, ist die Ungenauigkeit der in die Berechnung eingehenden Kerndaten zur dominierenden Fehlerquelle bei den Berechnungen geworden. Gleichzeitig sind die Arbeiten zur Bestimmung und Einschätzung von nuklearen Kerndaten in den letzten Jahren weltweit, aber besonders in Deutschland, auf ein sehr geringes Niveau reduziert worden, obwohl der Kenntnisstand vieler nuklearer Daten noch unbefriedigend ist.

Es erschien daher von Interesse, sowohl eine Überprüfung der vorhandenen Kerndatenbibliotheken für Neutronentransportrechnungen im Außenbereich des Reaktors vorzunehmen, als auch die vorhandenen Datenbibliotheken durch Aufnahme neuer Daten und Erhöhung der Gruppenzahlen weiterzuentwickeln. Um die Bestimmung der Ungenauigkeit der Berechnungsergebnisse auf eine zuverlässigere Basis zu stellen, sollten an Hand eines eindimensionalen Reaktormodells Kovarianzen der berechneten Gruppenfluenzen bestimmt werden.

Im Physikalisch-Energetischem Institut Obninsk besteht eine bis Anfang der 60-er Jahre zurückreichende Entwicklungstradition zu Gruppendatenbibliotheken (=Gruppensätzen) vom Typ ABBN, die weltweit zunächst bei der Berechnung schneller Brutreaktoren eingesetzt wurden und bis jetzt in Rußland und weiteren Staaten für Reaktoren und andere nukleare Einrichtungen breite Verwendung finden. Diese Gruppensätze zeichnen sich vor allem durch eine sehr gute Überprüfung und Justierung an integralen Experimenten aus, was im allgemeinen, wie z.B. auch in /2/ gezeigt wurde, trotz der geringen Gruppenzahl gute Berechnungsgenauigkeiten ermöglicht. Die zeitgemäße Erweiterung der Gruppenzahl von 26 bzw. 28 auf 299 Neutronen- und 11 γ-Gruppen in Form des ABBN/MULTIC-Gruppensatzes ist seit mehreren Jahren in Arbeit, konnte aber u.a. wegen unzureichender Finanzierung bisher nicht zum Abschluß gebracht werden. Erforderlich ist eine umfangreiche Testung der Daten und des Programmsystems zur Datenaufbereitung (=Berechnung makroskopischer Querschnitte für Gemische unter Berücksichtigung der Resonanzselbstabschirmung, Reduktion der Gruppenzahl u.a.) an einer Vielzahl integraler Experimente (> 100).

Im Rahmen des vorliegenden Projekts konnte nur ein kleiner aber wichtiger Teil der erforderlichen Arbeiten zur Überprüfung und Fertigstellung der Datenbibliothek geleistet werden. Diese Arbeiten werden im folgenden sowie in /A1/ beschrieben.

4.2 Nachrechnung von einfachen Benchmark-Experimenten für Abschirmungen

Die Exerimente erfolgten an einer ^{252}Cf-Quelle in Eisenkugeln mit Radien zwischen 10 und 35 cm. Verglichen wurden die gemessenen und berechneten Neutronen- und γ-Ausflußspektren, wobei die Rechnungen sowohl mit dem neuen ABBN/MULTIC-Datensystem als auch mit dem 28-Gruppensatz ABBN-93 ausgeführt wurden. Dabei zeigte sich für beide Berechnungsvarianten eine vernünftige Übereinstimmung mit dem Experiment, wenn man berücksichtigt, daß insbesondere für den Energiebereich unterhalb 100 keV die Messungen mit größeren Fehlern behaftet sind. Die Übereinstimmung der γ-Ausflußspektren war unerwartet gut.

4.3 Vergleich von verschiedenen ABBN-Gruppensätzen und eines ENDF/B-VI-Gruppensatzes für Anwendungen im Außenbereich von WWER-Reaktoren

Ausgangspunkt der vier Berechnungsvarianten waren ABBN-Gruppensätze mit 28, 81

und 299 Neutronengruppen sowie der auf Basis von ENDF/B-VI hergestellte199-Gruppensatz VITAMIN-B6. Der Vergleich wurde für ein eindimensionales Modell eines typischen Druckwasserreaktors für jeweils einen Punkt in Reaktorkern, Downcomer, Druckbehälter (bei 1/4 Dicke) und Betonabschirmung durchgeführt.
Ergebnisse: Die berechneten Neutronenflußspektren stimmten für die ABBN-Rechnungen mit verschiedenen Gruppenzahlen an allen Positionen im Energiebereich oberhalb 10 eV gut überein. Die Abweichungen zu den VITAMIN-B6-Ergebnissen waren ebenfalls überall sehr gering außer in der Betonabschirmung, wo die ABBN-Flüsse im gesamten Energiebereich etwas höher liegen als die VITAMIN-B6-Werte. Die ebenfalls berechneten Photonenspektren lagen erwartungsgemäß für die ABBN-Daten generell niedriger als für die VITAMIN-B6-Daten, da die ABBN-Daten sowohl prompte als auch verzögerte γ-Ausbeuten einschließen. Die Differenzen zwischen den mit verschiedenen ABBN-Gruppenzahlen erhaltenen Photonenspektren erklären sich aus dem großen Einfluß der niederenergetischen Neutronen, was eine detaillierte Behandlung des thermischen Bereichs erfordert, die nur bei der 299-Gruppen-Rechnung gegeben war.

4.5 Vergleich von ABBN-Datenkovarianzen mit ENDF/B-VI-Datenkovarianzen
Die relativen Standardabweichungen (RSD) und Korrelationen der ABBN-93 28-Gruppendaten sind in der Obninsker Datenbibliothek LUND abgespeichert. In der gleichen Gruppenstruktur wurden auf Basis von ENDF/B-VI eine Reihe von RSD-Vektoren und Korrelationsmatrizen bestimmt und mit den LUND-Daten verglichen. Dabei wurden beträchtliche Unterschiede für n,γ-Reaktionen und geringe für Schwellwertreaktionen festgestellt.

4.6 Verbesserung der Kovarianzdatenbasis und Berechnung der Spektrumskovarianzmatrix für ein eindimensionales Modell des WWER-1000.
Die zu diesem Punkt beschriebenen Arbeiten wurden gemeinsam mit dem FZR durchgeführt und sind in /3/ näher beschrieben.
Die Kenntnis der Kovarianzmatrix des berechneten Fluenzspektrums ist Voraussetzung und gegenwärtiger Hauptschwachpunkt der Justierung berechneter Spektren an Experimenten. Sie erlaubt außerdem die statistisch exakte Bestimmung von praktisch benötigten abgeleiteten Größen, wie Fluenzintegralen und dpa-Werten. Deshalb wurde eine Analyse aller Fehlerquellen bei einer Monte-Carlo-Fluenzberechnung (d.h. bei vernachlässigbaren Fehlern der Berechnungsmethode) vorgenommen und deren Einfluß auf das Gruppenfluenzspektrum mit Hilfe eindimensionaler Transportrechnungen mit dem Programm ANISN auf der Basis einer einfachen Differenzenmethode bestimmt. Für jeden Typ von fehlerbehafteten Parametern wurde eine Matrix H_k der Empfindlichkeitender Spektrumswerte bezüglich der Parameter des Typs k berechnet. Die Spektrumskovarianzmatrix V wurde dann nach dem verallgemeinerten Fehlerfortpflanzungsgesetz nach der Gleichung

$$V = \sum_{k=1}^{n} H_k \, W_k \, H_k^T$$

bestimmt, wobei die W_k die Kovarianzmatrizen der Parameter vom Typ k sind. Berücksichtigt wurden dabei Fehler infolge der Unsicherheit folgender Parameter:
- Neutronenquerschnitte (inelastische, elastische und Einfangsquerschnitte von Eisen, elastische Gruppenquerschnitte von Wasserstoff und Sauerstoff),
- Neutronenquellverteilung (Spaltspektren, Ortsverteilung),

- Geometrische Ausmaße und Materialdichten.

Die Kovarianzen der Wirkungsquerschnitte und des Spaltspektrums wurden der LUND Bibliothek entnommen. Für die Ortsverteilung wurde ein Fehler des Flußgradienten in der äußeren Brennelementschicht abgeschätzt (15%). Die Unsicherheiten der Abmessungen und Dichten sind schwer zu definieren, da sie vom jeweiligen Kenntnisstand über den Reaktor abhängen und selbst zwischen Reaktoren gleichen Typs variieren können. Sie wurden abgeschätzt an Hand von Konstruktionstoleranzen, Informationen aus Konsultationen mit WWER-Experten und den in amerikanischen LEPRICON Reports /4/ verwendeten Unsicherheiten. Den bei weitem größten Einfluß auf die Spektrumskovarianzen am Außenrand des Druckbehälters hatten jedoch die Unsicherheiten der Eisen-Wirkungsquerschnitte und des Spaltspektrums.
Die erhaltene Spektrumskovarianzmatrix weist RSD der Gruppenflüsse zwischen 17% in der letzten Gruppe (21.5-46.5keV) und 43% in der ersten Gruppe (14-15MeV) aus. Die Korrelationskoeffizienten sind ausschließlich positiv und langreichweitig. Entsprechende LEPRICON-Berechnungen für 2 US-amerikanische Druckwasserreaktoren ergaben für die unteren Energien etwas höhere und für die hohen Energien etwas geringere RSD bei ähnlichen Korrelationen zwischen den Gruppen.
Die berechneten großen Unsicherheiten scheinen der vergleichsweise besseren Übereinstimmung zwischen gemessenen und berechneten Aktivitäten /5-7/ zu widersprechen. Möglicherweise wurden bei der Fehlereinschätzung der Kerndaten Ergebnisse neuerer integraler Messungen ungenügend berücksichtigt. Anderseits kann die häufig relativ gute Übereinstimmung auch das Ergebnis einer durch Parameteranpassungen begünstigten Fehlerkompensation sein.

Die erhaltenen Spektrumskovarianzen wurden zur Justierung mit TRAMO berechneter Fluenzspektren auf der Basis von gemessenen Aktivierungsraten und des Justierungsprogramms COSA2 benutzt. Gleichartige Justierungsrechnungen wurden mit Hilfe einfacherer früher verwendeter Näherungen für die Spektrumskovarianzen durchgeführt. Die Ergebnisse wurden verglichen. Damit ist auch eine Einschätzung der Größenordnung der durch die Unsicherheiten der Spektrumskovarianzen verursachten Fehler der interessierenden justierten Fluenzintegrale möglich.

4.7 Erweiterungen des ABBN/MULTIC-Systems und Überprüfung durch Nachrechnung internationaler Benchmarks

Die ABBN/MULTIC-Bibliothek wurde durch Multigruppendaten für Gadolinium erweitert. Im thermischen Gebiet wurden P0- und P1-Streumatrizen erzeugt. Neue Photonendaten für Wasserstoff, Sauerstoff und Eisen wurden auf der Basis von ENDF/B-VI generiert.
Die Genauigkeit und Zuverlässigkeit der neuen Version von ABBN/MULTIC einschließlich der Datenaufbereitungsprogramme wurde durch Nachrechnung von 63 kritischen Benchmark-Experimenten überprüft. Mit dem ABBN/ MULTIC-Gruppensatz und dem Monte-Carlo-Transportprogramm KENO-V berechnete Eigenwerte keff wurden sowohl mit dem experimentellen Wert (keff=1) als auch mit Eigenwerten verglichen, die mit Hilfe von drei verschiedenen Datensätzen (einer auf ENDF/B-V- und zwei auf ENDF/B-VI-Basis) erhalten wurden.
In allen Fällen wurde mit Hilfe der ABBN/MULTIC-Daten eine ähnlich gute oder bessere Übereinstimmung mit dem Experiment erhalten wie mit Hilfe von ENDF/B-VI-Daten.

5. Sammlung von Daten für die Nachrechnungen von Experimenten an WWER-Druckbehältern und Formulierung der Reaktormodelle /A2/

Für die Berechnung der Fluenzen und Aktivierungsraten am Außenrand der WWER-Druckbehälter der Reaktoren von Rovno-3 und Balakovo-3 werden benötigt:

- die Konstruktionsparameter (Abmessungen, Temperaturen, chemische Zusammensetzung mit Dichten)
- Ausgangsdaten zur Bestimmung der zeitabhängigen Spaltquelle (Anreicherungen, Abbrand) und der Reaktorgeschichte in der Bestrahlungsperiode
- die genauen Positionen der Aktivierungsdetektoren , die bei beiden Reaktoren in je einer azimutalen und einer vertikalen Detektorreihe an speziellen Rahmen befestigt waren.

Diese Daten wurden vom SEC gesammelt und beschrieben. Darauf aufbauend wurden detaillierte Berechnungsmodelle für beide Reaktoren erarbeitet. Für Rovno-3 erwies sich ein 30° Symmetriesektor als ausreichend für die Berechnung, während für das Balakovo-3-Modell ein 60°-Sektor benötigt wird.

Neben der geometrischen Beschreibung des Reaktors wird die zeitabhängige Neutronenquellverteilung in pro Zeiteinheit und Volumen emittierten Neutronen benötigt. Sie wurde berechnet aus

- der Leistungsverteilung über das Core,
- der kumulativen Abbrandverteilung,
- der mittleren Anzahl von Neutronen pro Spaltung,
- der mittleren Spaltenergie,
- der Brennstoffdichte.

Die zeitabhängigen Spaltquellenverteilungen wurden aus der totalen Reaktorleistung, die vom Reaktorkontrollsystem bereitgestellt wird, sowie aus den zeitabhängigen kumulativen Abbrandverteilungen berechnet. Für die äußeren Brennelementreihen wurden detaillierte stabweise Leistungsverteilungen für verschiedene über der Bestrahlungszeit verteilte Zeitpunkte und 8 Höhenschichten bestimmt.
Im Ergebnis der Arbeiten wurden für die Reaktoren Rovno-3 und Balakovo-3 folgende Dateien bereitgestellt, die eine dreidimensionale stabweise Beschreibung der Spaltquellenverteilung ermöglichen:

a) Datei der Reaktorleistungsdaten (Leistungsgeschichte), 2D-Leistungsverteilung der Brennelemente und der Kühlwassertemperaturdifferenzen
b) Datei der zeitabhängigen Spaltquelle mit
   - 2D und 3D-Leistungsverteilungen der Brennelemente,
   - 2D- und 3D-Abbrandverteilungen der Brennelemente,
   - 3D stabweisen Leistungsverteilungen in den peripheren Brennelementen,
   - 3D stabweisen Abbrandverteilungen in den peripheren Brennelementen,
   - den Konzentrationen der Schwermetalle in den Brennlementen,
   - den Abbrandabhängigkeiten der Neutronenemission.

Diese Daten wurden für Neutronentransportrechnungen mit deterministischen S_N-Methoden im Kurtschatov-Institut im Rahmen dieses Projekts sowie für Monte-Carlo-Rechnungen mit dem Programm TRAMO in Rossendorf im Rahmen des parallelen BMBF-Projekts 1501022 /5/ benutzt. Die Notwendigkeit einer stabweisen Beschreibung wird daran deutlich, daß die Quellstärke in den äußeren Brennelementen von innen nach außen bis etwa um den Faktor 3 abfällt.

6. Überprüfung und Weiterentwicklung der Methoden zur Berechnung der Neutronenfluenz im Bereich des Reaktordruckbehälters /A3-A6/

Im Rahmen des Projekts wurden im Kurtschatov-Institut deterministische S_N-Methoden zur Berechnung der Fluenzen und Aktivierungsraten an Druckbehältern der Reaktoren Rovno-3 und Balakovo-3 eingesetzt. Die Ergebnisse wurden mit Experimenten sowie mit alternativen Rechnungen verglichen, um die Genauigkeit der Berechnungsmethode einschätzen zu können. Die Ergebnisse dieser Arbeiten sind in den Berichten /A3-A6/ ausführlicher dargelegt.

6.1 Methodik

Das Problem ist charakterisiert durch die Notwendigkeit,

- den Neutronentransport durch dicke Eisen-Wasser-Schichten zu berechnen, wobei die Neutronenquelle im Reaktorkern liegt und vorgegeben wird,
- detaillierte Neutronenspektren für Energien oberhalb 0.1 MeV zu berechnen,
- die detaillierte zeitabhängige Ortsverteilung der Neutronenquelle im Reaktorkern zu berücksichtigen.

Für die Lösung des Problems wurde eine Synthese von Ergebnissen zwei- und eindimensionaler Transportrechnungen mit dem Programmen DOT-3 und ANISN zu einer dreidimensionalen Flußdichtefunktion $\varphi(r,\theta,z,E)$ vorgenommen:

$$\varphi(r,\theta,z,E) = \varphi(r,\theta,E)\, K(r,z,E)$$

$$\text{mit} \qquad K(r,z,E) = \varphi(r,z,E) / \varphi(r,E),$$

wobei $\varphi(r,\theta,E)$ und $\varphi(r,z,E)$ mit DOT-3 erhaltene zweidimensionale Lösungen für die Quellverteilungen $q(r,\theta,E)$ und $q(r,z,E)$ sind und $\varphi(r,E)$ eine mit ANISN erhaltene eindimensionale Lösung für die Quellverteilung $q(r,E)$ ist.

Die verwendeten Neutronenquellen (s. a. Abschnitt 3) beruhen auf Berechnungen mit den russischen Standardcodes BIPR und PERMAK und den für WWER-Kernberechnungen üblichen russischen Datenbibliotheken. Der BIPR-Code liefert eine dreidimensionale brennelementweise Quellverteilung, während das zweidimensionale Programm PERMAK eine stabweise Verteilung der Quellen für die äußeren Brennelemente bereitstellt.
Für den Neutronentransport wurden die Materialien im Reaktorkern homogenisiert außerhalb desselben jedoch detailliert beschrieben.
Für die Basisrechnungen wurde die amerikanische Datenbibliothek BUGLE-93 ausgewählt, die auf ENDF/B-VI-Daten und einer 47-Gruppen-Darstellung beruht. Es wurde jedoch auch der Einfluß der Verwendung von ENDF/B-IV-Daten untersucht /A3/.

6.2 Methode der Beitragsfunktionen

Sie geht davon aus, daß der Neutronentransport im Reaktorkern von Abbrand und Anreicherung praktisch nicht beeinflußt wird, was in guter Näherung gewährleistet ist. Es werden die Beiträge jedes einzelnen Brennelements zum Neutronenfluß an den interessierenden Punkten berechnet. Für Reaktoren mit gleichem konstruktiven Aufbau aber unterschiedlichen Beladungs- und Abbrandzuständen kann dann mit einmal berechneten Beitragsfunktionen die Bestimmung der Neutronenflußverteilung durch einfache Aufsummierung der mit den partiellen Quellstärken der einzelnen Brennelemente gewichteten Beitragsfunktionen erfolgen. Diese Methode kann breite

Anwendung finden, da alle in Rußland, der Ukraine und Bulgarien laufenden WWER-1000-Reaktoren (außer Novovoronesh-5) im wesentlichen den gleichen konstruktiven Aufbau von Reaktorkern und Einbauten innerhalb des Druckbehälteres haben. Die Methode ist auch für Rechnungen zur Optimierung der Beladung und des Brennstoffzyklus und in weiteren Fällen /8/ günstig anwendbar.
Entsprechende Beitragsfunktionen wurden für die Standardversion des WWER-1000 für einen 30° Symmetriesektor berechnet (s. Tab.1 und /A5/).
Die Tabelle 1 zeigt, daß die berücksichtigten äußeren 2 Reihen von Brennelementen mindestens 99.4% der Gesamtfluenz an den betrachteten Punkten verursachen und daß an jeder Winkelposition jeweils ein Brennelement 42 - 79% zur Fluenz beiträgt.

Tab. 1: Relative Beiträge der 8 äußeren Brennelemente zur Neutronenfluenz mit E>0.5MeV an den in ° angegebenen Winkelpositionen am inneren Rand des Druckbehälters

θ°	Nummer des Brennelements								Summe
	6	7	12	13	16	17	18	19	
0	0.005	0.103	0.039	0.786	0.005	0.053	0.0	0.003	0.994
5	0.005	0.079	0.037	0.789	0.005	0.075	0.001	0.006	0.997
10	0.004	0.045	0.035	0.723	0.009	0.161	0.001	0.018	0.996
15	0.003	0.026	0.035	0.532	0.016	0.311	0.003	0.068	0.994
20	0.002	0.013	0.030	0.275	0.026	0.418	0.010	0.222	0.996
25	0.001	0.005	0.019	0.102	0.035	0.325	0.021	0.490	0.998
30	0.001	0.003	0.012	0.042	0.037	0.221	0.027	0.656	0.999

6.3 Berechnungsergebnisse und deren Überprüfung
Die mit der beschriebenen Methodik erhaltenen Berechnungsergebnisse (Neutronenspektren, Fluenzintegrale, Reaktionsraten, Spektralindizes) wurden mit Experimenten und mit anderen Berechnungen verglichen. Die Ergebnisse der Vergleiche sind in /A3-A6/ beschrieben. Auf den Vergleich mit den Balakovo-3-Experimenten wird in Abschnitt 8 eingegangen.
Für den Reaktor Rovno-3 wurden Vergleichsrechnungen mit BUGLE-93 und ABBN-93 durchgeführt, um den Einfluß der Datenungenauigkeit zu testen. Außerdem wurden die Rechnungen für 4 unterschiedliche Annahmen über den Abfall der Quellstärke in der äußeren Brennelementschicht wiederholt. Damit kann der Einfluß ungenauer Angaben zur Quellverteilung in den äußeren Brennelementen eingeschätzt werden.

Im folgenden ist der für den Reaktor Balakovo-3, 5. Betriebszyklus, während des Rossendorfer Workshops /A7/ im September 1997 durchgeführte Vergleich zwischen drei Berechnungsergebnissen dargestellt. In Tab.2 werden Ergebnisse von deterministischen 2D-1D-Synthese-Rechnungen des RRC KI und des FRAMATOME miteinander sowie mit Monte-Carlo-Ergebnissen des Programms TRAMO des FZR verglichen.

Die Übereinstimmung zwischen den drei unabhängigen Berechnungen ist als gut einzuschätzen. Die maximale Abweichung zwischen Flußintegralen>1MeV beträgt 13% und wird im Gebiet mit minimaler Fluenz erreicht. Hier macht sich wahrscheinlich bemerkbar, daß für Balakovo-3 die bei den Rechnungen des RRC KI angenommene 30°-Symmetrie nicht exakt gegeben ist. Die anderen beiden Rechnungen wurden entsprechend den Balakovo-3-Ausgangsdaten für einem 60°-Symmetriesektor ausge-

führt. Der Vergleich der Spektralindizes zeigt, daß die Monte-Carlo-Rechnung mit 123-Gruppen-ENDF/B-VI-Daten ein etwas härteres Spektrum ergibt als die deterministische 2D-1D-Synthese-Rechnung mit 47-Gruppen-Daten der BUGLE-93-Bibliothek.

Tab. 2: Flußintegrale oberhalb E [MeV] in n/cm^2/s und Spektralindizes SI=$\Phi_{>0.5MeV}/\Phi_{>3.0MeV}$

θ	Datenursprung	E [MeV]				SI $\Phi_{>0.5}/\Phi_{>3.0}$
		0.1	0.5	1.0	3.0	
Max. Fluß	RRC	1.14+10	5.08+9	1.70+9	2.29+8	22.2
	FRAM	1.13+10	4.92+9	1.67+9	-	-
	FZR	1.18+10	4.90+9	1.60+9	2.12+8	23.1
	RRC / FRAM	1.01	1.03	1.02	-	-
	RRC / FZR	0.97	1.04	1.06	1.08	0.96
	FRAM/ FZR	0.96	1.00	1.04	-	-
Min. Fluß	RRC	6.72+9	2.68+9	8.26+8	1.06+8	25.3
	FRAM	6.59+9	2.50+9	7.70+8	-	-
	FZR	6.59+9	2.61+9	7.33+8	9.41+7	27.7
	RRC / FRAM	1.02	1.07	1.07	-	-
	RRC / FZR	1.02	1.03	1.13	1.13	0.91
	FRAM/FZR	1.00	0.96	1.05	-	-

7. Aktivierungsmessungen an den Reaktoren Rovno-3 und Balakovo-3 und deren Auswertung /A2/

Die Bestrahlung der Aktivierungsdetektoren erfolgte während des 7. Betriebszyklus des Reaktors Rovno-3 und während des 5. Betriebszyklus des Reaktors Balakovo-3. Neben den Detektoren des SEC wurden auch Detektoren des FZR und im Falle von Balakovo-3 zusätzlich solche von 2 weiteren russischen Instituten sowie des ECN Petten und von Skoda, Pilsen eingesetzt. Die Auswertung der Ergebnisse der Experimente am Reaktor Balakovo-3 erfolgte im Rahmen des Balakovo-3-Interlaborvergleichs /A7/.
Der vom SEC eingesetzte Satz von Detektoren ermöglicht die Auswertung folgender Reaktionen: $^{93}Nb(n,n')^{93m}Nb$, $^{237}Np(n,f)$, $^{238}U(n,f)$, $^{58}Ni(n,p)^{58}Co$, $^{54}Fe(n,p)^{54}Mn$, $^{46}Ti(n,p)^{46}Sc$, $^{63}Cu(n,\alpha)^{60}Co$, $^{55}Mn(n,2n)^{54}Mn$ und $^{59}Co(n,\gamma)^{60}Co$.
Die Messungen an den SEC-Detektoren erfolgten in einem eigens für diese Zwecke eingerichteten Laboratorium des SEC.
Die Auswertung der Messungen erfolgte durch Bestimmung der Aktivitäten am Ende der Bestrahlungsperiode (End of Irradiation Activity-EOIA) und der davon abgeleiteten Reaktionsraten (RR), Spektralindizes sowie der azimutalen und axialen Verteilungen der Fluenzintegrale. Von besonderen Interesse war dabei die beobachtete starke

azimutale Variation des Spektralindexes a = RR(^{237}Np(n,f)) / RR(^{54}Fe(n,p)^{54}Mn), der auf eine beträchtliche azimutale Variation des Neutronenspektrums hinweist.

8. Vergleich von Experimenten mit Neutronentransportrechnungen /A6/

Aus den vom Projekt unterstützten Vergleichen von Berechnungen mit Experimenten an Fe-Kugeln, der LR-0-Anordnung und Druckbehältern der Reaktoren Rovno-3 und Balakovo-3 /A1-A6,6,7/ soll hier nur ein Teil der Ergebnisse zu Balakovo-3 beschrieben werden, da er im Rahmen des Balakovo-3 Ex-Vessel Interlaborvergleichs erfolgte und am umfangreichsten und vollständigsten war. Die Tabellen 3 und 4 zeigen Vergleiche von Ergebnissen von Aktivierungsmessungen des SEC und des FZR mit Rechnungen des RRC und des FZR sowie der Berechnungen untereinander für einen Teil der Detektorpositionen.

Tab. 3: Vergleich von Berechnungsergebnissen des RRC und Meßergebnissen des SEC für die azimutale Verteilung der ^{54}Fe(n,p) -Reaktionsrate in Höhe von 149cm oberhalb des Kernbodens

Daten	θ°										
	6.8	9.4	15.6	23.4	32.0	37.0	47.0	50.8	55.8	58.4	62.1
C_{RRC}/ E_{SEC}	1.14	1.15	1.17	1.18	1.14	1.13	1.08	1.07	1.08	1.10	1.11

Tab. 4: Vergleich von Meß- und Berechnungsergebnissen des RRC und des FZR für verschiedene azimutale Winkel θ in Höhe von 149cm oberhalb des Kernbodens

θ °	Daten (C - Calcul. E - Exper.)	Reaktion							
		^{237}Np(n,f)	^{238}U(n,f)	^{93}Nb(n,n^{1})	^{54}Fe(n,p)	^{58}Ni(n,p)	^{46}Ti(n,p)	^{60}Ni(n,p)	^{63}Cu(n,α)
9.4	C_{RRC} / C_{FZR}	-	-	1.02	1.02	1.02	1.06	-	0.97
	C_{FZR} / E_{FZR}	-	-	1.01	1.02	1.08	1.00	-	1.02
	C_{RRC} / E_{FZR}	-	-	1.03	1.04	1.10	1.06	-	0.99
	C_{RRC} / E_{SEC}	0.87	-	-	1.15	1.13	-	0.88	1.06
32	C_{RRC} / C_{FZR}	-	-	1.09	1.08	1.08	1.12	-	1.00
	C_{FZR} / E_{FZR}	-	-	0.85	0.97	1.00	0.91	-	0.96
	C_{RRC} / E_{FZR}	-	-	0.93	1.05	1.08	1.02	-	0.96
	C_{RRC} / E_{SEC}	0.85	0.99	-	1.14	1.14	-	0.84	1.05
55.8	C_{RRC} / E_{SEC}	0.83	0.91	-	1.08	1.08	-	0.85	1.04

Die Vergleiche weisen eine Übereinstimmung im Bereich von 10% zwischen Berechnungen des RRC und den Messungen wie auch den Rechnungen des FZR aus.

Die Differenzen zwischen Berechnungen des RRC und Messungen des SEC sind größer (bis zu 18%). Die Übereinstimmung zwischen berechneten und gemessenen ^{237}Np(n,f)-Reaktionsraten kann durch Berücksichtigung der Photospaltung und Verwendung eines genaueren Wichtungsspektrums bei der Erzeugung der Gruppenquerschnitte um bis zu 4% verbessert werden. Trotzdem verbleibt eine Diskrepanz von 10-15% für diese Reaktion.

Der vollständige C/E - Vergleich für die Berechnungen und Messungen des FZR für Balakovo-3 ist in /5,7/ enthalten. Er ergab etwas bessere als die hier dargestellten Übereinstimmungen zwischen Rechnung und Experiment (besser als 9%, außer in einem Falle mit 16%). Die Berechnungen des FZR zeichneten sich aus durch eine noch exaktere geometrische Modellierung, durch eine echte Dreidimensionalität der Rechnungen und durch die Berücksichtigung der Änderung der Orts- und Energieabhängigkeit des Neutronenflusses während der Bestrahlung für die kurzlebigen Detektoren (^{58}Ni(n,p) und^{46} Ti(n,p)). Der letztere Effekt bewirkte Korrekturen der mittleren Reaktionsraten von bis zu 9%.

Von den Teilnehmern des Balakovo-3-Workshops wurde empfohlen, die Ergebnisse aller Teilnehmer einzuschätzen und auf dieser Grundlage ein Benchmark zur Überprüfung von Berechnungsverfahren für die Neutronenbelastung von Reaktordruckbehältern auszuarbeiten. Allen Experimentatoren wurde zu diesem Zweck die Möglichkeit gegeben ihre experimentellen Ergebnisse noch einmal überprüfen.

9. Schlußfolgerungen und Vorschläge für eine sicherere Betriebsführung

Im Rahmen der beschriebenen Arbeiten war es möglich, die gegenwärtig für die Bestimmung der Neutronenbelastung von WWER-Reaktoren verwendeten experimentellen und theoretischen Methoden in wesentlichen Aspekten zu überprüfen und teilweise weiter zu entwickeln. Das betrifft sowohl die in die Berechnungen eingehenden nuklearen Daten, einschließlich der für die Spektrumsjustierung benötigten Kovarianzdaten, als auch die verschiedenen Verfahren zur Berechnung des Neutronentransports und zur Messung von Aktivierungsraten.

An zwei WWER-1000-Reaktoren wurde für jeweils einen Betriebszyklus ein komplexer Test der von den Partnern entwickelten Verfahren durchgeführt. Mit Hilfe des vom SEC organisierten Interlaborvergleichs und des vom SEC und dem FZR gemeinsam organisierten Workshops konnten Ergebnisse weiterer 5 Forschungseinrichtungen aus Rußland, Tschechien, den Niederlanden und Frankreich mit in die Tests einbezogen werden, wobei ein Teil der experimentellen Ergebnisse jedoch noch vorläufigen Charakter hat. Der Vergleich der Ergebnisse zeigte für die Monitorreaktion ^{54}Fe(n,p)^{54}Mn eine gute Übereinstimmung der Messungen der verschiedenen Experimentatoren, während für andere Reaktionen und Bestrahlungspositionen größere Differenzen auftraten. Eine gute Übereinstimmung war zwischen den deutschen, russischen und französischen Berechnungen hinsichtlich der verglichenen Fluenzintegrale festzustellen. Die Übereinstimmung von Berechnung und Experiment entsprach deren Fehlergrenzen. Wesentliche Probleme bestehen noch bei der experimentellen Bestimmung von ^{93}Nb(n,n')^{93m}Nb-, ^{237}Np(n,f)- und ^{238}U(n,f)-Reaktionsraten,

wo teilweise nicht konsistente oder mit unbefriedigend großen Fehlern behaftete Meßergebnisse erhalten wurden. Da die Ansprechfunktionen dieser Reaktionen jedoch am besten mit der Energieabhängigkeit des dpa-Wirkungsquerschnitts übereinstimmen, sind für diese Reaktionen weitere Testvergleiche und Überprüfungen der Meßverfahren notwendig. Deshalb wurden während des Rossendorfer Balakovo-3 Workshops zusätzliche Interlabor-Vergleichsmessungen an gleichartig bestrahlten Nb-Proben initiiert.

Die Arbeiten haben gezeigt, daß die "Ex-Vessel"-Dosimetrie in Zusammenhang mit fortgeschrittenen Berechnungsmethoden eine zuverlässige Bestimmung der Neutronenbelastung des Außenbereichs des WWER-1000-Reaktordruckbehälters ermöglicht und so zu einer sichereren Überwachung der Neutronenbelastung beiträgt. Weitere Experimente zur Bestimmung der Neutronenbelastung der Innenseite des Druckbehälters sind jedoch erforderlich. Das Gesamtproblem der genaueren und zuverlässigeren Bestimmung der ortsabhängigen Neutronenbelastung über das gesamte Druckgefäß ist nur lösbar durch eine Kombination von "Ex-Vessel"-Messungen mit Mock-up-Experimenten (z.B. am LR-0), Messungen der Druckbehälteraktivität (an Kratzproben, Schiffchenproben und Bohrproben), sowie Experimenten an einfachen Benchmarks (z.B. an der KORPUS-Anordnung und Fe-Kugeln mit Cf-Quellen).
Eine beträchtliche praktische Bedeutung für die Optimierung der Betriebsführung im Hinblick auf die Neutronenbelastung des Druckbehälters kann die Anwendung der Methode der Beitragsfunktionen erhalten.

Im Interesse einer sichereren Betriebsführung der WWER wird vorgeschlagen:

- die zur Überwachung der Neutronenbelastung von RDB eingesetzten Meß- und Berechnungsmethoden mit den erhaltenen Daten zu validieren, dazu auf der Basis der beim Balakovo-3-Experiment erzielten Ergebnisse ein Benchmark auszuarbeiten, an welchem alle zur Bestimmung der Neutronenbelastung von Reaktordruckbehältern benutzten Neutronentransportprogramme und Auswertungsverfahren von Messungen überprüft werden können,

- Ex-vessel Dosimetrieexperimente routinemäßig zur Überwachung der Neutronenbelastung des RDB einzusetzen,

- zur Qualitätssicherung Interlaborvergleiche von Meßmethoden und Berechnungsverfahren in größeren Abständen zu wiederholen,

- die Methode der Beitragsfunktionen routinemäßig bei der Beladungsplanungsplanung zur Gewährleistung einer minimalen Neutronenbelastung des Druckbehälters anzuwenden. Bei jeder Neubeladung kann damit auf einfache Weise der zu erwartende Fluenzbeitrag bestimmt werden.

10. Literatur

/1/ G. Borodkin, O. Kovalevich, Interlaboratory VVER-1000 Ex-Vessel Experiment at Balakovo-3 NPP, Proceedings of the Ninth International Symposium on Reactor Dosimetry, Prag Sept. 2-6, 1996

/2/ H.-U. Barz, B. Böhmer, J. Konheiser, I. Stephan, Ermittlung der Neutronendosis von bestrahlten WWER-Reaktordruckbehältermaterialien, FZR-87, 1995, (Abschlußbericht zu BMBF-Vorhaben 150 0917)

/3/ B. Böhmer, G. Manturov, Influence of Input Neutron Spectrum Covariances on Results of Pressure Vessel Neutron Spectrum Adjustments, REACTOR DOSIMETRY, Proceedings of the 9th International Symposium on Reactor Dosimetry, Sept. 2-6, 1996, Eds H. Aït Abderrahim, P. D'hondt, B. Osmera, World Scientific Publishing, Singapore (1998) ISBN 981-02-3346-9, pp 294-301

/4/ R.E. Maerker, B.L. Broadhead, J.J. Wagschal, Nucl. Sci. Eng. 9 (1985) 369-392

/5/ Abschlußbericht zum BMBF Forschungsvorhaben 1501022 "Ermittlung einer fortgeschrittenen Methodik zur Bestimmung der Neutronenbelastung des Druckbehältermaterials vom Reaktor des Typs WWER-1000" (1996-1998), in Vorbereitung als FZR Report 1998

/6/ H.-U. Barz, G. Borodkin, B. Boehmer, J. Konheiser, I. Stephan, Determination of Pressure Vessel Neutron Fluence Spectra for a Low Leakage Rovno-3 Reactor Core Using Three Dimensional Monte Carlo Neutron Transport Calculations and Ex-vessel Neutron Activation Data, Proceedings of the 9th International Symposium on Reactor Dosimetry, Sept. 2-6, 1996, Eds H. Aït Abderrahim, P. D'hondt, B. Osmera, World Scientific Publishing, Singapore (1998) ISBN 981-02-3346-9, pp 58-75

/7/ H.-U. Barz, B. Böhmer, J. Konheiser, K. Noack, I. Stephan, Monte Carlo Fluence Calculations and Spectrum Adjustment for the Pressure Vessel of thre VVER-1000 "Balakovo-3", Trans. Am.. Nucl. Soc. 77, 343 (1997)

/8/ H.-U. Barz, W. Bertram, Calculation of neutron fluence in the region of the pressure vessel for the history of different reactors by using the Monte-Carlo-method, Nuclear Engineering and Design 137(1992)71-75

Danksagung

Unser Dank gilt Herrn Dr. H.-U. Barz, Herrn J. Konheiser, Herrn Dr. K. Noack und Frau Dr. I. Stephan für Hilfe und gute Zusammenarbeit.

Herrn Prof. Dr. F.-P. Weiß danken wir für die Unterstützung der Arbeiten und die kritische Durchsicht des Manuskripts.

Für die finanzielle Unterstützung des BMBF und die Hilfe durch die Forschungsbetreuung der GRS sei allen Beteiligten an dieser Stelle herzlich gedankt.

ANHANG

/A1/ Abschlußbericht des IPPE Obninsk

/A2/ Abschlußbericht des SEC GOSATOMNADZOR

/A3/ 1. Zwischenbericht des RRC KI

/A4/ 2. Zwischenbericht des RRC KI

/A5/ 3. Zwischenbericht des RRC KI

/A6/ Abschlußbericht des RRC KI

/A7/ Protokoll, der Beiträge und Teilnehmer des "International Workshop on the Balakovo-3 Interlaboratory Dosimetry Experiment"

A1

Abschlußbericht des IPPE Obninsk

Final Report

on the Cooperation Agreement on the Project

«Increasing the accuracy of determination of the neutron load of VVER-1000 reactor components to get additional information for a safer operation of reactors»

A.M.Tsiboulia and G.N.Manturov

**Institute of Physics and Power Engineering,
Obninsk, Kaluga Region, Russia**

OBJECTIVES

Improvement and testing of the modern Russian group data set ABBN/MULTIC in order to apply these data for determination of neutron fluences.

TASK AND TERMS

1. Comparison of neutron shielding calculations with the last version of MULTIC multigroup data with calculations of reduced group numbers for a simple one-dimensional model.
2. Comparison of covariances of neutron cross sections calculated by the international code NJOY with covariances on the basis of ABBN/MULTIC.
3. Improvement of covariance data bases and calculation of neutron spectrum covariances for a one-dimensional model of the VVER-1000 reactor.
4. Development of the ABBN/MULTIC system by comparisons with international data respectively including of new data.

ABSTRACT

This time the verification of the new version of the ABBN-93 group data set and the CONSYST2 system comes to the finish. The verification is concerning the ABBN/MULTIC multigroup (299 group) data set and to the new code CONSYST for supplying material cross sections to different applications. The main attention is applied to VVER shielding and pressure vessel dosimetry applications with help of the transport S_n calculations by the code TWODANT and by Monte-Carlo codes KENO-V and VI and MCNP too. All of these codes are now based on identical group cross sections which are supplied by the code CONSYST. Under this verification some errors were found in the previous FORAN code. New algorithms were involved for calculations within the thermal region below 4eV using P_n scattering matrices for moderators. The multigroup library ABBN/MULTIC was filled by new data.

1. Comparison of neutron shielding calculations with the last version of ABBN/MULTIC multigroup data with calculations of reduced group number for a simple one-dimensional models

1.1. Background

ABBN-93 [1] is a recently released new Russian group data set. It was developed for calculations of neutron and gamma-ray radiation fields and their functionals. The ABBN-93 system consists of two main parts:

a. ABBN-93/MULTIC system - 28 group and 299 multigroup nuclear data set for calculation of neutron and photon radiation fields and their functionals.

b. CONSYST2 system - the ABBN-93/MULTIC processing data code system which prepares group average cross sections for material regions (it calculates self-shielded microscopic neutron group cross sections, weighted spectra, neutron and photon few group average cross sections of real material compositions and others). Main program of the CONSYST2 data code system is the CONSYST FORTRAN code. The CONSYST code communicates the ABBN-93 group constants with such transport codes as ANISN, DOT4, TWODANT and with such Monte-Carlo codes as KENO-V and VI as well as with German TRAMO code.

The ABBN-93 is the newer ABBN multigroup data set. The previous version of this data set was included to RSIC collection as DLC-182/ABBN-90 data library. The ABBN-93 is a modification of the ABBN-90. It differs by changing of scope included materials and improving of the CONSYST code especially within the thermal energy region. Some errors in the algorithms were eliminated too.

The ABBN-93 as well as the ABBN-90 rests on the FOND-2 nuclear data library (File Of evaluated Neutron Data) which includes selected data from BROND-2, ENDF/B-VI, JENDL-3, JEF-2 evaluated nuclear data libraries and some other sources. Majority of the data files were modified and data were converted to the group constants by GRUCON [2] and NJOY [3] codes.

The ABBN-93 set presents group cross sections for basic 28 neutron energy groups - from the thermal to 15 MeV, for the important reactor materials as well as 299 neutron group data set - from the thermal energies to 20 MeV, and for 15 photon groups - from 0 to 11 MeV. The 299 and the 28 data sets both are processed by the CONSYST program simultaneously.

Resonance self-shielding effects are taken into account by using Bondarenko factors. Nikolaev's subgroup as optimized multiband parameters are also included to the 28 and the 299 data sets and they can be used in the cases when the spatial dependence of group constants is essential.

Thermalization effects are taking into account by using thermalized P_0 and P_1 scattering matrices depending on neutron temperatures in the energy region below 4.65 eV (within ABBN groups 22, 23, 24, 25 and 26). It means in this energy region there is a possibility of upscatterings and in case of using thermalized matrices full scattering matrix will be constructed for material regions.

Table 1.1, 1.2 and 1.3 present information about the ABBN-93 neutron and photon energy group-wise structure.

Table 1.1. ABBN wide group energy structure (28 groups)

ABBN wide group number	amount of fine groups	group lower energy (eV)	group upper energy (eV)	group lethargy wide	fine group lethargy wide
-1	5	13.9818+6	20.0+6	0.07160	0.071595
0	4	10.5 +6	13.9818+6	0.28638	0.071595
1	6	6.5 +6	10.5 +6	0.47957	0.079929
2	6	4.0 +6	6.5 +6	0.48551	0.078334
3	6	2.5 +6	4.0 +6	0.47000	0.080918
4	8	1.4 +6	2.5 +6	0.57982	0.072477
5	8	0.8 +6	1.4 +6	0.55962	0.069953
6	9	0.4 +6	0.8 +6	0.69315	0.077017
7	9	0.2 +6	0.4 +6	0.69315	0.077017
8	9	100.0 +3	200.0 +3	0.69315	0.077017
9	12	46.4159+3	100.0 +3	0.76753	0.063961
10	12	21.5443+3	46.4159+3	0.76753	0.063961
11	12	10.0 +3	21.5443+3	0.76753	0.063961
12	12	4.64159+3	10.0 +3	0.76753	0.063961
13	12	2.15443+3	4.64159+3	0.76753	0.063961
14	12	1000.0	2.15443+3	0.76753	0.063961
15	12	464.1589	1000.0	0.76753	0.063961
16	12	215.4434	464.1589	0.76753	0.063961
17	12	100.0	215.4434	0.76753	0.063961
18	12	46.41589	100.0	0.76753	0.063961
19	12	21.54434	46.41589	0.76753	0.063961
20	12	10.0	21.54434	0.76753	0.063961
21	12	4.641589	10.0	0.76753	0.063961
22	12	2.154434	4.641589	0.76753	0.063961
23	12	1.0	2.154434	0.76753	0.063961
24	12	0.4641589	1.0	0.76753	0.063961
25	12	0.2154434	0.4641589	0.76753	0.063961
26	25	0.0253	0.0253	(see detailed)	

Table 1.2. Energy structure of the last ABBN group

fine group number	group lower energy (eV)	group upper energy (eV)	fine group lethargy wide
275	1.89574-1	2.15443-1	0.127922
276	1.66810-1	1.89574-1	0.127922
277	1.46780-1	1.66810-1	0.127922
278	1.29155-1	1.46780-1	0.127922
279	1.13646-1	1.29155-1	0.127922
280	1.00000-1	1.13646-1	0.127922
281	8.25404-2	1.00000-1	0.191883
282	6.81292-2	8.25404-2	0.191883
283	5.62341-2	6.81292-2	0.191883
284	4.64159-2	5.62341-2	0.191883
285	3.83119-2	4.64159-2	0.191883
286	3.16228-2	3.83119-2	0.191883
287	2.61016-2	3.16228-2	0.191883
288	2.15443-2	2.61016-2	0.191883
289	1.77828-2	2.15443-2	0.191883
290	1.46780-2	1.77828-2	0.191883
291	1.21153-2	1.46780-2	0.191883
292	1.00000-2	1.21153-2	0.191883
293	6.81292-3	1.00000-2	0.383766
294	4.64158-3	6.81292-3	0.383766
295	3.16227-3	4.64158-3	0.383766
296	2.15443-3	3.16227-3	0.383766
297	1.00000-3	2.15443-3	0.767532
298	1.00000-4	1.00000-3	2.302585
299	1.00000-5	1.00000-4	2.318282

Table 1.3. ABBN Photon Group Energy Structure

Photon group number	Energy low (eV)	Energy high (eV)
1	9.00+ 6	11.00+ 6
2	7.00+ 6	9.00+ 6
3	5.50+ 6	7.00+ 6
4	4.50+ 6	5.50+ 6
5	3.50+ 6	4.50+ 6
6	2.50+ 6	3.50+ 6
7	1.75+ 6	2.50+ 6
8	1.25+ 6	1.75+ 6
9	0.75+ 6	1.25+ 6
10	0.35+ 6	0.75+ 6
11	0.15+ 6	0.35+ 6
12	0.08+ 6	0.15+ 6
13	0.04+ 6	0.08+ 6
14	0.02+ 6	0.04+ 6
15	0.01+ 5	0.02+ 6

1.2. Shielding Benchmarks

Series integral iron experiments were performed at the IPPE (in Obninsk) [4]. They were identified as benchmarks and as useful for the purpose of testing nuclear data and numerical methods.

The experiments were performed with iron spheres of different widths (20, 30, 40, 50, 60 and 70 cm in diameter) with californium source of power 10^9 n/sec which was positioned at the center of each iron sphere. Leakage neutron and photon as neutron induced energy-wise flux spectra were measured. These experiments give an information about the iron cross sections.

The leakage flux spectrum calculations were performed by using the code TWODANT applying group 28 and 299 the ABBN-93 iron cross sections. The angular approximation was S_{16} with P_5 scattering. When solving the problem the source region volume was conserve as $1cm^3$. The neutron and photon flux spectra were calculated at the distance 2R from the surface of the iron.

The calculation results are presented in Figures 1.1 through 1.9 as functions $4\pi R^2\phi(E)$ with comparison to the measured spectra.

The agreement can be considered as fairly reasonable taking into account that the accuracy of the neutron spectra measurements is about 10-20% within the each fine group and about 5-10% within the wide group (and below 0.1 MeV not less 30%). The accuracy of the photon spectra measurements is about 15-20% below 4 MeV and about 30-50% above 6 MeV. For the 60 cm iron sphere the calculated and the measured neutron flux spectra were compared for both the fine and the wide group energy-wise structures.

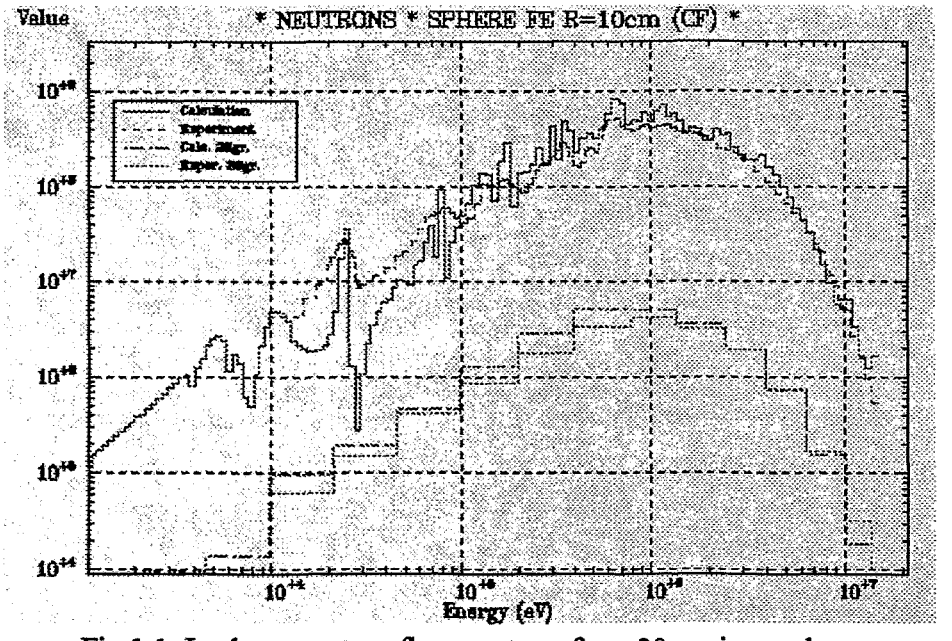

Fig.1.1. Leakage neutron flux spectrum from 20 cm iron sphere
(28 group data multiplied by factor 10^{-2})

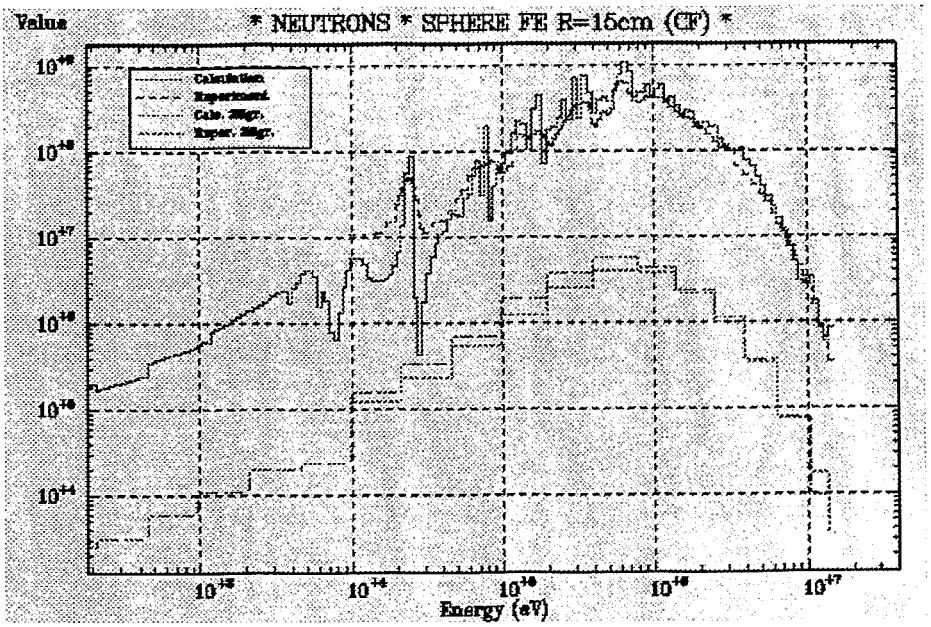

Fig.1.2. Leakage neutron flux spectrum from 30 cm iron sphere
(28 group data multiplied by factor 10^{-2})

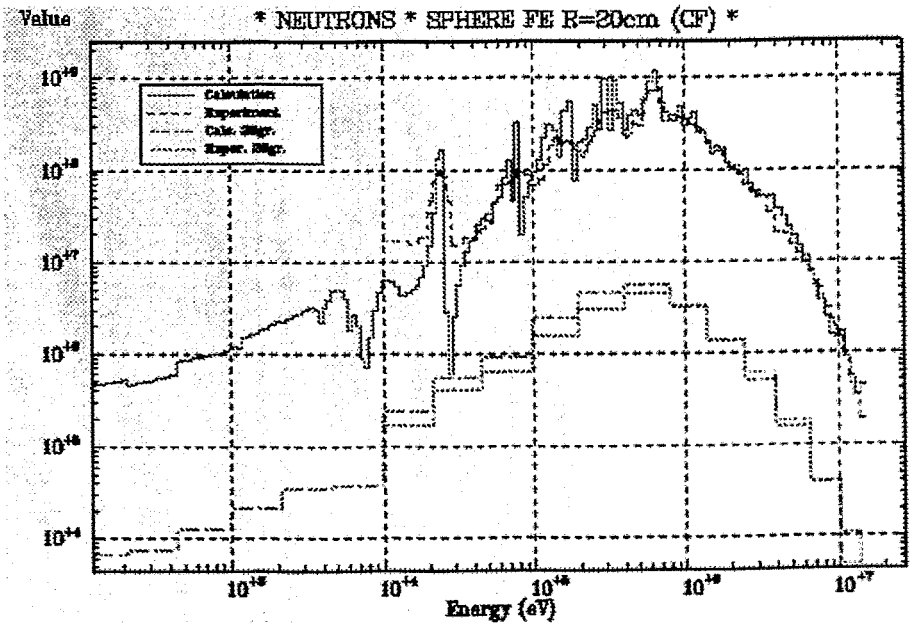

Fig.1.3. Leakage neutron flux spectrum from 40 cm iron sphere
(28 group data multiplied by factor 10^{-2})

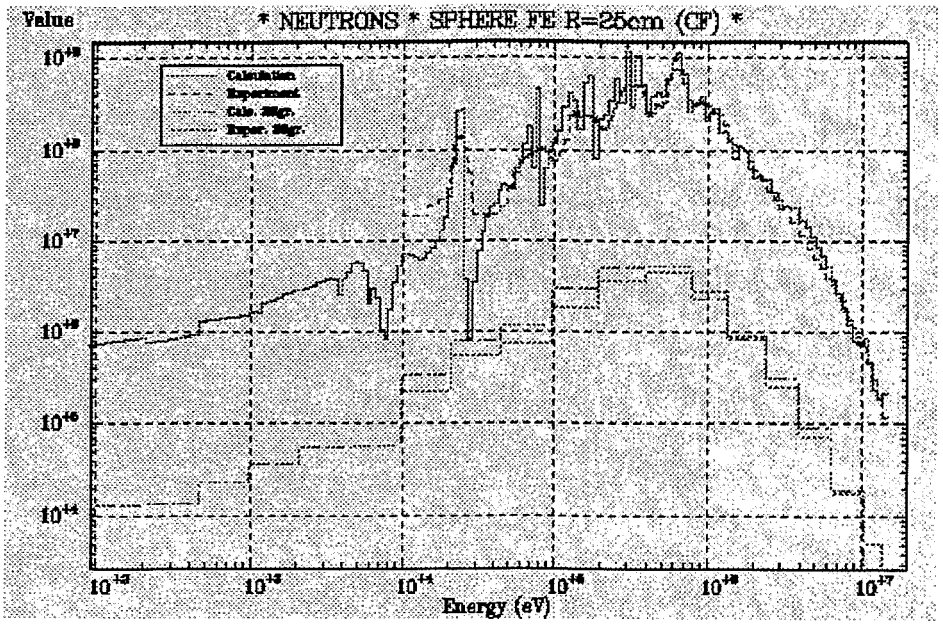

Fig.1.4. Leakage neutron flux spectrum from 50 cm iron sphere
(28 group data multiplied by factor 10^{-2})

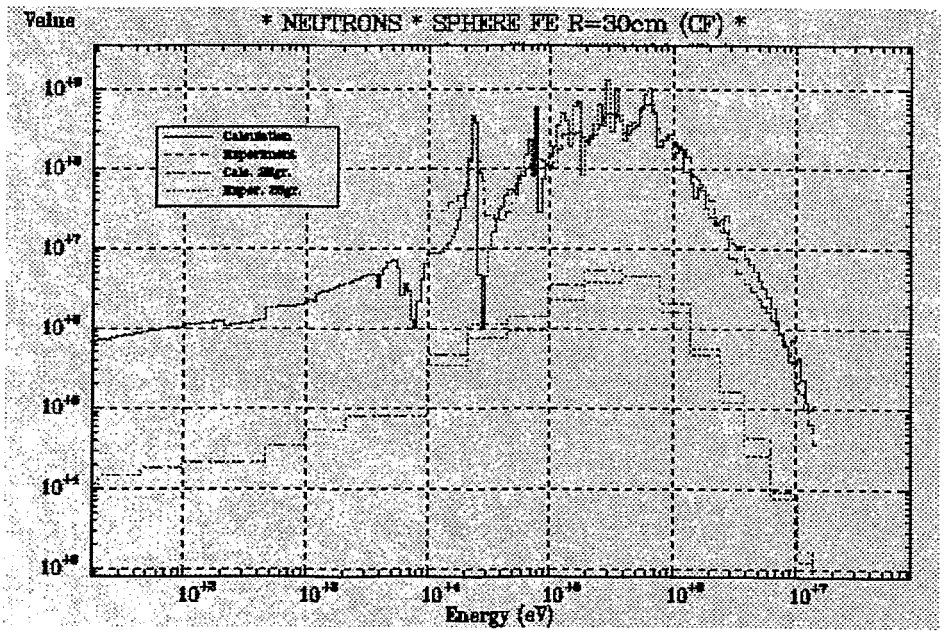

Fig.1.5. Leakage neutron flux spectrum from 60 cm iron sphere
(28 group data multiplied by factor 10^{-2})

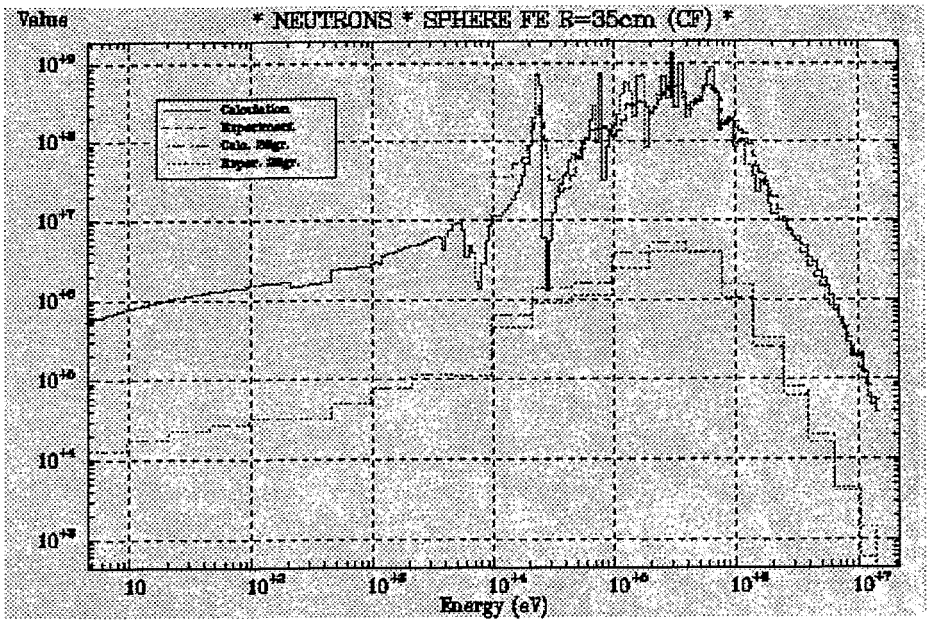

Fig.1.6. Leakage neutron flux spectrum from 70 cm iron sphere
(28 group data multiplied by factor 10^{-2})

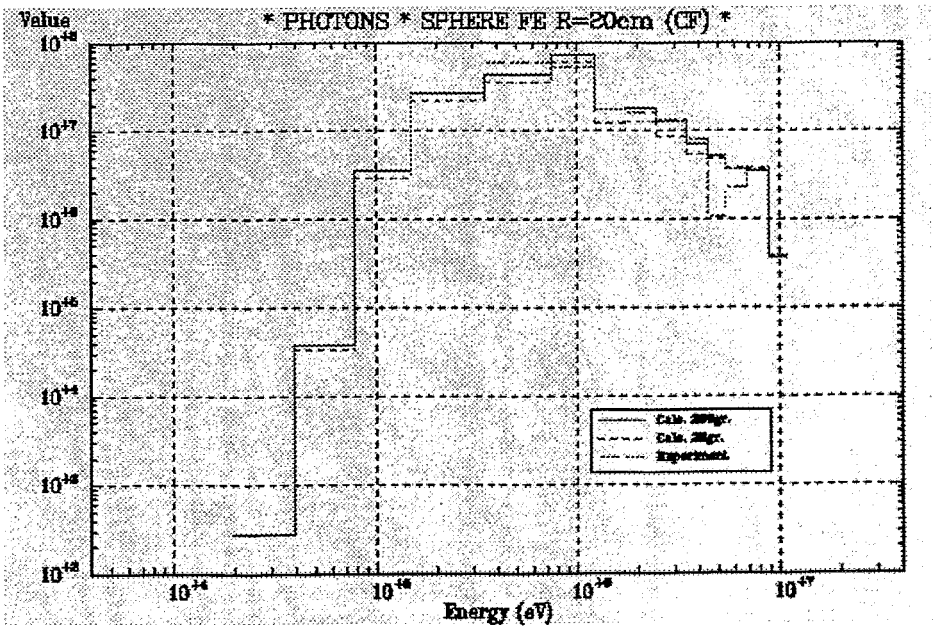

Fig.1.7. Leakage neutron induced photon flux spectrum from 40 cm iron sphere

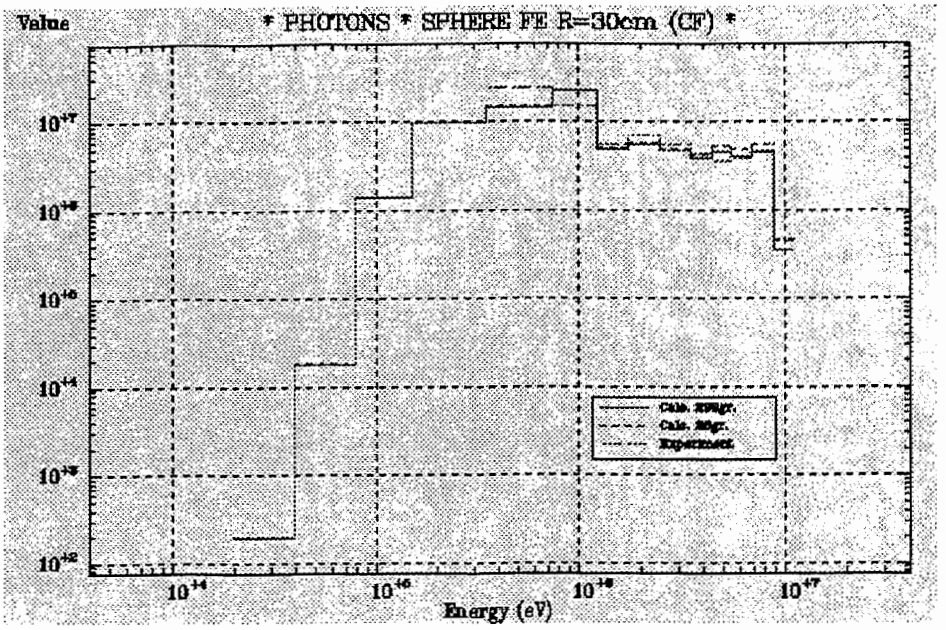

Fig.1.8. Leakage neutron induced photon flux spectrum from 60 cm iron sphere

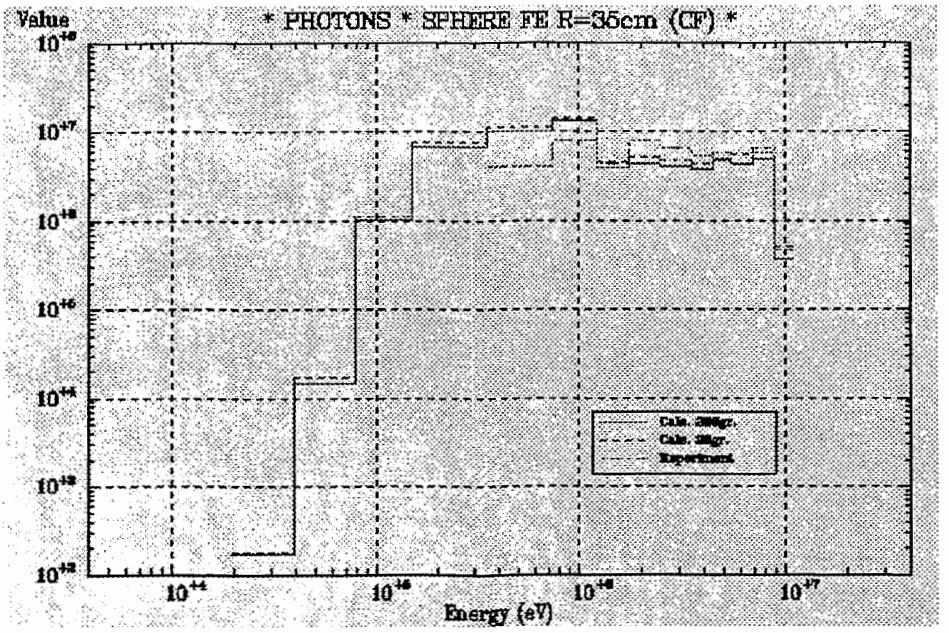

Fig.1.9. Leakage neutron induced photon flux spectrum from 70 cm iron sphere

1.2. VVER reactor shielding and reactor pressure vessel dosimetry applications

For comparative study of VVER calculations it was considered a one-dimensional model of PWR typical reactor plant used for testing of BUGLE-80 and BUGLE-93 broad-group cross-section libraries for LWR shielding applications and reactor pressure vessel dosimetry [5,6]. The BUGLE-93 was derived from VITAMIN-B6 199 group cross-section library [6].

The calculation model of PWR reactor is shown in Fig.1.10. Number densities and key parameters of pin cell used in the PWR calculations are presented in Tables 1.4 and 1.5.

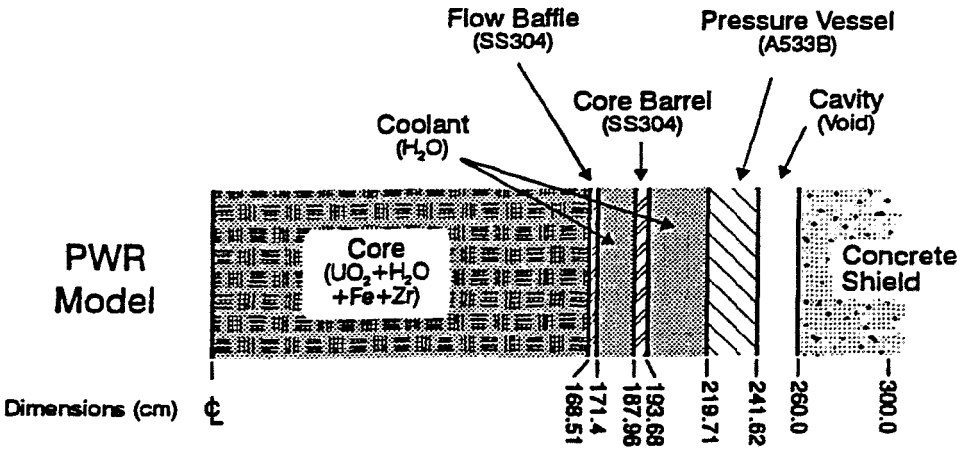

Fig.1.10. One-dimensional model of PWR reactor

Neutron and photon flux spectra from four specific locations within the PWR model were than selected corresponding to: (1) Point #37 - off-center in the PWR core region, (2) Point #69 - the downcomer region, (3) Point #82 - within the pressure vessel at a depth of 1/4 the total thickness, (4) Point #106 - within the concrete shield surrounding the reactor vessel.

The calculations were performed with the transport code TWODANT. The angular approximation was S_{16}. The order of scattering used for both neutrons and photons was P_5. The calculations with the ABBN/MULTIC were performed for 28, 81 and 299 neutron group structure. The 81 group results were produced for comparative study and they differ from the 28 group calculations by detailed representation of the resonance energy region only.

The calculated neutron and photon flux spectra as functions $4\pi R^2\phi(E)$ are compared with VITAMIN-B6 calculations in Figures 1.11 through 1.18. The comparison gives next conclusion:

- the 299 group ABBN neutron flux spectra are very close to the VITAMIN-B6 ones for all specific locations excepting the concrete shield point where the 299 group spectra are lower in all neutron energy range;
- for 1/4T PV location the difference between ABBN and VITAMIN-B6 results are it seems to us due to the last does not take into account the thermalization effects under spectrum calculation;
- the 28 and 81 group ABBN neutron flux spectra agree with the 299 group ones;
- in photon case the ABBN results are higher than the VITAMIN-B6 ones for all specific locations but it is due to the ABBN-93 photon production group cross sections include prompt and delayed gamma-ray yields;

- in photon case the broad (28 or 81) and the 299 group ABBN flux spectra are different and only the detailed representation of thermal energy region gives right results.

Table 1.4. Number densities[a] used in PWR model

	CORE	COOLANT
Hydrogen	2.768-2	4.714-2
Oxygen	1.384-2	2.357-2
Boron-10	2.466-6	4.200-6
Zirconium	4.257-3	
Iron	1.444-5	
U-235	1.903-4	
U-238	6.515-3	
Fuel Oxygen	1.343-2	

	STEELS		CONCRETE	
	SS-304	A533B	Type 04	
Carbon	2.37-4	9.81-4	Hydrogen	7.77-3
Silicon	8.93-4	3.71-4	Carbon	1.15-4
Chromium	1.74-2	1.27-4	Oxygen	4.38-2
Manganese	1.52-3	1.12-3	Sodium	1.05-3
Iron	5.83-2	8.19-2	Magnesium	1.48-4
Nickel	8.55-3	4.44-4	Aluminum	2.39-3
			Silicon	1.58-2
			Potassium	6.93-4
			Calcium	2.29-3
			Iron	3.13-4

[a] In units of $b^{-1} \times cm^{-1}$

[b] Read as 1.535×10^{-2}

Table 1.5. Key parameters for PWR pin cell

Inner radius clad (cm)	0.41783
Outer radius clad (cm)	0.47498
Outer radius cell (cm)	0.71079
Region temperature (K)	
Pellet	921
Clad	672
Moderator	551
Pellet nuclear density ($b^{-1}cm^{-1}$)	
U-235	6.325-4
U-238	2.166-2
Oxygen	4.465-2
Moderator density ($b^{-1}cm^{-1}$)	
Hydrogen	4.714-2
Oxygen	2.357-2
Boron-10	4.200-6

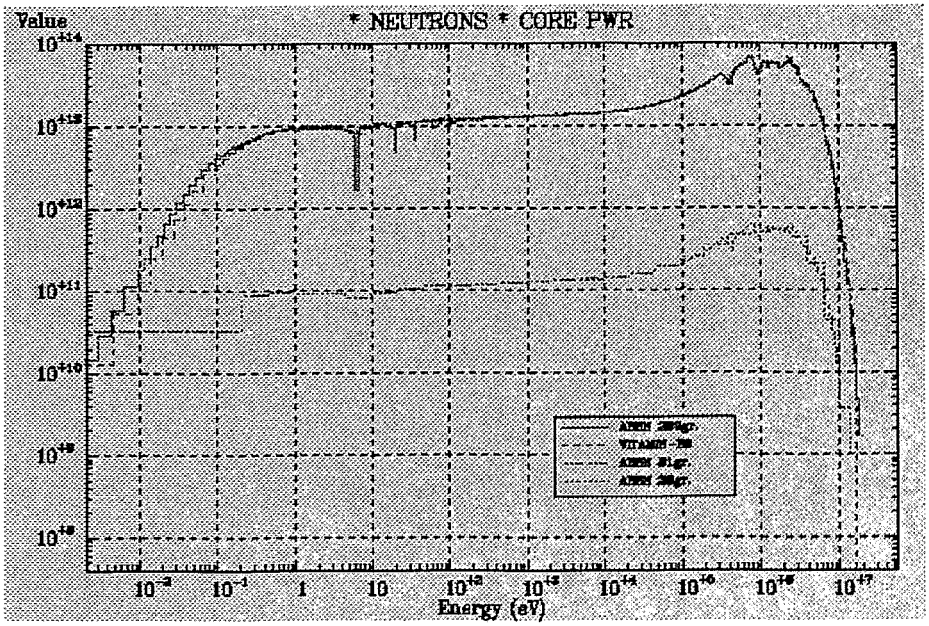

Fig.1.11. Comparison of PWR Core (Point #37) neutron flux spectra (28 and 81 group data multiplied by factor 10^{-2})

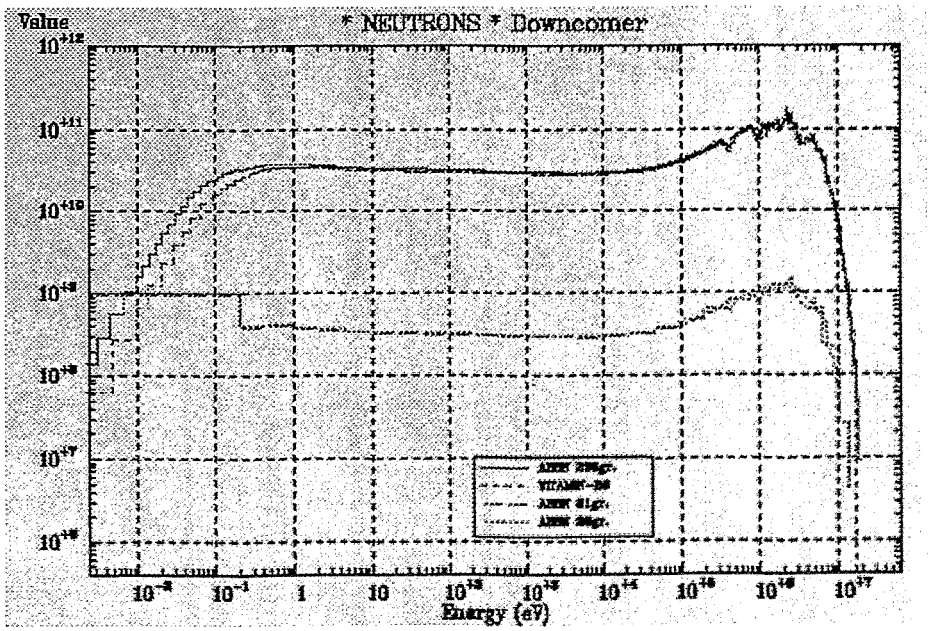

Fig.1.12. Comparison of PWR Downcomer (Point #69) neutron flux spectra (28 and 81 group data multiplied by factor 10^{-2})

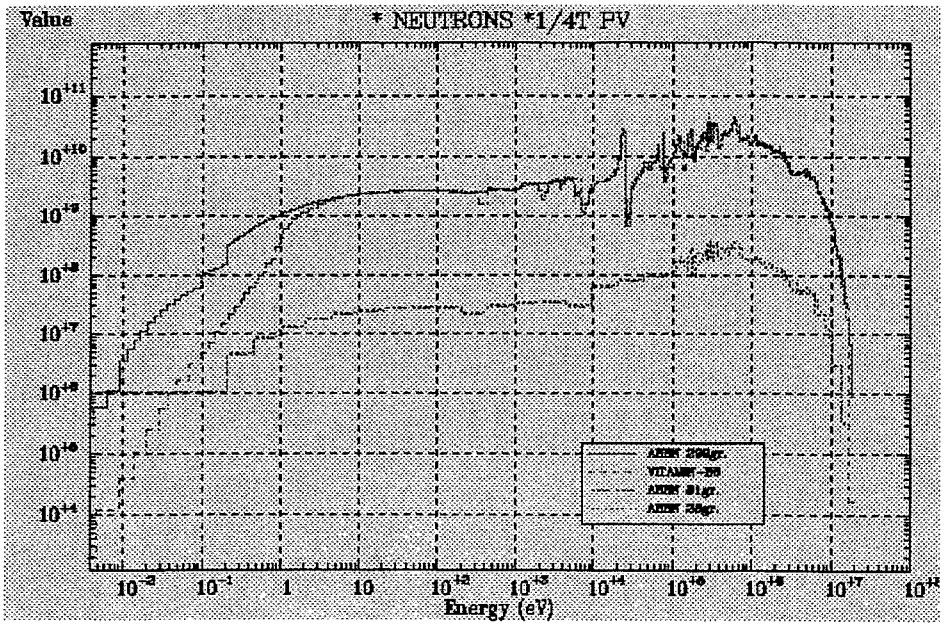

Fig.1.13. Comparison of PWR 1/4T Pressure Vessel (Point #82) neutron flux spectra (28 and 81 group data multiplied by factor 10^{-2})

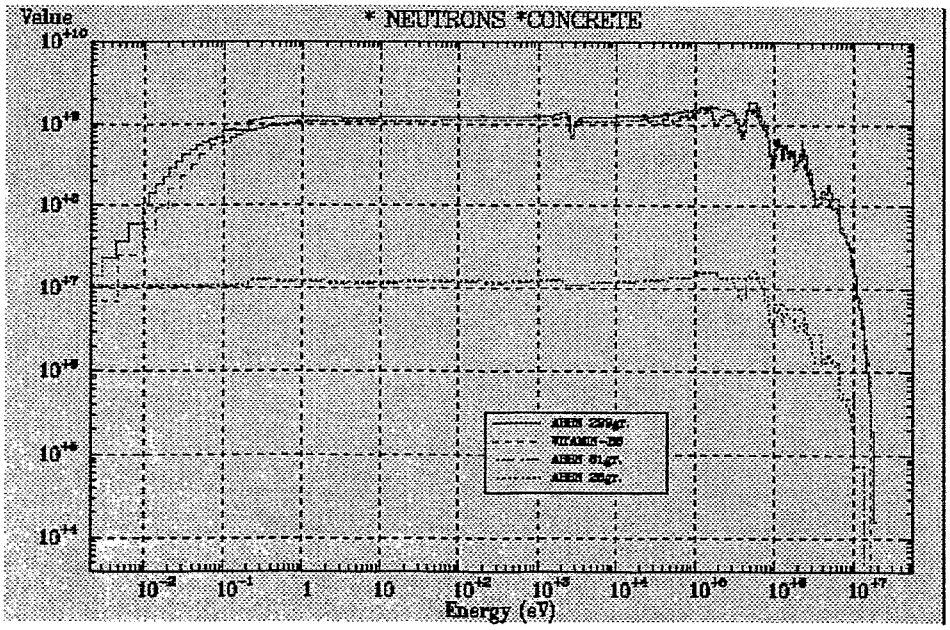

Fig.1.14. Comparison of PWR Concrete Shield (Point #106) neutron flux spectra (28 and 81 group data multiplied by factor 10^{-2})

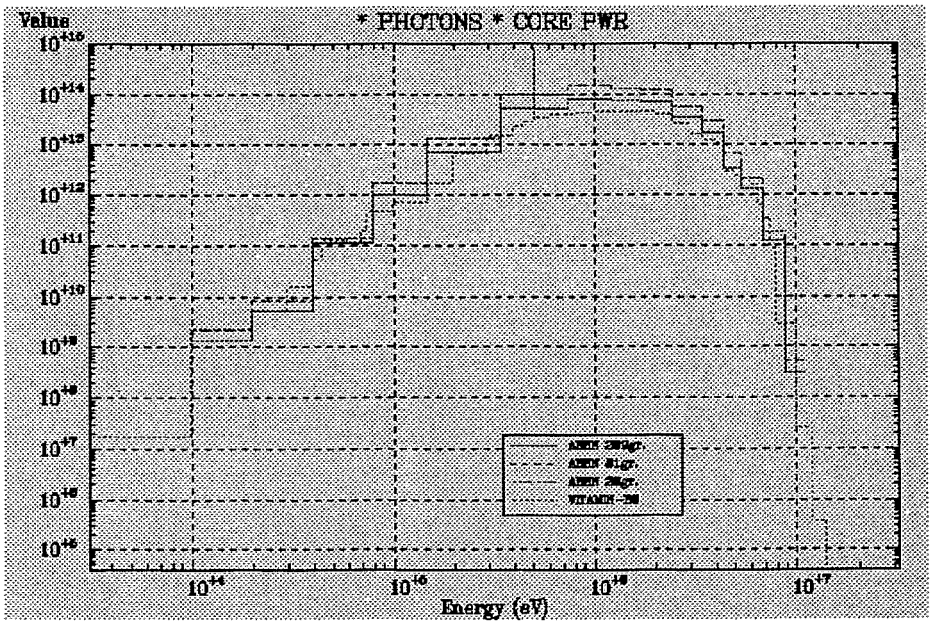

Fig.1.15. Comparison of PWR Core (Point #37) gamma-ray flux spectra

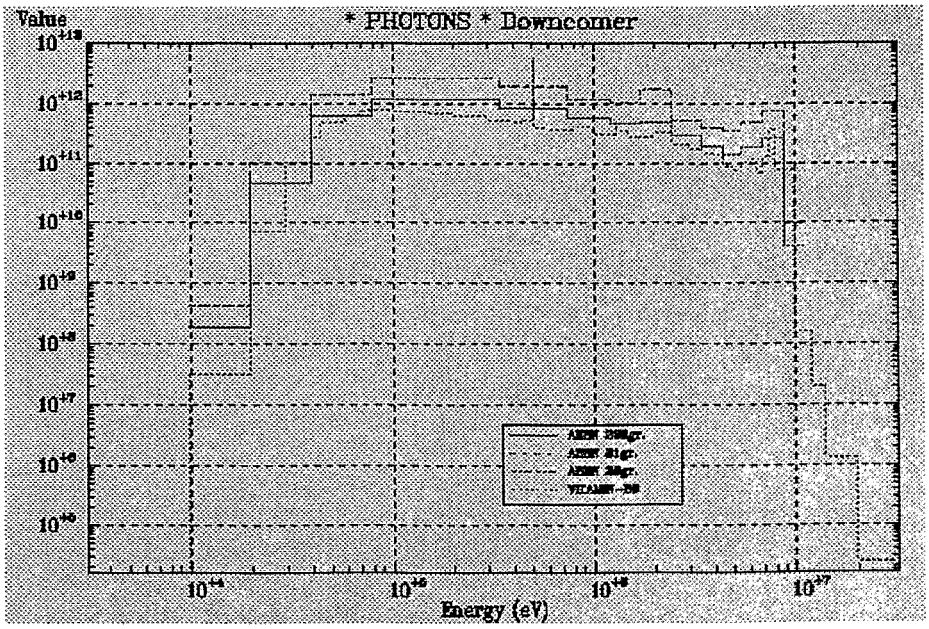

Fig.1.16. Comparison of PWR Downcomer (Point #69) gamma-ray flux spectra

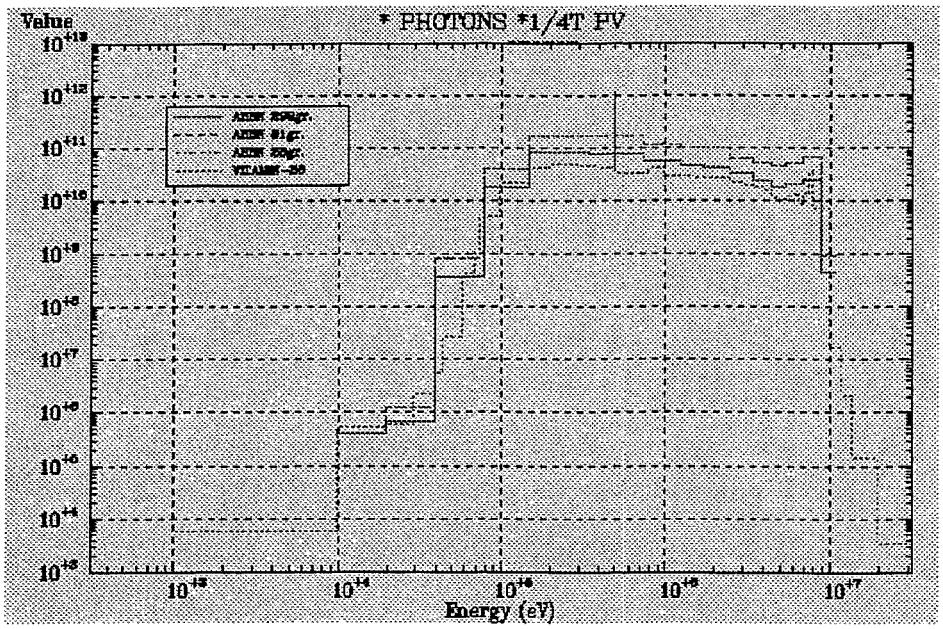

Fig.1.17. Comparison of PWR 1/4T Pressure Vessel (Point #82) gamma-ray flux spectra

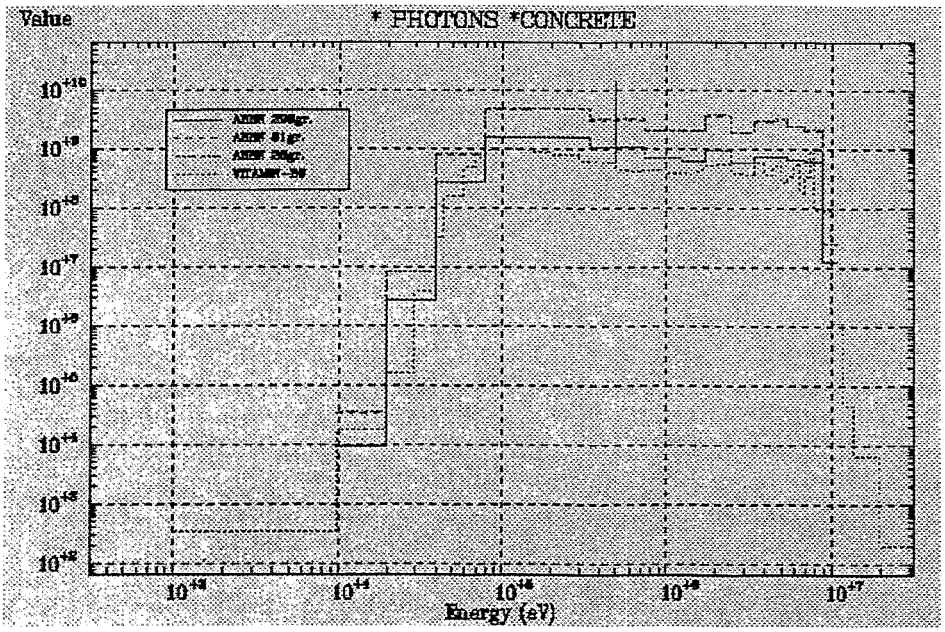

Fig.1.18. Comparison of PWR Concrete Shield (Point #106) gamma-ray flux spectra

2. Comparison of covariances of neutron cross sections calculated by the international code NJOY with covariances on the basis of ABBN/MULTIC

The LUND library (Library of Uncertainties of Nuclear Data) is a basis of uncertainties of the ABBN-93 28 group cross-section library. The LUND basis now presents more than 500 covariance matrices of uncertainties for reactions (n,γ), (n,f), (n,n'), (n,n), (n,p), (n,α), (n,2n) but also total cross section and average number of neutrons per fission for about 100 nuclides - light and structure materials, fission products, fissile and fertile nuclides, all actinides. A part of this information is presented in Table 2.1 and Fig.2.1 shows an example of the LUND data for 28 group matrices of ^{239}Pu fission and ^{238}U capture cross sections.

The LUND constructed matrices are based on analyzing of applied experimental technics and their sources of uncertainties. They also take into account of uncertainty the theoretical description of the cross section energy-wise dependence.

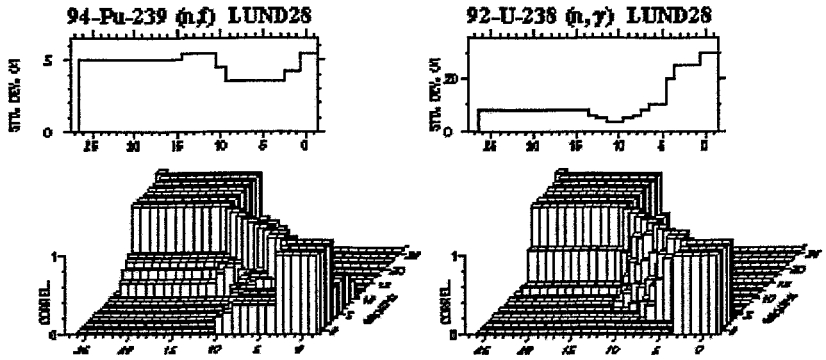

Fig.2.1. An example of the LUND data

The ENDF/B-VI file contents an information for calculation covariance matrix (MF=32 and MF=33) and it is interesting to compare the LUND and the ENDF/B-VI data. The ENDF/B-VI covariance matrices were derived by NJOY code for light elements ^{7}Li, ^{12}C, ^{19}F, and structure materials ^{23}Na, Si, ^{27}Al, Cr, ^{55}Mn, Fe, Ni and Cu.

Fig.2.2 shows the comparison of the LUND ^{23}Na(n,γ) cross section covariance matrix and the derived from the ENDF/B-VI. There are discrepancies in standard deviations of group cross section uncertainties as well as in their correlations. The same situation was observed for (n,γ) cross sections of other materials. But for threshold reactions as (n,p), (n,α) and (n,2n) the LUND and the ENDF/B-VI covariance data are very similar.

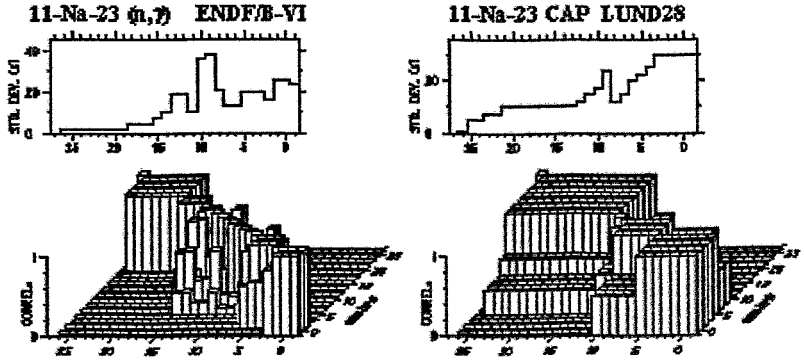

Fig.2.2. Comparison of ^{23}Na (n,γ) cross section covarience data

Table 2.1. Information about covariance matrices in the LUND library

Nuclide	tot	nn	nn'	n2n	μ	nγ	np	nd	nt	nα
1-H - 1	+	+								
3-Li- 6									+	
3-Li- 7	+	+		+		+			+	
4-Be- 9	+			+	+	+				+
5-B -10			+				+			+
5-B -11							+			+
6-C -12	+	+	+		+					+
7-N -14	+		+		+		+			+
8-O -16	+	+	+		+	+	+			+
9-F -19				+			+		+	+
11-Na-23	+	+	+	+	+	+				+
13-Al-27			+			+	+			+
14-Si						+				
14-Si-28				+		+	+			+
16-S						+				
16-S -32							+			+
22-Ti-46				+			+			
22-Ti-47							+			
22-Ti-48							+			+
22-Ti-49							+			
22-Ti-50							+			+
23-V -51				+			+			+
24-Cr	+	+	+			+				
24-Cr-50				+		+	+			+
24-Cr-52				+		+	+			+
24-Cr-53							+			+
24-Cr-54							+			+
25-Mn-55			+	+		+	+			+
26-Fe	+	+	+	+	+	+				
26-Fe-54				+			+			+
26-Fe-56				+		+	+			
26-Fe-57							+			
26-Fe-58						+	+			
26-Co-59				+		+	+			+
28-Ni	+	+	+			+				
28-Ni-58			+				+	+	+	+
28-Ni-60							+			
28-Ni-61							+			
28-Ni-62							+	+		+
28-Ni-64						+	+	+		+

3. Improvement of covariance data bases and calculation of neutron spectrum covariances for a one-dimensional model of the VVER-1000 reactor[7]

3.1. Introduction

Spectrum adjustment procedures are used in reactor dosimetry to combine information from neutron transport calculations and activation measurements in order to get more precise neutron spectra and their uncertainties, whereby the spectrum is defined as the absolute fluence level as a function of energy. The main disadvantage of neutron spectrum adjustments, based on the generalized least squares method, was in the past the lack of reliable covariance matrices, needed for all input data: reaction rates, detector cross sections and calculated spectra. The reaction rates covariances are relatively simply to evaluate and by using calibrated sources for all detector reactions the correlations between different detectors are small. The detector cross section covariances can be calculated now with available codes and data (NMF-90, NJOY + ENDF/B6, ..). The influence of the remaining uncertainties of the uncertainties of detector cross sections on adjustment results is not large.Very unsatisfactorily is the situation with the spectrum covariances. Their exact calculation is more difficult and expensive than the calculation of the spectrum itself. It includes the calculation of sensitivity coefficients relatively to all input parameters of the transport calculation and requires the availability of the uncertainties of all input parameters and their mutual correlations i.e. of the complete parameter covariance matrix. Therefore, in the past usually different coarse approximations for this matrix, or matrices calculated for other reactors, have been used for spectrum adjustment. The only adjustment system, which includes rigorous calculations of spectrum covariance matrices is up to now, to our knowlegde, the LEPRICON[8] methodology. Unfortunately it implicates the use of special transport programs and a special data base. Both are not tested for VVER type reactors. Highly specialized for VVER reactors 3-dimensional Monte Carlo codes with other data bases could not be used in the frame of LEPRICON. Therefore and for other reasons a spectrum adjustment system based on the STAYSL type least squares code COSA2[10,11] was developed and has been used for VVER neutron embrittlement and other problems. At first simple analytical models were applied as spectrum covariances. Later a combination of own estimations of relative standard deviations and a LEPRICON correlation matrix was employed. In this work an attempt has been made to evaluate the covariance matrix of the neutron spectrum in the VVER-1000 reactor cavity calculated with the Monte Carlo code TRAMO[9,12]. The effect of using this matrix relatively to formerly used approximations will be demonstrated.

3.2. Method of Spectrum Covariance Calculations

The covariances of the group spectra values, i.e. their errors and mutual correlations, are caused by the uncertainties of all input parameters of the calculation, by the inadequacy of the calculational model and by the approximations in the calculational method. As it is possible to calculate with the Monte Carlo code TRAMO the reactor in all details and with sufficient energy and angular resolution it can be assumed that errors in the calculational model and in the calculational method will be negligible. There remain the uncertainties of the input data. The following particular sources of uncertainties considered as most important have been taken into account:

a)Neutron cross sections:

- the inelastic, elastic, and capture group cross sections of iron
- the elastic group cross sections of hydrogen and oxygen.

b)Neutron source distributions:

- the uncertainty of the source energy distributions (fission spectra)
- the uncertainty of the spatial source distribution.

c)Geometrical dimensions and material densities:

Their uncertainties are difficult to specify. They can change even from reactor to reactor of the same type and depend on the quality of available information. They were estimated using tolerances prescribed by the constructors, consultations with German and Russian VVER specialists as well as the corresponding uncertainties found in LEPRICON reports. Following uncertainties were assumed:

- water thickness in the downcomer due to out-of-roundness of pressure vessel: ±0.5cm
- the steel cladding thickness: ±0.1cm
- the pressure vessel thickness: ±0.2 cm
- the pressure vessel steel density: ±1 %
- the coolant water density: ±2 %.

Fortunately, this type of uncertainty sources has not shown a decisive influence on the summary spectrum covariances although the uncertainties had been assumed larger than known tolerances.

3.2.1. Calculation of partial and total spectrum covariance matrices

For each uncertainty source a partial fluence covariance matrix is calculated. The total group spectrum covariance matrix V is obtained as sum of partial matrices:

$$V = \sum_{k=1}^{n} (H_k \; W_k \; H_k^T)$$

Here H_k is the matrix of sensitivity coefficients relatively to the parameter type k and W_k is the covariance matrix of the parameters of type k. This formula is valid also for relative covariance and sensitivity matrices usually used in computations, whereas the results are presented in form of correlation matrices and vectors of relative standard deviations (RSD).

The sensitivity matrices H_k were calculated by a direct perturbation method with help of the one-dimensional transport code ANISN. The replacement of the 3-dimensional model by a one-dimensional model is an essential approximation, however it is sufficient for the considered uncertainties and spectrum covariances for spectra at given positions. To calculate correlations between different vertical or angular positions would indeed afford at least two-dimensional calculations. But that was not the aim of this work.

The W_k matrices are obviously quite simple for the first category of the considered sources of uncertainties. In the case of uncertainties associated with neutron cross sections and the energy distribution of the fission source the corresponding W_k matrices were taken from the group nuclear data uncertainty data base LUND. The LUND data base is included in the INDECS data code system[6] and it presents uncertainties and covariances for the ABBN-93 group data set for the 28 energy group structure[14]. Some comparative calculations have been made with ENDF/B6 group cross sections calculated with code NJOY.

3.2.2. Results of the Spectrum Covariance Calculations

The uncertainty of the inelastic scattering cross sections of iron is in our case the largest contributor to the uncertainties of the spectrum in the cavity. In Table 3.1 the relative standard deviations and the correlation matrix of the iron inelastic group cross sections are given together with the group energy boundaries for the first 12 ABBN groups. The cross sections are obtained from the ABBN-93 data library, which takes into account all experiments from the LEMEX data base of the INDECS System[13]. The corresponding ENDF/B-6 uncertainties are somewhat lower in most groups.

Summarized fluence uncertainty data associated with nuclear data and neutron source uncertainties are given in Table 3.2. Table 3.3 shows the analogous data for the uncertainties of geometrical dimensions and densities.

Table 3.1. Energy group boundaries, relative standard deviations (RSD) and correlation matrix of the iron inelastic group cross sections.

GR	E_{upper} (MeV)	$\delta\sigma/\sigma$ (RSD) %	correlation coefficients mult. by 100										
1	15.0	7.8	100										
2	13.98	7.8	56	100									
3	10.5	7.8	49	70	100								
4	6.5	7.8	41	58	81	100							
5	4.0	7.8	11	5	25	25	100						
6	2.5	6.2	-23	-31	-50	-43	-23	100					
7	1.4	6.2	-15	-18	-28	-28	-43	62	100				
8	0.8	7.0	-10	-12	-18	-15	-25	40	70	100			
9	0.4	6.3	-7	-9	-11	-5	-10	20	46	73	100		
10	0.2	14.9	-1	-1	-2	-5	-7	9	7	30	55	100	
11	0.1	14.9	0	0	-1	-2	-3	9	9	9	25	55	100
12	0.0465	14.9	0	0	-1	-2	-3	9	9	9	25	25	55 100

E_{lower}(12th group) = 0.0215MeV.

Table 3.2. Summarized fluence correlation matrix associated with neutron cross sections and neutron source uncertainties

GR	RSD %	correlation coefficients mult. by 100										
1	42.6	100										
2	36.7	60	100									
3	35.1	50	71	100								
4	35.1	44	61	86	100							
5	29.8	36	43	66	73	100						
6	23.2	32	39	49	59	74	100					
7	22.4	32	43	56	64	73	95	100				
8	21.4	35	45	61	69	81	93	96	100			
9	20.1	33	46	61	69	81	90	94	98	100		
10	19.7	31	45	60	68	80	88	92	96	98	100	
11	18.7	32	45	60	68	80	88	92	96	98	98	100
12	17.4	30	45	58	66	77	86	89	93	96	97	98 100

Table 3.3. Summarized fluence correlation matrix associated with geometrical dimensions and densities

GR	RSD %	correlation coefficients mult. by 100										
1	11.4	100										
2	10.4	98	100									
3	11.4	98	98	100								
4	12.3	97	98	98	100							
5	12.4	95	97	98	98	100						
6	12.1	92	95	96	97	98	100					
7	11.1	83	88	89	91	94	96	100				
8	10.4	68	76	77	80	84	89	96	100			
9	10.4	55	64	65	69	74	81	91	97	100		
10	10.6	49	58	59	63	69	76	88	96	98	100	
11	10.7	48	58	58	62	69	76	87	95	98	98	100
12	11.0	47	56	57	61	67	75	86	95	98	98	98 100

3.3. Spectrum Adjustment

For these tests the transport calculations and experiments described in paper[5] have been used. The spectrum adjustment has been performed with the program system COSA2. Detector cross sections and their covariances were calculated on the basis of the newest version of IRDF-90. The input spectra were calculated with the TRAMO code for 29 groups above 21.875 keV, a subset of the VITAMIN/N175 group structure. The group boundaries were rearranged in order of increasing energies (see Table 3.4).

Table 3.4. Group boundaries used for the adjustment procedure

GR	E	GR	E	GR	E	GR	E	GR	E
1	2.187E-02	2	2.700E-02	3	4.631E-02	4	7.200E-02	5	9.804E-02
6	1.291E-01	7	1.576E-01	8	2.024E-01	9	2.732E-01	10	3.020E-01
11	4.076E-01	12	5.502E-01	13	6.721E-01	14	8.208E-01	15	9.617E-01
16	1.165E+00	17	1.423E+00	18	1.827E+00	19	2.307E+00	20	2.466E+00
21	3.012E+00	22	4.066E+00	23	4.966E+00	24	5.769E+00	25	6.592E+00
26	7.788E+00	27	9.512E+00	28	1.221E+01	29	1.455E+01		1.964E+01

The used reaction rates results from German and Russian activation measurements[12] with detectors irradiated at the Rovno-3 NPP during cycle 7 at 15 positions at the outer boundary of the pressure vessel. Rather large errors - 6% for $^{54}Fe(n,p)^{54}Mn$, 8% for $^{58}Ni(n,p)^{58}Co$, $^{46}Ti(n,p)^{46}Sc$, $^{63}Cu(n,\alpha)^{60}Co$ and 10% for $^{93}Nb(n.n')^{93m}Nb$, $^{237}Np(n,f)$ - have been assumed for these reaction rates based not only on the known sources of uncertainties of the measurements but also on the internal consistency of results. As for each detector an independent calibration source was available, correlations between detectors at one position caused by measurements were negligible. There has been additionally a 3% power normalization error included in the covariances of reaction rates which is fully correlated.
The calculated before 28 ABBN group spectrum covariances and the different LEPRICON covariance matrices were transformed to our 29 group structure by COSA2 subroutines.
The following spectrum covariance matrices were used in the adjustments:
1. ABBN/LUND WWER-1000 - this work
2. REAL88/ANO/LEPRICON - ANO covariance data distributed for the REAL-88 exercise
3. ABBN/LUND WWER-1000 - with reduced RSD (15% in all groups, used in paper[12])
4. REAL88/PS2/LEPRICON correlations combined with own relative standard deviations
5. GAUSS1 - Gaussian distributed correlations
6. GAUSS2 - Gaussian distributed plus constant correlations.

The calculated in this work VVER-1000 correlation matrix and the relative standard deviations (first case) are presented in Table 3.5. The REAL88/ANO/LEPRICON correlation matrix is a very similar one. Only the relative standard deviations are for the VVER case in the most groups (with exception of the lowest) somewhat higher than in the ANO case. In both cases such large uncertainties are a little surprising having in mind the comparatively better agreement between activation experiments and calculations and the not so large differences usually obtained in calculations with different cross section files. Possibly the error estimations given in the nuclear data files are too pessimistic. (ENDF/B-6 cross section covariances would probably give somewhat smaller spectrum covariances as calculations for iron cross section showed.) At the other side there may be a compensation of errors in practical pressure vessel dosimetry work, connected with the effect that usually errors are searched for and corrected only so long as the agreement between theory and experiment is not satisfyingly.

3.4. Results of the Spectrum Adjustments and Conclusions

The spectrum adjustment obtained with different spectrum covariance matrices were performed for a detector position at angle 118.5° and 149 cm height about the core bottom (Experiment h118.5). The different adjusted spectra agree well for higher energies and disagree to some extend by lower energies. The reason is that the C/E - values for the Nb and Np detectors are rather low, whereas the high energy detectors have C/E - values near 1. With different spectrum covariances the adjustment procedure handles this situation in different ways. In dependance from the uncertainties more or less information is taken from the experiment. In cases where the agreement between measured and calculated reaction rates is better the difference between the adjustment results with different matrices is lower. This can be observed in Table 3.6, where similar adjustment results for the fluence integrals $\Phi_{E>1.0MeV}$ at 3 positions are compared to the unadjusted $\Phi_{E>1.0MeV}$. In all cases the differences between results with different spectrum matrices were lower than their errors ($\leq 7\%$).

Table 3.5. ABBN/LUND VVER-1000 29-group correlation matrix with RSD

```
GR RSD    correlation coefficients multiplied with 100
     %
 1 20.6 100
 2 20.6 100100
 3 21.5  97 97100
 4 21.5  97 97100100
 5 22.3  97 97 97 97100
 6 22.4  97 97 97 97100100
 7 22.4  97 97 97 97100100100
 8 22.6  96 96 97 97 97 97 97100
 9 22.6  96 96 97 97 97 97 97100100
10 22.6  96 96 97 97 97 97 97100100100
11 23.8  92 92 95 95 95 95 95 97 97 97100
12 23.8  92 92 95 95 95 95 95 97 97 97100100
13 23.8  92 92 95 95 95 95 95 97 97 97100100100
14 25.0  87 87 90 90 91 91 91 93 93 93 95 95 96100
15 25.0  87 87 90 90 91 91 91 93 93 93 95 95 96100100
16 25.0  87 87 90 90 91 91 91 93 93 93 95 95 96100100100
17 26.2  82 82 85 85 85 85 85 88 88 88 92 92 92 95 95 95100
18 26.2  82 82 85 85 85 85 85 88 88 88 92 92 92 95 95 95100100
19 26.2  82 82 85 85 85 85 85 88 88 88 92 92 92 95 95 95100100100
20 30.1  77 77 81 81 81 81 81 83 83 83 86 86 86 82 82 82 84 84 84100
21 32.2  73 73 77 77 77 77 77 79 79 79 81 81 81 76 76 76 77 77 77 99100
22 37.2  63 63 65 65 66 66 66 68 68 68 70 70 70 67 67 67 64 64 64 76 77100
23 37.2  63 63 65 65 66 66 66 68 68 68 70 70 70 67 67 67 64 64 64 76 77100100
24 37.0  63 63 65 65 66 66 66 68 68 68 70 70 70 67 67 67 64 64 64 77 77100100100
25 36.9  56 56 58 58 58 58 58 60 60 60 62 62 62 59 59 59 55 55 55 69 70 87 87 88100
26 36.9  56 56 58 58 58 58 58 60 60 60 62 62 62 59 59 59 55 55 55 69 70 87 87 88100100
27 35.5  56 56 58 58 58 58 58 60 60 60 62 62 62 59 59 59 55 55 55 68 69 86 86 87 99 99100
28 37.8  44 44 45 45 45 45 45 47 47 47 47 47 47 47 47 47 45 45 45 49 49 64 64 65 73 73 82100
29 44.1  30 30 32 32 32 32 32 34 34 34 38 38 38 37 37 37 38 38 38 42 41 48 48 48 53 53 57 64100
```

Table 3.6. Fluence integrals $\Phi_{E>1.0MeV}$ in units of 10^{16} n/cm^2 and their RSD at 3 positions for input spectrum and adjusted spectra using different spectrum covariance matrices.

Spectrum Covariances	Experim h118.5		Experim. h114.7		Experim. h92.0	
	$\Phi_{E>1.0MeV}$	$\delta\Phi/\Phi$ %	$\Phi_{E>1.0MeV}$	$\delta\Phi/\Phi$,%	$\Phi_{E>1.0MeV}$	$\delta\Phi/\Phi$,%
not adjusted	3.35	21	3.47	21	2.03	21
ABBN/LUND VVER-1000	3.88	7	3.76	9	2.03	9
REAL88/ANO/LEPRICON	3.75	7	3.69	8	2.04	9
ABBN/LUND/VVER-1000/R	3.70	6	3.65	7	2.01	7
REAL88/PS2/LEPRICON	3.62	6	3.63	7	2.01	7
GAUSS-1	3.77	7	3.68	8	2.01	9
GAUSS-2	3.73	7	3.67	8	2.00	8

The dominating uncertainty sources for the calculated VVER-1000 fluence covariance matrix at the outer surface of the pressure vessel are the uncertainties of neutron cross sections and fission spectrum. The high uncertainty level obtained for the calculated spectra seems to be somewhat contradictory to the usually better agrement between precise calculations and measurements. The calculated covariances are in reasonable agreement but somewhat higher than results of LEPRICON calculations for a similar position in an US pressure vessel reactor. The effect of using different spectrum covariances on the adjustment results was relatively low, so that older adjustment results may be not so bad, provided that the discrepancies between theory and experiment have been not too large and that the detectors are sensitive in the whole interesting energy region. To get optimal results in all situations realistic spectrum covariances are needed. Further investigations with improved data and methods are recommended.

4. Development of the ABBN/MULTIC system by comparisons with international data respectively including of new data

4.1. Including of New Data

The ABBN/MULTIC cross-section library was filled by gadolinium multigroup neutron data.

The thermalized scattering multigroup library was extended to P_0 and P_1 scattering matrices and they are now presented for files:

Name	Temperature , Kelvin Degree
H(BENZ)	300,400,450,500,600,800,1000
H(CH2)	300,350
H(FREE)	300,350,400,450,500,600,800,1000
H(H2O)	300,350,400,450,500,600,800,1000
H(ZRH)	300,400,500,600,700,800,1000
D(D2O)	300,350,400,450,500,600,800,1000
D(FREE)	300,350,400,450,500,600,800,1000
BE(FREE)	300,400,500,600,700,800,1000,1200
BE(BE)	300,400,500,600,700,800,1000,1200
BEO(BEO)	300,400,500,600,700,800,1000,1200
C(FREE)	300,350,400,450,500,600,700,800,1000,1200,1600,2000
C(GRAPH)	300,400,500,600,700,800,1000,1200,1600,2000
O(FREE)	300,350,400,450,500,600,800,1000
ZR(FREE)	300,400,500,600,700,800,1000,1200
ZR(ZRH)	300,400,500,600,700,800,1000,1200

The revised photon data were included to the ABBN-93 cross-section library for nuclides hydrogen, oxygen and iron derived by code NJOY from ENDF/B-VI nuclear data files.

4.2. Thermal and Fast Reactor Data Testing

The calculation of criticality benchmarks help to establish the reliability of the resulting fine-group cross-section library and the cross-section processing methods for fuel and moderator materials. The testing included the calculation of several CSEWG (Cross Section Evaluation Working Group) fast and thermal critical experiments [14] and a few additional non-CSEWG benchmarks [15].

Table 4.1 lists the physics benchmarks used in the testing.

The KENO-V and VI of the SCALE system [16] calculation results of thirty-seven CSEWG and twenty-six non-CSEWG critical experiments are presented in this report. The KENO calculations used 1000 generations at 1000 neutrons per generation. Ten generations were skipped before averaging.

The KENO calculations were performed in the P_3 and P_5 approximation with the 299 group ABBN-93 data set. The CONSYST2 system with the code CONSYST were used for calculation the mixed material cross-sections and for converting these data to the CCC-254/ANISN format.

Calculated eigenvalues were compared to results obtained with the SCALE LAW-238 library (238 groups) based on ENDF/B-V data and with the VITAMIN-B6 library based on ENDF/B-VI data. In some cases, results were compared with those obtained by researchers at other organizations as MCU (RRC KI, Moscow) results.

The ABBN/MULTIC calculation results of all thirty-seven CSEWG and twenty-six non-CSEWG critical experiments show fairly agreement to the experiment and to the other ones.

Table 4.1. Reactor physics benchmarks used for data testing

Thermal reactor CSEWG benchmarks [14]:

ORNL-1,-2 -3,-4,-10	Unreflected spheres of ^{235}U (as uranyl nitrate) in H_2O
TRX-1,-2	H_2O moderated uranium lattices
BAPL-1,-2,-3	H_2O moderated uranium oxide critical lattices
PNL-1,-2,-3,-4 -5,-6,-8,-9	Unreflected spheres of plutonium nitrate in H_2O
PNL-7,-10, -11,-12	Reflected spheres of plutonium nitrate in H_2O
PNL-30,-31,-32, -33,-34,-35	Square lattices of mixed oxide rods with 2wt % plutonium

Thermal reactor non-CSEWG benchmarks [15]:

MIX-COMP-THERM Series	Square lattices of (PuO_2+UO_2) rods in a water with 20 wt % plutonium
MIX-SOL-THERM Series	Mixed plutonium and uranium solutions
PU-SOL-THERM Series	Plutonium nitrate solutions with low content of ^{240}Pu

Fast reactor CSEWG benchmarks [14]:

GODIVA	Bare sphere of enriched uranium metal
JEZEBEL	Bare sphere of plutonium metal
JEZEBEL-PU	Bare sphere of plutonium metal of 20.1% ^{240}Pu
JEZEBEL-23	Bare sphere of uranium metal (98.13 atom % ^{233}U)
BIG TEN	Reflected cylinder of uranium of 10% ^{235}U
FLATTOP-25	Reflected sphere of enriched uranium metal
FLATTOP-PU	Reflected sphere of plutonium metal
FLATTOP-23	Reflected sphere of uranium metal (98.13 atom % ^{233}U)

Table 4.2. ABBN-93 calculation results of non-CSEWG benchmarks

Variant	Experiment	k-eff, KENO-Va, ABBN-93
MIX-COMP-THERM-001 Case 2	1.000	0.99089 ± 0.00116
MIX-COMP-THERM-001 Case 1	1.000	0.99055 ± 0.00109
MIX-COMP-THERM-001 Case 3	1.000	0.98547 ± 0.00117
MIX-COMP-THERM-001 Case 4	1.000	0.98956 ± 0.00117
MIX-SOL-THERM-002 Number 058	1.000	0.99446 ± 0.00052
MIX-SOL-THERM-002 Number 059	1.000	0.99627 ± 0.00050
MIX-SOL-THERM-002 Number 061	1.000	0.99627 ± 0.00051
PU-SOL-THERM-001 Case 6	1.000	0.99406 ± 0.00088
PU-SOL-THERM-001 Case 5	1.000	1.00084 ± 0.00091
PU-SOL-THERM-001 Case 1	1.000	0.99842 ± 0.00087
PU-SOL-THERM-002 Case 1	1.000	0.99923 ± 0.00088
PU-SOL-THERM-003 Case 1	1.000	0.99756 ± 0.00081
PU-SOL-THERM-010 Case 9-1	1.000	1.01269 ± 0.00092
PU-SOL-THERM-010 Case 9-2	1.000	1.00684 ± 0.00088
PU-SOL-THERM-010 Case 9-3	1.000	1.00258 ± 0.00087
PU-SOL-THERM-010 Case 11-1	1.000	1.00740 ± 0.00090
PU-SOL-THERM-010 Case 11-2	1.000	1.00652 ± 0.00086
PU-SOL-THERM-010 Case 11-3	1.000	1.00476 ± 0.00087
PU-SOL-THERM-010 Case 11-4	1.000	0.99752 ± 0.00084
PU-SOL-THERM-010 Case 11-5	1.000	0.99997 ± 0.00084
PU-SOL-THERM-010 Case 11-6	1.000	1.00977 ± 0.00088
PU-SOL-THERM-010 Case 11-7	1.000	0.99890 ± 0.00088
PU-SOL-THERM-010 Case 12-1	1.000	1.00564 ± 0.00088
PU-SOL-THERM-010 Case 12-2	1.000	1.00524 ± 0.00084
PU-SOL-THERM-010 Case 12-3	1.000	1.01100 ± 0.00082
PU-SOL-THERM-010 Case 12-4	1.000	1.00731 ± 0.00081
Average		**0.9995**

Table 4.3. Benchmark calculation results of uranium systems

Benchmark	*Type*	*Fuel*	H/Fuel	*k - effective*					
				Exp.	ENDF/B-5	ENDF/B-6	MCU BNAB	KENO ABBN-90	KENO ABBN-93
GODIVA-g -m	Unrefl	U	95%U	1.000	.9966	.9960	1.002(2)	.9986(5) .9991(5)	.9984(5) .9993(5)
BIGTEN-g -m	Refl.	U	U	.996	1.0144	1.0171		1.0037(3) 1.0041(3)	1.0030(3) 1.0026(3)
FLATTOP-25-g -m	Unrefl	U	U	1.000	1.0047	1.0018		1.0033(4) 1.0037(4)	1.0030(5) 1.0027(4)
FLATTOP-23-g -m	Refl.	U^3	98.13%U	1.000	-	1.0032		1.0039(5) 1.0024(5)	1.0018(5) 1.0031(5)
JEZEBEL-23-g -m	Unrefl	U^3	98.13%U	1.000	.9935	.9934		.9972(5) .9968(5)	.9978(5) .9963(5)
Average					**1.0039**	**1.0023**	**1.002**	**1.0012**	**1.0008**
ORNL-1-g -m	Unrefl	U	1378	1.0003	1.0007	.9965	.993(2)	.9982(6) .9979(6)	.9973(5) .9979(5)
ORNL-2-g -m	Unrefl	U	1177	.9998	1.0005	.9964	1.002(2)	.9970(6) .9966(5)	.9964(6) .9973(6)
ORNL-3-g -m	Unrefl	U	1023	1.000	.9975	.9935	.999(3)	.9943(5) .9934(5)	.9912(5) .9934(5)
ORNL-4-g -m	Unrefl	U	972	1.000	.9989	.9950	1.002(2)	.9956(6) .9951(5)	.9937(5) .9953(5)
ORNL-10-g -m	Unrefl	U	1835	1.0003	.9993	.9961	.998(2)	.9977(4) .9964(4)	.9968(4) .9973(4)
Average					**.9994**	**.9955**	**.999**	**.9959**	**.9962**
TRX-1-m	Lattices	U	2.35*	1.000	.9915	.9894	.994(1)	.9918(6)	1.0016(8)
TRX-2-m	Lattices	U	2.02*	1.000	.9959	.9915	.995(1)	.9942(5)	.9993(8)
Average					**.9937**	**.9905**	**.995**	**.9930**	**1.0005**
BAPL-1-m	Pin	U	1.43*	1.000	.9947	.9975	.998(2)	.9988(4)	1.0062(5)
BAPL-2-m	Pin	U	1.78*	1.000	.9965	.9971	.999(1)	.9988(4)	1.0028(4)
BAPL-3-m	Pin	U	2.40*	1.000	.9965	.9972	.998(1)	.9987(5)	.9995(7)
Average					**.9959**	**.9973**	**.998**	**.9988**	**1.0028**

*V_m/V_f for pin cells

Table 4.4. Benchmark calculation results of plutonium systems

Benchmark	*Type*	*Fuel*	H/Fuel	*k - effective*					
				Exp.	ENDF/B-5	ENDF/B-6	MCU BNAB	KENO ABBN-90	KENO ABBN-93
JEZEBEL-g								.9912(6)	.9914(6)
-m	Unrefl	Pu	95.5%Pu	1.000	.9982	.9970	.998(2)	.9910(6)	.9906(6)
JEZEBEL-PU-g								.9965(6)	.9957(6)
-m	Unrefl	Pu	80%Pu	1.000	.9983	.9980	1.009(1)	.9946(6)	.9956(5)
FLATTOP-PU-g								.9993(5)	.9982(5)
-m	Unrefl	Pu		1.000		1.0029		.9991(5)	.9983(5)
THOR-g								1.0006(5)	1.0016(5)
-m	Refl.	Pu	94.9%Pu	1.000				1.0013(5)	1.0019(5)
Average					**.9983**	**.9993**	**1.0035**	**.9965**	**.9966**
PNL-1-g								1.0077(6)	1.0029(6)
-m	Unrefl	Pu	700	1.000	1.0166	1.0089	1.003(2)	1.0052(6)	1.0062(6)
PNL-2-g								.9965(6)	.9922(9)
-m	Unrefl	Pu	125	1.000	1.0092	1.0037	1.000(2)	.9976(6)	1.0001(9)
PNL-3R-g								.9889(5)	.9844(8)
-m	Unrefl	Pu	1204	1.000	.9978	.9942	.986(2)	.9877(5)	.9877(8)
PNL-4R-g								.9878(5)	.9847(8)
-m	Unrefl	Pu	911	1.000	1.0049	1.0013	.993(2)	.9942(5)	.9965(8)
PNL-5R-g								.9991(6)	.9922(8)
-m	Unrefl	Pu	578	1.000		1.0065	.998(2)	.9988(6)	1.0009(9)
PNL-6B-g								.9957(6)	.9902(9)
-m	Unrefl	Pu	131	1.000		1.0025	.997(2)	.9986(9)	.9993(9)
PNL-7A-g								1.0061(5)	1.0018(7)
-m	Unrefl	Pu	985	1.000		1.0052		1.0023(8)	1.0023(7)
PNL-8A-g								1.0061(5)	.9976(8)
-m	Unrefl	Pu	795	1.000		1.0066		1.0023(8)	1.0023(8)
PNL-9-m	Unrefl	Pu	910	1.000	1.0071		.993(2)	.9996(8)	
PNL-10-m	Refl.	Pu	210	1.000	1.0057		.996(2)	.9933(9)	
PNL-11-m	Refl.	Pu	623	1.000	1.0089		.999(2)	.9952(6)	
PNL-12A-m	Refl.	Pu	1118	1.000		1.0066	1.003(2)	1.0028(8)	1.0041(7)
Average					**1.0072**	**1.0040**	**.997**	**.9981**	**.9997**
PNL-30-m	Lattices	Pu		1.000	.9931			.9966(7)	1.0017(7)
PNL-31-m	Lattices	Pu		1.000	9994			.9986(7)	1.0049(6)
PNL-32-m	Lattices	Pu		1.000	.9980			.9991(8)	1.0033(7)
PNL-33-m	Lattices	Pu		1.000	1.0019			1.0027(6)	1.0082(6)
PNL-34-m	Lattices	Pu		1.000	1.0024			1.0002(7)	1.0056(6)
PNL-35-m	Lattices	Pu		1.000	1.0074			1.0031(6)	1.0066(6)
Average					**1.0004**			**1.0000**	**1.0050**

REFERENCES:

1. G.N. Manturov, M.N. Nikolaev, A.M. Tsiboulya, "ABBN-93 Group Data Set. Part I: Nuclear Data for Calculation of Neutron and Photon Radiation Fields" (Rus. Systema Gruppovich Konstant BNAB-93. Chasti I: Yadernye Konstanty dlya Rascheta Neitronnich i Fotonnich Polei Izlucheniya), Jornal VANT, Series Nuclear Data (1996), vol.1, p.59-98.

2. V.V. Sinitsa, "Code for Group Constants Calculations with Evaluated Nuclear Data Libraries", Jornal VANT, Series Nuclear Data (1984), vol.5(59), p.34 (Rus.).

3. R.E. MacFarlane, D.W. Muir, R.M. Boicourt, "The NJOY Nuclear Data Processing System", Volume I: User's Manual, LA-9303-M (ENDF-324), Los Alamos National Laboratory, 1982.

4. L.A. Trikov, Yu.I. Kolevatov, A.N. Nikolaev, et al, "Experimental Investigations of Leakage Neutron Spectra and Gamma-Ray Radiation for Iron Spheres", Report FEI-943, Obninsk, 1979 (Rus.)

5. R.W. Roussin, "BUGLE-80: Coupled 47 Neutron, 20 Gamma-Ray, P3 Cross-Section Library for LWR Shielding Calculations", RSIC Data Library Collection, DLC-075, ORNL.

6. D.T. Ingersoll, J.E. White, et al, "Producing and Testing of the VITAMIN-B6 Fine-Group and the BUGLE-93 Broad-Group Neutron/Photon Cross-Section Libraries derived from ENDF/B-VI Nuclear Data", Report ORNL-6795, (January 1995).

7. B. Boehmer and G. Manturov, "Influence of Input Neutron Spectrum Covariances on Results of Pressure Vessel Neutron Spectrum Adjustments", *Proc. Intern. Conf. in Prague* (1996).

8. Maerker, B.L. Broadhead, J.J. Wagschal, Nucl. Sci. Eng. 91, 369-392 (1985).

9. H-U. Barz, TRAMO - a Flexible Multigroup Neutron Transport Code on the Basis of the Monte Carlo Method for Flux Calculations, *ZfK- 705*, Rossendorf 1990

10. B.Böhmer, COSA2 - Ein Spektrumsjustierungsprogramm zur Auswertung von Aktivierungsmessungen auf der Basis der verallgemeinerten Methode der kleinsten Quadrate, *ZfK-735*, Rossendorf 1991.

11. H-U. Barz, B. Böhmer, J. Konheiser, I. Stephan, Ermittlung der Neutronendosis von bestrahlten WWER-Reaktordruckbehältermaterialien, *FZR-87*, 1995.

12. H-U. Barz, G. Borodkin, B. Boehmer, J. Konheiser, I. Stephan Determination of Pressure Vessel Neutron Fluence Spectra for a Low Leakage Rovno-3 Reactor Core Using Three Dimensional Monte Carlo Neutron Transport Calculations and Ex-vessel Neutron Activation Data, Contribution to this Symposium.

13. Manturov, "Influence of Neutron Data Uncertainties on the Accuracy of Prediction of Advanced Reactor Characteristics", Proc. of Intern. Conf. on Nuclear Data for Science and Technology, Gatlinburg, Tennessee, USA, (1994), Vol.2, p.993-999.

14. ENDF-202. Cross Section Working Group Benchmark Specifications, DNL-19302, BNL (November 1974).

15. NEA Nuclear Science Committee, "International Handbook of Evaluated Criticality Safety Benchmark Experiments", NEA/NCS/DOC(95)03, OECD.

16. SCALE 4.3: RSIC Computer Code Collection, CCC-545, ORNL.

A2

Abschlußbericht des SEC GOSATOMNADZOR

FINAL REPORT

on the Cooperation Agreement on the Project

„Increasing the accuracy of determination of the neutron load of VVER-1000 reactor components to get additional information for a safer operation of reactors"

Gennady I. Borodkin, project leader
and
Victor P. Gorbunov, project participant

Scientific and Engineering Center for Nuclear and Radiation Safety of Russian GOSATOMNADZOR
14/23 Avtozavodskaya ul., 109280 Moscow, Russia

SCIENTIFIC GOAL:

Collection and preparation of all needed data of the reactor Balakovo-3 and Rovno-3 together with the formulation of basic reactor models for the calculation of neutron fluences in the region of the reactor pressure vessel and evaluation of activation measurements.

TASKS AND TERMS:

1. Collection of basic data of the VVER-1000 (geometrical measures, compositions).
2. Establishment of reactor models including first information for the time dependent fission source distributions.
3. More accurate determination of time dependent fission source distributions with a sufficient fine space distribution in the outer fuel elements nearer to the reactor pressure vessel.
    - Collection of the needed information
    - completion of the calculation of detailed fission sources
4. Performing of activation measurements and evaluation on a certain VVER-1000 pressure vessel.

INTRODUCTION

VVER pressure vessel integrity is a main criterion of safe operation of these reactor types. The main reason of the degradation of properties of pressure vessel steel at operation, in particular radiation embrittlement, is a neutron radiation. For the determination of the characteristics of the pressure vessels neutron load the methods of neutron dosimetry are used. The neutron dosimetry includes the determination of the fluence, fluence rate, spectrum of neutrons in critical points of a pressure vessel. To reach this objective the calculated-measured methods of neutron dosimetry are used. By using the neutron transport calculations the neutron field characteristics and their functionals in RPV thickness and near RPV space are determined. The experiments are used for testing and validation of methods and results of calculations.
Ex-vessel dosimetry experiments performed at Balakovo NPP, unit 3, and Rovno NPP, unit 3, allow to validate the calculated values in the ex-vessel reactor cavity.
The reliability and the quality of the neutron transport calculational data depends on correct modeling of the reactor and completeness of initial data for neutron transport calculations with reference to the experiment, taking into account all features of reactor operating and fluence measurement technique.
In frame of this project the collection and preparation of all needed data of the reactor Balakovo-3 and Rovno-3 together with the formulation of a basic reactor models for the calculation of neutron fluences in the region of the reactor pressure vessel have been performed. The ex-vessel measurement data obtained by activation technique have been evaluated.

1. COLLECTION OF BASIC DATA OF THE VVER-1000 (GEOMETRICAL MEASURES, COMPOSITIONS).

The basic data of the VVER-1000 include the design parameters, the space sizes of an investigated design, the type of used materials and their compositions.

The design construction data of VVER-1000, incorporated in mathematical model of neutron transport calculations of Balakovo-3 and Rovno-3 are indicated In table 1.

Table 1. *Design construction data of VVER-1000, used in reactor modeling.*

PARAMETERS	VALUE
1. Reactor core	
Nominal thermal power	3000 MW
Nominal electrical power	1000 MW
Coolant	
Pressure at core inlet	15.9 MPa
Net flow	80 000 m^3/h

PARAMETERS	VALUE
Inlet temperature	288 degr.C
Outlet temperature	317 degr.C
Number of fuel assemblies	163
Effective core radius	158 cm
2. Fuel assembly	
Fuel assembly pitch	23,4 cm
Step of assemblies placement	23,6 cm
Assembly shell	no
Fuel assembly gap	0,2 cm
Number of fuel pins	312
Lattice pitch	1,275 cm
Spacer grid	
Number	14
Distance between spacer grids	25,5 cm
Material	Stainless steel
Density	7.85 g/cm^3
Mass	654 g
Instrumentation tube	
Material	Stainless steel
Outer radius	0,56 cm
Wall thickness	0,08 cm
Control rod tube	
Number	18
Material	Stainless steel
Outer radius	0,630 cm
Wall thickness	0,085 cm
3. Fuel element	
Cladding	
Material	Zirconium alloy (Zr + 1% Nb)
Density	6.52 g/cm^3
Outer radius	0,455 cm
Wall thickness	0,069 cm
Pellet	
Material	UO_2
Density	10,22 g/cm^3
Outer radius	0,3775 cm
Central hole radius	0,024 cm
Height of UO_2	355 cm
Mass of UO_2	1560 g
4. Control absorber	
Number	18

PARAMETERS	VALUE
Clad material	Stainless steel
Inner diameter of clad	0,7 cm
Clad thickness	0,06 cm
Absorber diameter	0,7 cm
Absorber material	BC_4
Absorber density	1,8 g/cm^3
5. Burnable absorber	
Number	18
Clad material	Zirconium alloy (Zr + 1% Nb)
Inner diameter of clad	0,772 cm
Clad thickness	0,069 cm
Absorber diameter	0,772 cm
Absorber material	91.7%Al+1,26%B + Stainless steel

It is clear that it is impossible to model in details a real construction of power reactor, moreover, it is unnecessary in case of neutron transport calculations. Proceeding from physical reasons a integration and homogenization of various constructive details, as well as simplification of a complex configuration of separate details, is carried out. The reasons resulting from the neutron transport calculational technique and experience of variant calculations with different degree of detailization are in this case used.

The choise of the geometrical model for individuel calculations depends from the VVER symmetry approximation, experimental technique and operating parameters of reactors.

The positions of the experimental racks near the pressure vessels of the Balakovo-3 and Rovno-3 reactors are presented on the fig.1.

Proceeding from the azimuthal position of the experimental racks and possible asymmetry of a specific power in reactor core sector of interest the 60 degree sector of periodicity is recommended for calculation of Balakovo-3 reactor. This sector is shown on the fig.2.

The 30 degree sector of symmetry may be used for Rovno-3 calculations.

The axial-radial geometrical scheme is the same for both reactors.The dimensions of calculation area are 352 cm on radius and 519 cm on height with elevation marks of 470 cm higher and 49 cm below than level of reactor core bottom. This scheme has been transmited to the FZR.

The following simplifications on the materials compositions may be considered for preparation of the VVER-1000-size-material model:

- the reactor core is made as completely homogenious with contemination: fuel (U-238 and U-235), zirconium, stainless steel, water
- the stainless steel consists of iron, cromium and nickel
- zirconium alloy - pure zirconium
- pressure vessel - pure iron.

In accordance with above mentioned approximation the final data for composition have been prepared and submitted in table 2.

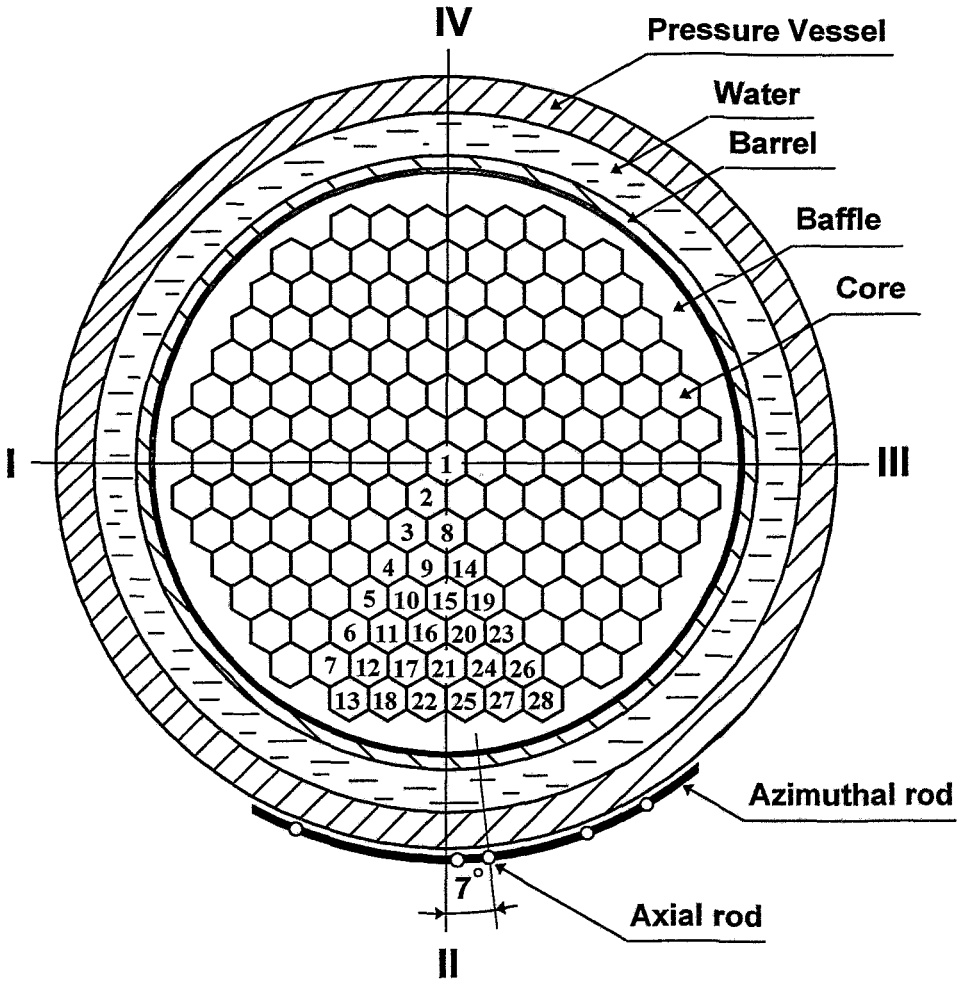

Figure 1. Schematic view of the experimental rack arrangement near the VVER-1000 pressure vessel

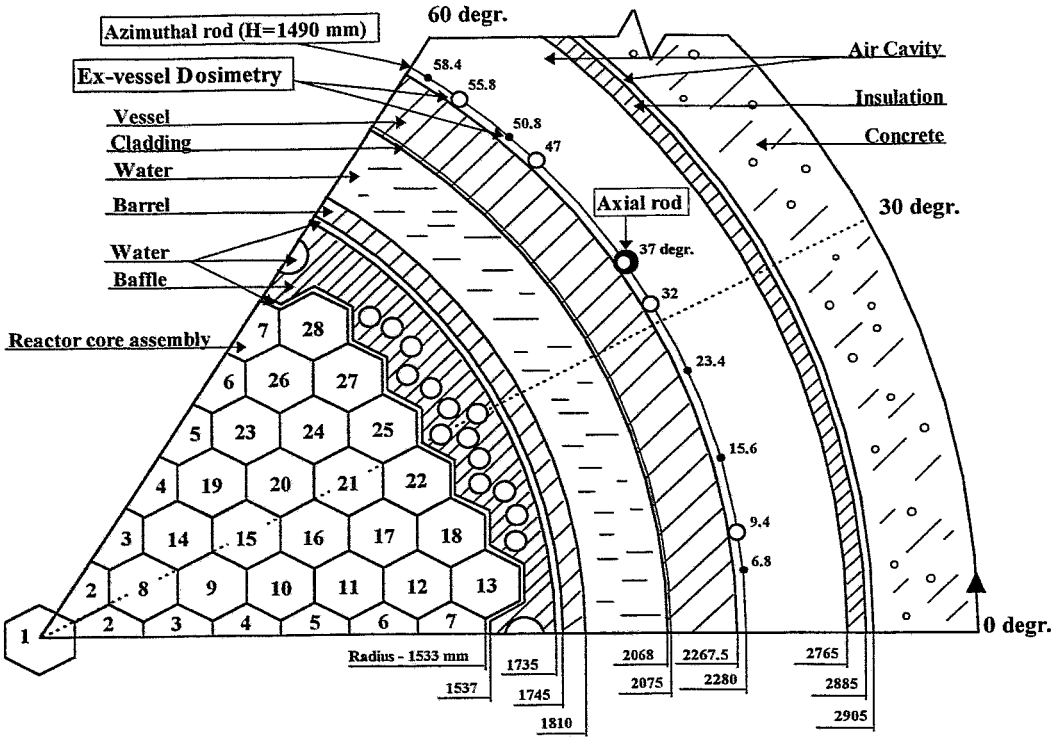

Fig.2. Radial-Azimythal Scheme of the Periodical Sector with Installed Dosimeters (o - Capsule, • - Fe-54 Monitor) near the Balakovo-3 Pressure Vessel

The 1D scheme of radial layers (zones), as recommended for the S_n calculations of the VVER-1000 reactor, is shown on fig. 3. The numbering of layers is indicated according to table 2.

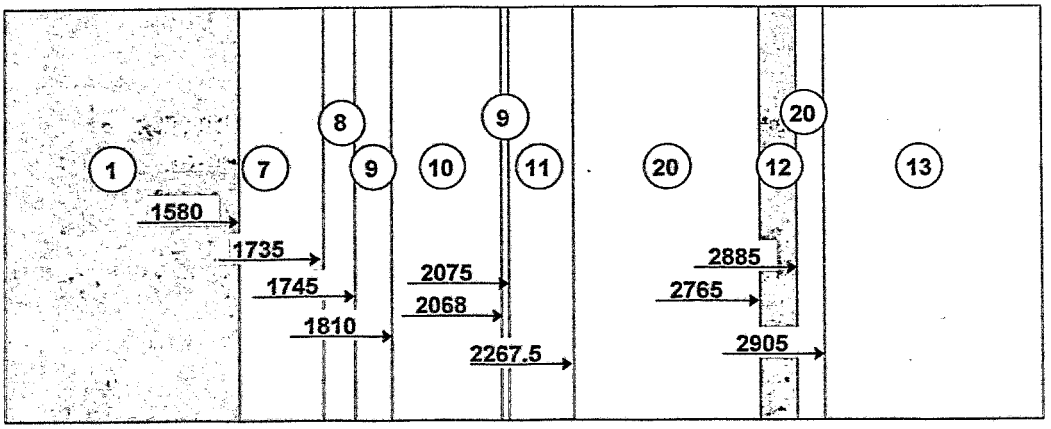

Fig.3. R-approximation of the VVER-1000 reactor model

Table 2. *Element concentration in zones of the calculational model of the VVER-1000 (nuclear density of elements), 10^{24} cm^{-3}*

Zone	No	H	O	Fe	Cr	Ni	Zr	Si	U238	U235
Reactor core	1	2,674E-02	2,524E-02	1,141E-03	3,454E-04	1,674E-04	4,754E-03		5,839E-03	9,615E-05
Steel-Water-Zr	2	2,900E-02	1,450E-02	4,200E-03	1,260E-03	6,170E-04	1,480E-02			
Steel-Water-Zr	3	2,850E-02	1,420E-02	1,990E-02	5,950E-03	2,920E-03	4,230E-03			
Steel-Water	4	3,360E-02	1,680E-02	1,990E-02	5,950E-03	2,920E-03				
Steel-Water	5	3,500E-02	1,750E-02	1,800E-02	5,410E-03	2,650E-03				
Steel-Water	6	4,680E-02	2,340E-02	4,200E-03	1,260E-03	6,170E-04				
Baffle	7	1,300E-02	6,480E-03	4,380E-02	1,330E-02	5,870E-03				
Water	8	4,959E-02	2,479E-02							
Steel	9			6,019E-02	1,730E-02	8,064E-03				
Water	10	5.067E-2	2.533E-2							
Pres-sure vessel	11			8,480E-02						
Insola-tion	12			9,670E-03	7,890E-04	3,490E-04				
Con-crete	13	2,260E-02	3,840E-02	4,790E-03				2,39E-02		
Steel-Water-Zr	14	2,540E-02	1,270E-02	1,100E-03	3,240E-04	1,580E-04	5,050E-03			
Steel-Water-Zr	15	2,470E-02	1,240E-02	4,400E-03	1,320E-03	6,440E-04	1,300E-02			
Water	16	4,773E-02	2,386E-02							
Steel-Water	17	3,720E-02	1,860E-02	1,100E-02	3,240E-03	1,580E-03				
Steel-Water	18	1,030E-02	5,130E-03	4,650E-02	1,390E-02	6,820E-03				
Steel-Water	19	2,780E-02	1,390E-02	2,320E-02	6,940E-03	3,410E-03				
Air cavity	20		1,000E-05							
Speci-mens	21	2,390E-02	1,190E-02	2,710E-02	6,990E-03	3,390E-03		4,10E-03		
Steel-Water	22	4,160E-02	2,080E-02	4,830E-04	1,440E-04	7,080E-05				

2. ESTABLISHMENT OF REACTOR MODELS INCLUDING FIRST INFORMATION FOR THE TIME DEPENDENT FISSION SOURCE DISTRIBUTIONS.

The neutron source is defined as the total number of fission neutrons emitted per unit volume. The total source is calculated from the power distribution over the core, cumulated burnup (MW*days/kgU), the average number of neutrons emitted per fission, the average energy per fission and the fuel density, and it is distributed in energy according to a theoretical fission spectrum. To obtain the time-dependent fission source distribution the reactor total power history, an assemblies power and cumulated burnup distribution over the reactor core during the irradiation period must be taken into account.

The total power history during the fluence detector irradiation is controled and fixed by the reactor operation control system.

The relative assembly power distributions for the irradiation period have been obtained from the results of the neutron-physical calculations and corrected by the measured data obtained from the operating control system. As example, the first information for core power distribution of Balakovo-3 reactor is presented in Fig.4 and tables 3 and 4. The time periods are expressed in Effective Full Power Days (EFPD). It is adopted that in fig.4 and table 4 the total power of the reactor core is the same for these time moments.

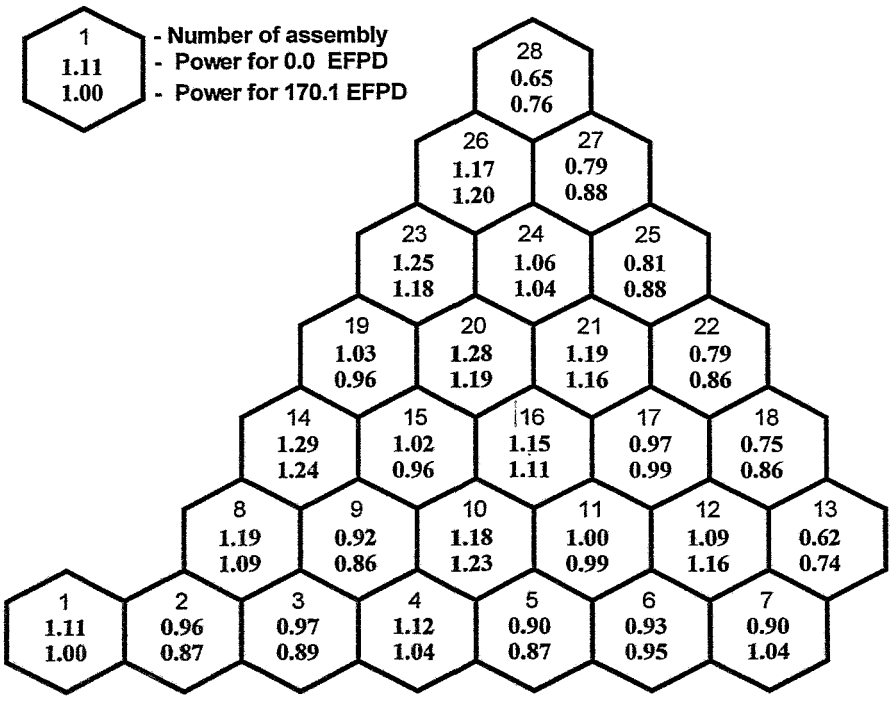

Fig.4. The Relative Assembly Power Distributions During the Dosimeters Irradiation for the Balakovo-3 Experiment.

Table 3. *The monthly total power history during detector irradiation in time of 5th cycle of Balakovo-3.*

Datum	EFPD's	Average Power(a), MW
17.03.94	0.0	0.0
17.04.94	24.80	2400
17.05.94	28.60	380
17.06.94	29.00	39
17.07.94	45.70	1670
17.08.94	71.50	2497
17.09.94	98.50	2613
17.10.94	112.10	1360
17.11.94	130.00	1732
17.12.94	148.70	1870
17.01.95	166.40	1713
24.01.95	170.10	1586

a - the averaged total power for previous month

Table 4. *The relative variation of the peripheral assemblies powers during the irradiation for Balakovo-3.*

	Number of the periphery assemblies						
EFPD	7	13	18	22	25	27	28
0	1.0	1.0	1.0	1.0	1.0	1.0	1.0
40	1.01	1.02	1.01	1.01	1.01	1.01	1.02
80	1.04	1.08	1.07	1.04	1.04	1.05	1.06
120	1.09	1.13	1.11	1.08	1.06	1.09	1.11
138	1.11	1.15	1.12	1.08	1.07	1.09	1.12
154	1.13	1.18	1.13	1.09	1.07	1.10	1.14
170	1.16	1.19	1.15	1.09	1.09	1.11	1.17

The cumulated burnup distribution for the peripheral assemblies is presented in table 5.

Table 5. *The peripheral assemblies burnup during the irradiation period of fifth cycle of Balakovo-3.*

	Assembly Burnup, MW*Day/kgU	
Assembly number	0.0 EFPDs	170 EFPDs
7	0	7.39
13	0	5.21
18	0	6.22
22	0	6.42
25	0	6.55
27	0	6.48
28	0	5.38
12	10.70	19.41
17	25.89	33.55
21	13.19	22.35
24	25.71	33.89
26	10.70	19.88

The axial time-dependent assembly power distributions have been obtained by the same way as azimuthal power distributions. These data are in the FZR utilization.
In accordance with the same procedure such information for the Rovno-3 reactor have been collected and prepared. Full data files had been transmited to the FZR.

3. MORE ACCURATE DETERMINATION OF TIME DEPENDENT FISSION SOURCE DISTRIBUTIONS WITH A SUFFICIENT FINE SPACE DISTRIBUTION IN THE OUTER FUEL ELEMENTS NEARER TO THE REACTOR PRESSURE VESSEL.

To obtain more accurate time-dependent fission source distributions taking into account fine space distributions in the peripheral assemblies a set of detailed neutron-physics calculations has been run. In neutron transport calculations of VVER-1000 it is important to take into account the pin-to-pin power distributions of the peripheral assemblies, which play a dominant role in neutron irradiation of the pressure vessel. The detailed pin-by-pin power distributions for the periphery assemblies were calculated for the various time instants during detectors irradiations for Balakovo-3 and Rovno-3 reactors. Moreover, the pin-by-pin power distributions were obtained for 8 axial levels of each peripheral assembly.

Let's consider the main features of pin-to-pin distributions on the example of Balakovo-3 experiment.

The distributions of the specific power over the section the peripheral assemblies (from center of the reactor to the pressure vessel through the assembly center) are submitted on fig. 5-8. The peripheral assemblies are considered for 30 degree

symmetry sector. A tendency of power distributions in the symmetric assemblies for the 60 degree sector is the same. It is visible that the power reduction over the section of assemblies (over the fuel pins) is essential. However, from the beginning of fuel cycle the change of this dependence is weak. The comparison of power reduction for different assemblies is shown on fig. 9. The most essential reduction is observed for assembly 13. This is the assembly with the closest placement to the reactor pressure vessel. The most week power reduction has been found for the assembly 7. This assembly is more profound in core and is closer to the centre. No systematic dependence of the specific power reduction over the assembly has been found out for the peripheral assemblies of second row.

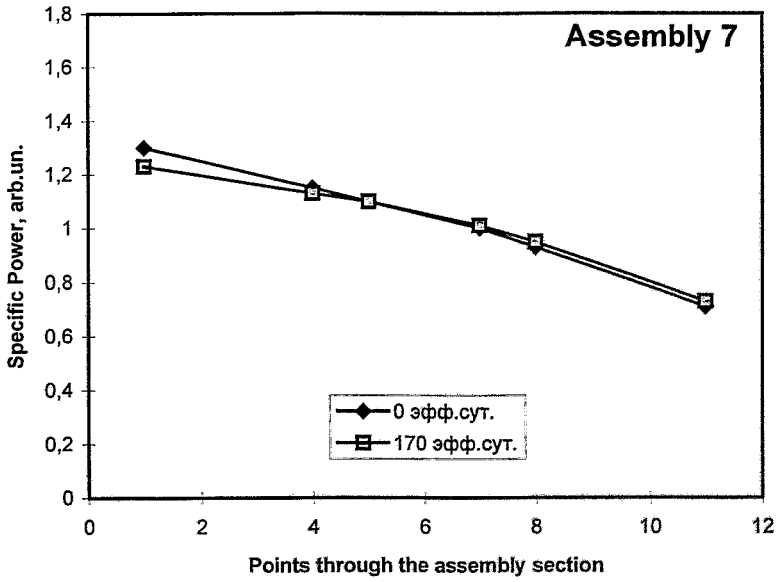

Fig.5. Power reduction over the assembly 7 of Balakovo-3, cycle 5

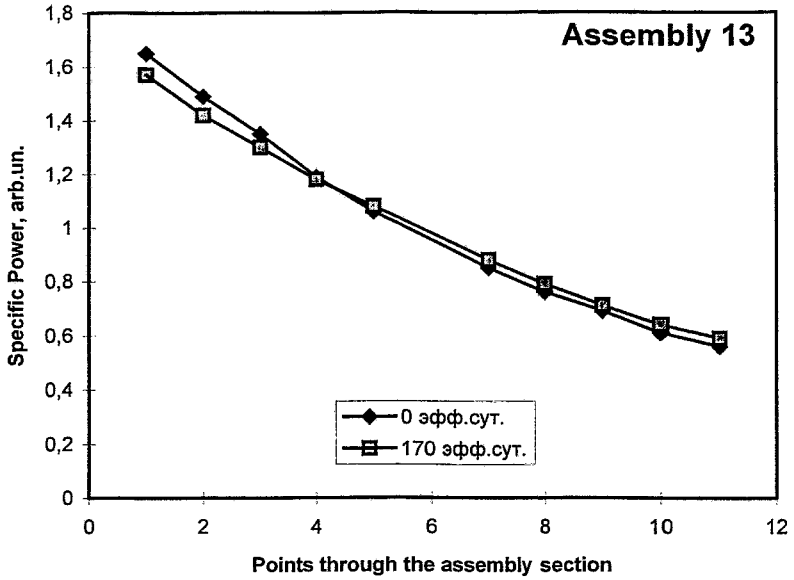

Fig.6. Power reduction over the assembly 13 of Balakovo-3, cycle 5

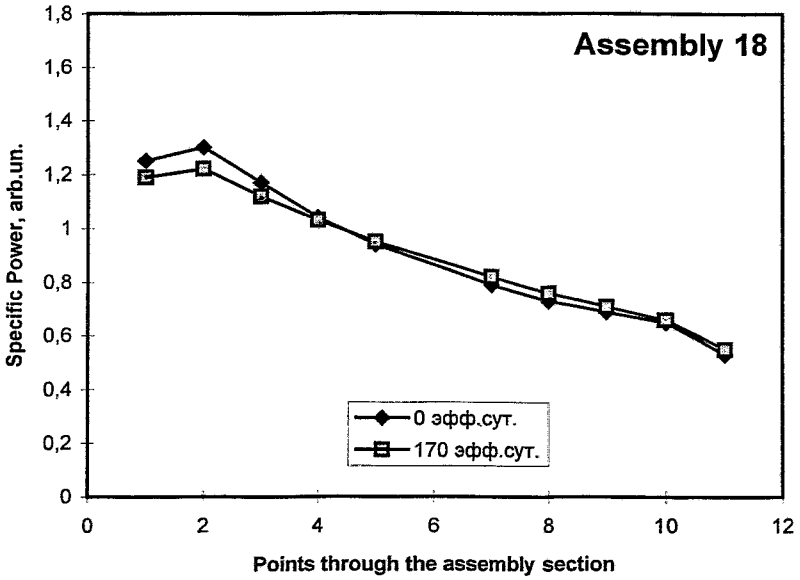

Fig.7. Power reduction over the assembly 18 of Balakovo-3, cycle 5

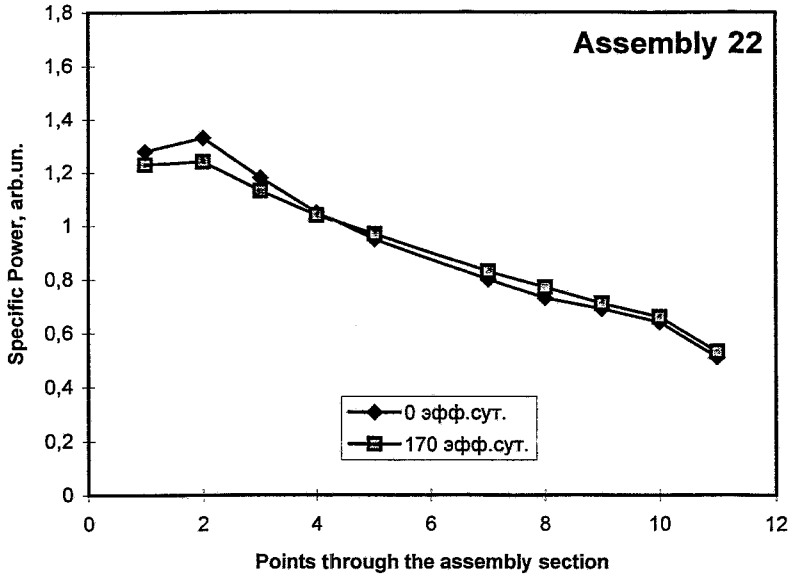

Fig.8. Power reduction over the assembly 22 of Balakovo-3, cycle 5

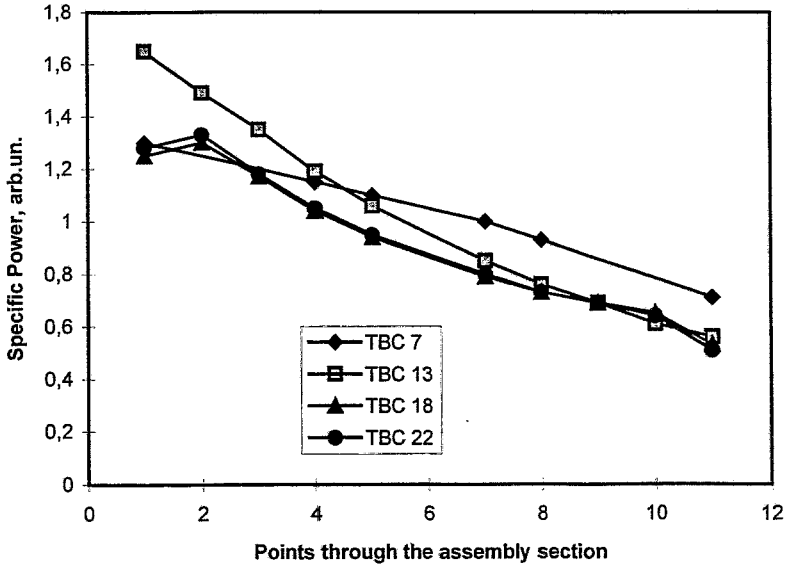

Fig.9. Power reduction over the periphery assemblies of Balakovo-3, cycle 5

4. PERFORMING OF ACTIVATION MEASUREMENTS AND EVALUATION ON A CERTAIN VVER-1000 PRESSURE VESSEL.

The experimental technique used for validation of the calculational results is the neutron-activation method. The set of activation detectors were installed near the pressure vessels of Balakovo-3 and Rovno-3. The typical detector set used in fluence measurements by SEC is shown in table 6. The characteristics of fluence detectors are presented in table 7.

After the completion of irradiation of the neutron fluence detectors installed near the outer surface of the reactor pressure vessels the measurements of gamma-rays emitted by detectors have been performed. The activity measurements of the SEC's detectors and monitors have been carried out at the SEC's laboratory designed for such works.

The activity of detectors is measured by counting of the emitted gamma rays from activation reaction products in the detector material. Every detector has the reaction product with an individual energy of gamma rays. The quantity of gamma rays with different energy must be detected by the special gamma-spectrometry equipment.
The End Of Irradiation Activity (EOIA), A_o, of detectors is derived by the following expression:

$$A_o = \frac{S_f \cdot \exp(\lambda \cdot T_c)}{N_n \cdot \varepsilon \cdot \eta \cdot C_c \cdot C_h \cdot C_r \cdot C_s}$$

where:

S_f - count rate of the full-energy peak yield of the gamma-ray with subtraction of the background and correction, taking into account the deadtime of apparatus,
λ - decay constant,
T_c - cooling time from the end of the irradiation to the middle of the counting period,
N_n - nuclide number in detector,
ε - counter efficiency,
η - gamma-ray emission,
C_c - factor, taking into account a self-absorption of gamma-ray in detector material,
C_h - factor, taking into account a distance of radioactive material from the counter,
C_r - detector radius factor, taking into account the fact that the detector is not a "point",
C_s - factor, taking into account a coincidence summing of cascade gamma-rays.

Table 6. *SEC NRS Dosimeters Used in Ex-vessel Dosimetry Experiments at Balakovo-3 and Rovno-3.*

Element	Material	Contamination/Purity	Mass (mg)/Nuclei
Iron	foil	99.9 % ^{54}Fe	20
Iron	foil	pure	200
Nickel	foil	pure	15
Nickel-58	foil	95.9 % ^{58}Ni	10
Nickel-60	foil	92.6 % ^{60}Ni	100
Niobium	foil	5 ppm Ta	60
Copper	foil	99.6 % ^{63}Cu	300
Titanium	foil	alloy with Al, Mo	150
Titanium-46	powder	TiO_2, 70.8% ^{46}Ti	60
Manganese	powder	MnO_2	250
Cobalt	foil	alloy with Al	30
Cobalt	foil	pure	1
Neptunium-237	powder	NpO_2	5E+19
Uranium-238	powder	UO_2, 3 ppm ^{235}U	1E+20

Table 7. *The characteristics of fluence detectors.*

Detector, reaction	Half-life period, days	Effective energy (MeV)	Interval of 5 % activation (MeV)	Interval of 95 % activation (MeV)
$^{237}Np(n,f)$	11020	0.5	0.21	3.4
$^{93}Nb(n,n')$	58900	1.0	0.34	5.6
$^{238}U(n,f)$	11020	1.5	1.2	8.0
$^{58}Ni(n,p)$	70.86	2.35	1.5	9.3
$^{54}Fe(n,p)$	312.3	3.0	2.1	9.5
$^{46}Ti(n,p)$	83.79	4.0	4.2	11.2
$^{63}Cu(n,\alpha)$	1925.5	6.4	5.4	12.6
$^{55}Mn(n,2n)$	312.3	12	11.4	16.4

The reaction rate, RR, is derived from the detector activity measurements as follows:

$$RR = \frac{A_o}{\gamma \cdot k_e \cdot k_o}$$

where:
γ - cumulative yield of radioactive nuclide per reaction of a neutron with a parent nuclide (used for fission reactions),
k_e - factor of neutron field perturbation caused by detector material,
k_o - factor which takes into account the decay of a radioactive nuclide over irradiation period.

Coming from the specific feature of the activation detector technique, the last factor must be determined by a particular method. The expression for this factor may be as:

$$k_o = \sum_{n=1}^{N} f_n \cdot (e^{\lambda \cdot t_{o,n}} - 1) \cdot e^{-\lambda \cdot (T_o - t_n)}$$

where:
N - number of irradiation periods with steady-state totel power levels,
f_n - factor taking into account the level of the neutron flux in the detector position during the interval *n* (local neutron flux),
T_o - calender time of the irradiation,
t_n - time of the beginning the interval *n*,
$t_{o,n}$ - time duration of the interval *n*.

In case of the direct proportionality of the neutron flux in the detector position and the total power of the reactor during the irradiation, this factor may be obtained as:

$$f_n = \frac{P_n}{P_{nom}}$$

where:
P_{nom} , P_n - nominal reactor power and power for the interval *n*,

By this procedure the evaluation of measured results has been performed. The azimuthal distributions of fast neutron fluences derived by reaction $^{54}Fe(n,p)^{54}Mn$ have been presented in the fig.10 (Balakovo-3) and 11 (Rovno-3).
The comparison of measured reaction rates is presented in the table 8.

A comparison of azimuthal distributions of the fast and epithermal neutron field parameters derived for Balakovo-3 reactor has shown significant differences. The epithermal fluence was measured by the cobalt detector, covered by the cadmium, using the reaction $^{59}Co(n,\gamma)^{60}Co$. As an indicator of the fast neutron fluence was used the iron detector with the reaction $^{54}Fe(n,p)^{54}Mn$. The comparison results have been presented in the table 9. It can be seen that the relation of the maximum to minimum for the fast neutrons is 2.31, while this value for the epithermal neutrons is 1.15. Earlier for VVER-1000 [1] such difference has been obtained for the thermal neutrons (azimuthal irregularity was 1.2). Now this fact has been also shown for the epithermal neutrons.

Moreover, the neutron spectrum in range of high energies, as can be seen in comparison of $^{54}Fe(n,p)$ and $^{237}Np(n,f)$ reactions [2], differs in azimuthal direction of VVER-1000. That fact that the neutron spectrum in the relation of the thermal, epithermal and fast neutrons differs in the azimuth must result in the azimuthal variation of the effective cross section values and needs the introduction of a suitable correction during the analysis of the fluence distributions obtained from the activity measurements.

The cadmium ratio for the $^{59}Co(n,\gamma)^{60}Co$ reaction has been found to be equal 1.31 what gives a good agreement with the results obtained at the other VVER-1000 reactors [3]. Such value of the cadmium ratio says that there is an rather small part of thermal neutrons in the ex-vessel position of the VVER-1000 in comparison with the total amount of neutrons. Therefore, it can be supposed that the influence of the impurity activities in the neptunium, uranium, nickel and copper detectors is very small. This opportunity increases significantly the quality of the experimental data and reduces the measurement uncertainty.

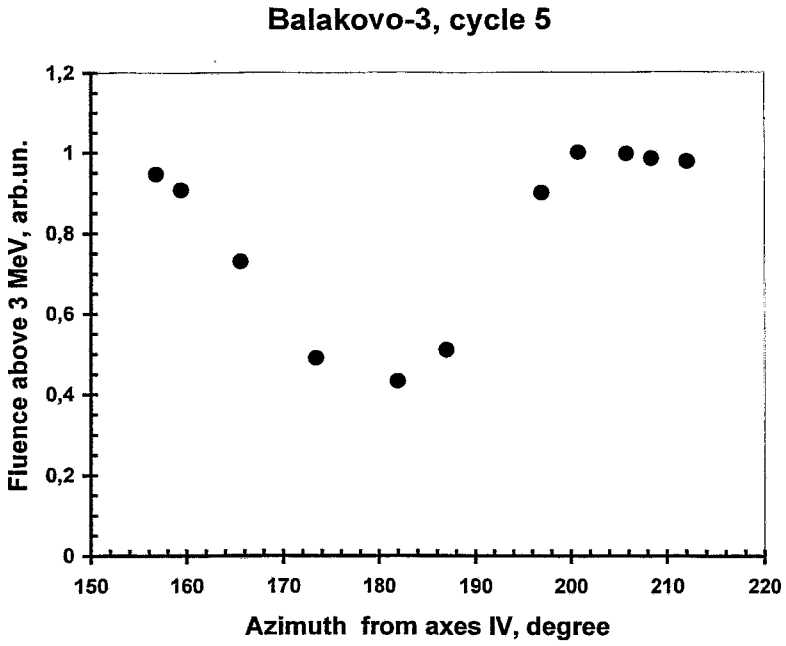

Fig.10. Azimuthal distribution of fast neutron fluence in the ex-vessel position of Balakovo-3 derived in the experiment

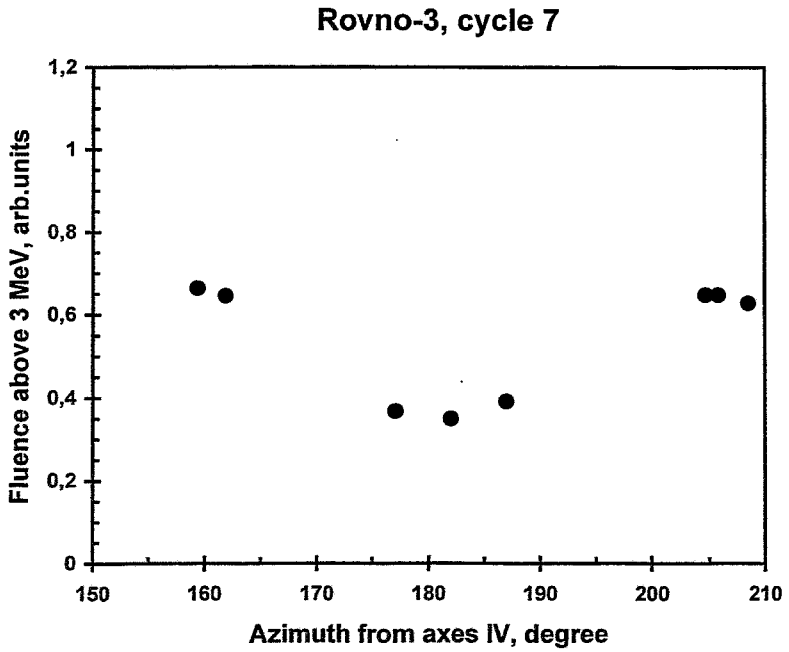

Fig.11. Azimuthal distribution of fast neutron fluence in the ex-vessel position of Rovno-3 derived in the experiment

Table 8. *Maximum reaction rates* (Bq/nucl.) *in the Balakovo-3 and Rovno-3 ex-vessel positions.*

Reaction	Balakovo-3, cycle 5	Rovno-3, cycle 7
$^{237}Np(n,f)$	7.70E-15	6.80E-15
$^{238}U(n,f)$	5.74E-16	---------
$^{58}Ni(n,p)$	1.27E-16	1.08E-16
$^{54}Fe(n,p)$	9.28E-17	7.97E-17
$^{60}Ni(n,p)$	5.18E-18	---------
$^{63}Cu(n,\alpha)$	1.19E-18	1.12E-18

Table 9. *Relative azimuthal distributions of the fast and epithermal neutron fluences in the Balakovo-3 ex-vessel position*

Azimuthal angle, degr.	$^{54}Fe(n,p)^{54}Mn$	$^{59}Co(n,\gamma)\ ^{60}Co$ + Cd
9.4	0.910	0.981
32	0.433	0.871
37	0.511	0.901
47	0.901	0.962
55.8	1.000	1.000

CONCLUSIONS

The scientific goal of the cooperation agreement has been reached and all tasks are fully completed.
On the basis of two ex-vessel experiments at Balakovo-3 and Rovno-3 reactors the reactor models for neutron transport calculations have been prepared. These models include:

- design description of VVER-1000 reactors
- description of the experiments
- azimuthal-radial geometrical approximation of reactors
- axial-radial geometrical approximation
- material composition of modelled zones
- nuclear concentrations of zones
- reactor operating data during the fluence detector irradiations (total power history, 2D assemblies power distributions, coolant temperature variations)
- descriptions of time-dependent fission sources:
    - 2D and 3D assemblies power distributions
    - 2D and 3D assemblies burnup distributions
    - 3D pin-to-pin power distributions of the peripheral assemblies
    - 3D pin-to-pin burnup distributions of the peripheral assemblies
    - heavy metal concentration in assemblies
    - burnup-dependence of neutron emission

The activation measurements of fluence detectors irradiated at ex-vessel positions of these reactors have been performed. The results of measurements include:

- specific end-of-irradiation activities
- specific reaction rates
- azimuthal distributions of neutron fluence
- axial distributions of neutron fluence
- evaluation of the spectral indexes in azimuthal directions

The analysis of ex-vessel neutron spectrum on the basis of spectral indexes evaluations has been made. It has been experimentally established that the neutron spectrum in the relation of the thermal, epithermal and fast neutrons differs in the azimuth of VVER-1000.

REFERENCES

1. G.I.Borodkin et al., *Pressure Vessel Fluence Monitoring at NPP with VVER: Routine Thechnique and New Approaches*, Proc. of 8th ASTM-EURATOM Symposium on Reactor Dosimetry, 29 Aug. - 3 Sep. 1993, Vail, Colorado, ASTM STP 1228, Harry Farrar IY et al., Eds., Philadelphia, 1994, pp.55-65

2. G.I.Borodkin and O.M.Kovalevich, *Interlaboratory VVER-1000 Ex-vessel Experiment at Balakovo-3 NPP*, Report on the 9th International Symposium on Reactor Dosimetry, 2 - 6 Sep. 1996, Prague, Czech Republic, Report E-147, 1996

3. G.I.Borodkin et al., *Neutron Flux Measurements Vicinity Pressure Vessel of the General Reactor of VVER-1000 Type*, In collected volume: Radiatsionnaya bezopasnost i zathchita AES, Moscow, ENERGOATOMIZDAT, 1987, Issue 12, p.10-12 (in russian)

A3

1. Zwischenbericht des RRC KI

"Increasing of the accuracy of the determination of neutron load of WWER-1000 reactor components to get additional information for a safer operation of reactors"

Preparation of Basic Data and Carrying out of First Test Calculations

Interim Report

E.B. Brodkin, A.L. Egorov, S.M. Zaritsky
Nuclear Reactors Institute RRC "Kurchatov Institute"

April 1996

1. BACKGROUND AND TARGET

The accurate determination of the neutron fluence in the WWER pressure vessel (PV) is a very actual problem from the point of PV safety guarantee.

The goal of the Project is carrying out calculations of neutron fluences by the data and codes using in Russia and comparison with the results of other calculations and measurements.

2. MILESTONES

This report is the first milestone in the Project.

The total schedule of milestones:
- Preparation of Basic Data and Carrying out of First Test Calculations, 15th April 1996.
- Completion of transport calculations for Balakovo-3, 15th October 1996.
- Completion of transport calculations for Rovno-3, 15th April 1997.
- Evaluation of results and comparison with other calculations, 15th October 1997.

In this first interim report we review the codes and data using in Russia (RRC Kurchatov Institute) and our experience in using them.

3. THE CODES AND CROSS SECTION LIBRARIES FOR MULTIGROUP CALCULATIONS OF NEUTRON TRANSPORT IN THE WWER PV DOSIMETRY

3.1. THE CODES FOR SOURCE AND NEUTRON TRANSPORT CALCULATIONS

For neutron transport calculations we use the discrete ordinates method realised in the codes ANISN, DOT, TORT .

The 3-dimensional distributions of the neutron flux in the vicinity and inside of the PV are calculated by the code TORT or - in the more simple cases - by the synthesis of 2- dimensional ($r\theta$, rz) and 1- dimensional calculations [1] by codes DOT and ANISN respectively.

The source distributions are calculated as a rule by the standard design codes like BIPR and PERMAK. Sometimes we use the data obtained from NPP too(the distributions of the fuel burn-up)

3.2. THE CODE AND DATA SYSTEM FOR PRERARATION OF CROSS SECTION LIBRARIES

The code system for preparation of cross sections libraries was developed by authors as a compilation of well known codes NJOY, AMPX, ANISN and DOT-3 adapted for NDP Fortran on IBM PC/AT. The 171-group library DLC-41/VITAMIN-C (with Bondarenko factors) based on the ENDF/B-4 is introduced to the system as a main data library. The modification and development of this library are realised by NJOY code on the base of ENDF/B-6 files. The 171-group problem-oriented data library is usually used in 1D calculations by the code ANISN. This library is being generated by the AMPX modules (BONAMI and others). Data libraries with smaller number of groups are being used in 2D calculations by DOT-3 and 3D calculations by TORT. The data in these libraries have been gotten from 171-group problem-oriented data which are averaged by corresponding spectra obtained from 1D calculations.

The cross section generation procedure is shown on Fig.1. The library DLC-41/VITAMIN-C, based on the ENDF/B-4, contains data for 66 nuclides, 3 temperatures, 5-6 dilution cross sections for each nuclide in AMPX Master Interface Format. The 171-group data for all isotopes of Cr, Fe, Ni and O-16 and H-1, based on ENDF/B-6 data, were added to the VITAMIN-C by NJOY code. It is used here the new module MIAML to transform CCCC format into AMPX Master format. The 171-group set of self-shielded cross sections for each nuclide mixture is being generated by the standard AMPX modules (AJAX, BONAMI, NITAWL) in ANISN format. These modules were adapted for NDP Fortran on IBM PC/AT.

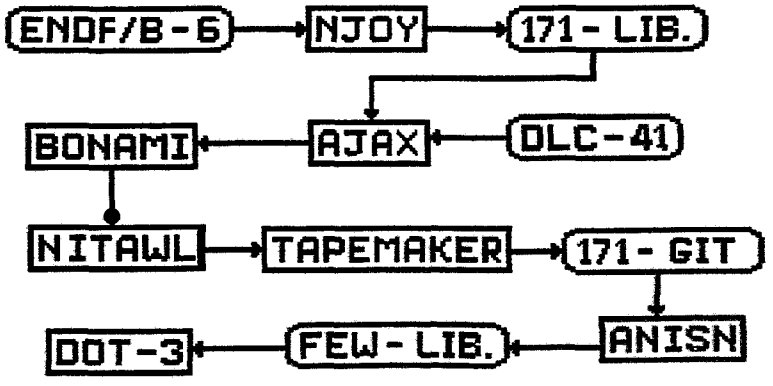

Fig.1. Cross sections generating procedure

4. THE EXAMPLES OF THE TEST CALCULATIONS

The several WWER mock-ups and benchmark experiments have been carried out during the last decade on LR-0 reactor for experimental validation of calculations of the WWER pressure vessel radiation load [2]. The code system, described above, was used to calculate the neutron spectra, measured in these experiments, and to choose the best cross sections for neutron transport calculations outside the core of the light water power reactors (WWER-440, 1000).

4.1. LEAKAGE SPECTRUM FROM IRON SPHERE

These calculations demonstrate the role of Fe cross-sections refining.

The calculations of the leakage spectra from the iron sphere (radius 25 cm), with central point californium-252 source were carried out using the 171-group Fe cross sections from ENDF/B-4 to ENDF/B-6. The ratio of ENDF/B-6 to ENDF/B-4 group fluxes on outer surface of iron sphere is shown on Fig. 2.

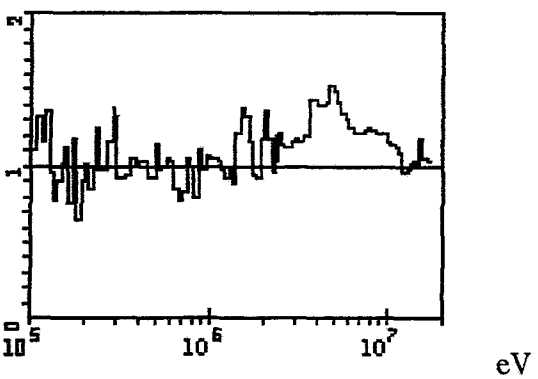

Fig.2. The ratio of ENDF/B-6 to ENDF/B-4 group fluxes on outer surface of iron sphere

Both calculations were carried out with the same source spectrum. The ratio depends only on the difference between Fe cross sections in ENDF/B-6 and ENDF/B-4 libraries. One can see that ENDF/B-6 increase the neutron penetration through the iron in comparison with the ENDF/B-4 in the energy region above 1 MeV. This effect correlate with the reducing of the inelastic cross section up to 13% in ENDF/B-6 in comparison with the ENDF/B-4 in the same energy region [3]. The ratios of some responses, calculated in the both leakage spectra, are presented in Table 1.

Table 1.

Ratios of Reaction Rates with ENDF/B-6 and ENDF/B-4 Iron Data

($RR = {}_0\int^{\infty} f(E) \cdot \sigma_R(E) dE$, where f(E)-neutron spectrum, $\sigma_R(E)$-response cross section)

RR	$^{27}Al(n,a)$	$^{63}Cu(n,a)$	$^{24}Mg(n,p)$	$^{27}Al(n,p)$	$^{46}Ti(n,p)$	$^{54}Fe(n,p)$
ratio	1.200	1.245	1.200	1.300	1.304	1.227
RR	$^{58}Ni(n,p)$	$^{47}Ti(n,p)$	$^{93}Nb(n,n')$	Flux>1MeV	Flux> 0.5MeV	
ratio	1.173	1.160	1.017	1.060	0.979	

One can see that the higher energy threshold in response the greatest response ratio. Ratios of integral fluxes above 1 and 0.5 Mev are smaller. The results of Table 1 also demonstrate increasing of high-energy neutrons penetration through the iron with ENDF/B-6 data. The integral flux above 0.5 MeV is changed insufficiently. So the ratios of the integral cross sections:

$$\sigma_R(E_0) = {}_0\int^{\infty} \sigma_R(E) * f(E) dE \; / \; {}_{E_0}\int^{\infty} f(E) dE,$$

calculated with ENDF/B-6 and ENDF/B-4 for E_0=0.5 MeV and all responses from Table 1 will be the same as the ratios of responses. The same responses are used in the power reactor pressure vessel dosimetry. If the form of neutron spectrum can be correctly calculated in the point of response measurement, the integral cross section and the integral flux can be calculated also correctly.

4.2 COMPARISON OF CALCULATED AND MEASURED BENCHMARK SPECTRA

The comparison of calculated and measured spectra for benchmark experiment is described here. The measurements have been carried out on the experimental reactor LR-0 [4]. The reactor core were composed of 19 WWER-1000 type cassettes. The neutron spectrum was measured in the dry channel of central cassette; in this cassette the fuel pins were replaced by the steel ones. The wrench size of cassette equal to 23.5 cm. The neutron spectrum in the channel has been formed by fission neutrons from core, penetrating through water-steel composition of central cassette. The benchmark core is given in the Fig.3. The steel to water volume ratio in the central cassette is equal to 0.5. The diameter of dry channel is 7.3 cm. The neutron spectrum is calculated in the cylindrical geometry, core and water-steel region are homogenised. The calculation has been carried out by code ANISN with 171 group libraries , based on the ENDF/B-4 and ENDF/B-6

data files. The ratio of ENDF/B-6 and ENDF/B-4 group fluxes in the experimental channel is shown in the Fig.4. In the energy range 1-8 MeV ratio do not exceed 1.06. This result is agreed with the preceeding data, as the amount of Fe is small in the region, where the neutron spectrum is formed.

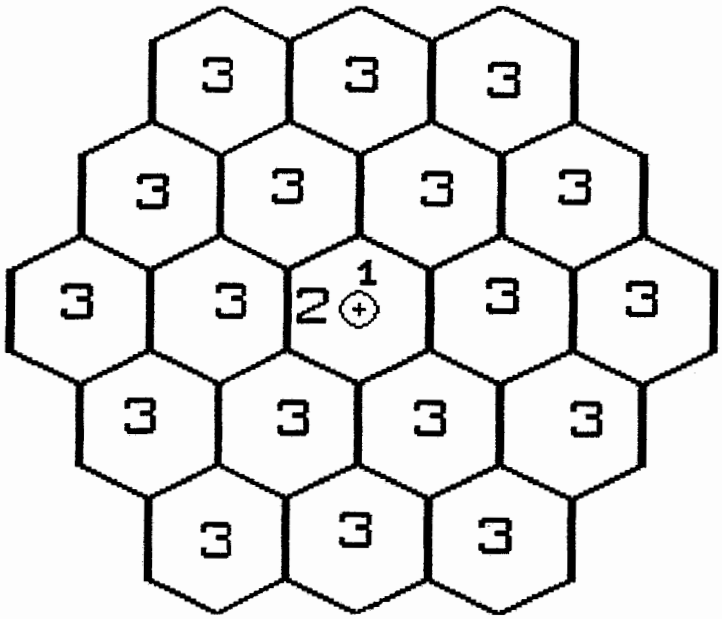

Fig.3. The Benchmark Core: 1-dry channel, 2-cassette with steel pins, 3-cassette with fuel pins

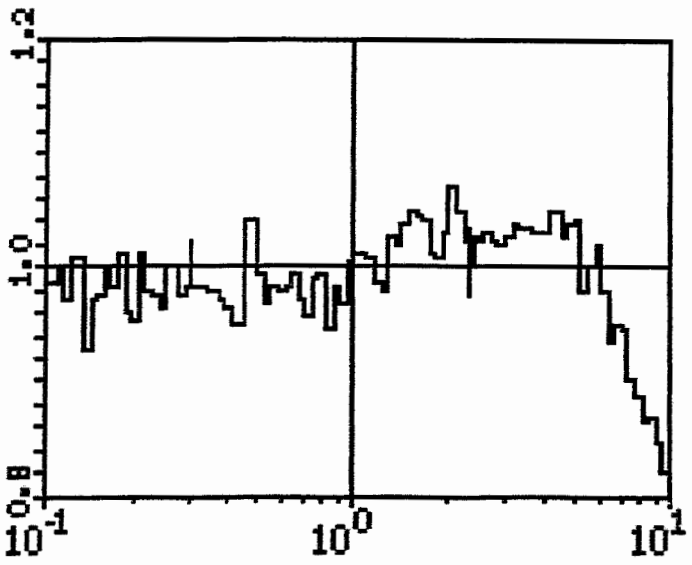

Fig.4 The Ratio of ENDF/B-6 to ENDF/B-4 Neutron Fluxes in the Benchmark

In the range above 8 MeV, the ratio is less than 1, as the ^{235}U fission spectrum from ENDF/B-4 library is harder than ENDF/B-6 spectrum.

The measured and the calculated (ENDF/B-6) spectra are given in the Fig.5. In the both cases integral flux above 1 MeV equal to 1. In the range under 2 MeV both spectra are likewise, above 3 MeV the measured spectrum is harder than the calculated one. The same correlation of the measured and calculated spectra is observed when some other cross sections libraries (SAILOR, DLC-23/CASK) are used for the calculation of the neutron spectrum.

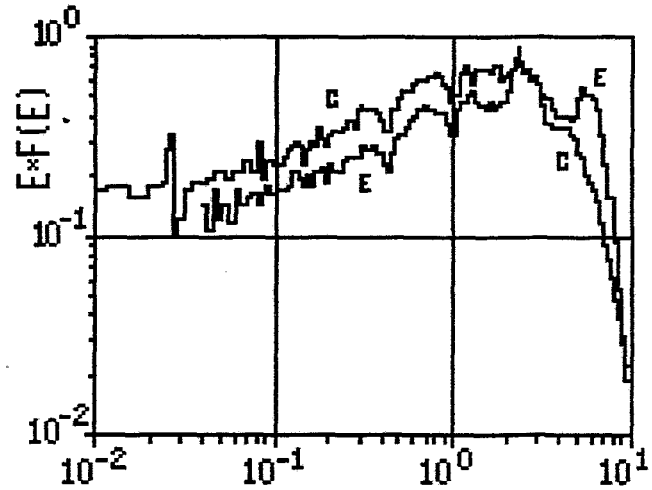

Fig.5. The measured (E) and calculated (C) neutron spectra in the benchmark experiment

The independent activation measurements give the possibility for the other comparison of the spectra in the energy range above 2 MeV. Some measured spectral indices and some spectral indices, calculated in different spectra, are given below.

The first two columns of Table 2 include data from [4]. The rest of them are calculated here using IRDF-90 activation cross sections, the measured spectrum from [4] (third column), and calculated spectra (columns 4-6). The measured spectrum consists of the results of two different measurements: by the stilbene spectrometer (fast part) and by the hydrogen chamber. There is a discrepancy between the hydrogen chamber and stilbene detector in energy range below 2 MeV. The presented in [4] stilbene spectrum above approximately 2 MeV and measured spectral indices seem to be consistent- except the Ni and Ti cases. The "best" calculated spectrum do not correlate with the measured spectral indices for Mg and especially AlP. This discrepancy depends on the unusual maximum in the measured spectrum in the range approximately 4.5-7.0 Mev (see Fig.5). This

maximum is not seen in the calculated spectrum. As all indices are normed on the high- energy-

Table 2.

The Comparison of the Spectral Indices.

	measured spectral indices		calculated spectral indices			
Spectral indices	exp. ratio	uncert.[%]	exp. spectrum	calculated spectra		
				b4-b4	b4-b6	b6-b6
Ni/Al[a]	116.63	5.5	105.41	98.88	110.13	114.06
Mg/Al[a]	2.3035	8.0	2.33	2.077	2.1	2.1
Fe/Al[a]	83.544	6.0	82.29	74.86	83.24	86.28
Ti/Al[a]	24.161	12.0	20.94	20.86	23.29	24.11
Al[p] /Al[a]	5.5109	6.0	5.57	4.112	4.434	4.558

Notes: Al[a] - ^{27}Al(n,α), Ni- ^{58}Ni(n,p), Mg- ^{24}Mg(n,p), Fe- ^{54}Fe(n,p), Ti- ^{47}Ti(n,p), Al[p] - ^{27}Al(n,p); b4-b4 : first index-cross section data, second index - ^{235}U fission spectrum data.

threshold reaction ^{27}Al(n,α), we calculated the ratio of this response in the measured spectrum to the same value in calculated spectrum. This ratio is equal to 1.4-1.6 for various calculated spectra. The increasing of the response ^{27}Al(n,α) as 1.2 is observed (see Table 1) in the leakage spectrum from the iron sphere, when the Fe cross sections from ENDF/B-4 are replaced by ENDF/B-6. The benchmark spectrum is formed by the cylindrical water-steel layer (volume ratio 2) with the thickness approximately 10 cm. The influence of the various cross section data on the form of neutron spectrum in this case is small. The differential measurements have unkwown error in the energy range above 9 MeV and approximately 20% in range 8-9 MeV.

At the same time the measured spectral index Al^{p}/Al$^{\alpha}$, equal to 5.51, correlates with the one calculated in the measured spectrum (5.57) and exceeds the same index in calculated spectrum (4.56) on 17.2% (1σ of the measured index is equal to 6%). So this analysis does not give a good agreement with the measurements as with the ENDF/B-4 as the ENDF/B-6 nuclear data. The reason of this discrepancy is unknown.

4.3 COMPARISON OF CALCULATED AND MEASURED NEUTRON SPECTRA IN WWER-440 MOCK-UP EXPERIMENT

The measurements of neutron spectra have been carried out in the WWER-440 mock-up in LR0 reactor shown in Fig.6.

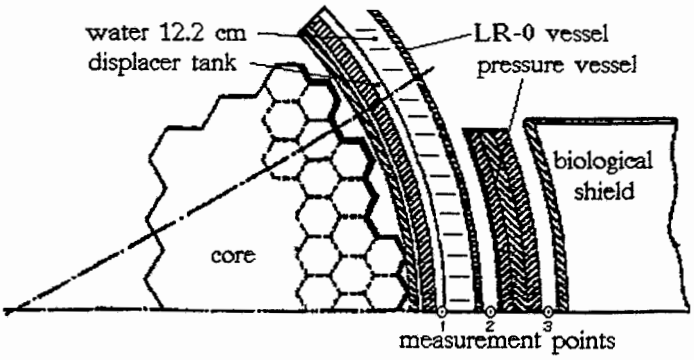

Fig.6. The WWER-440 mock-up in LR0 reactor

The measured and calculated spectra are shown in Fig.7 (1D calculation). These spectra are normalized to flux above 1 MeV in the inner surface of PV (point 2).

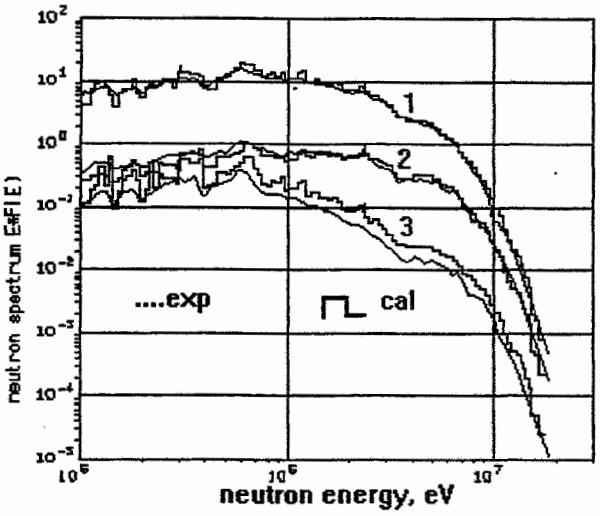

Fig.7. The measured and calculated neutron spectra in WWER-440 mock-up on LR0 reactor: 1- surveillance position; 2- inner surface PV; 3 - outer surface PV

Analysis of impact of nuclear data choice (ENDF/B-4 or ENDF/B-6) on the calculated spectrum and comparison with the measured spectrum were done on 1D model in direction of spectrometer location. The thickness of

the water gap between core and basket was taken equal to 2 cm. In each point the spectra have been normalized to flux above 0.5 MeV. The ratios of measured to calculated (ENDF/B-6 and ENDF/B-4) group fluxes in 3 points of WWER-440 mock-up are shown in the Fig.8.

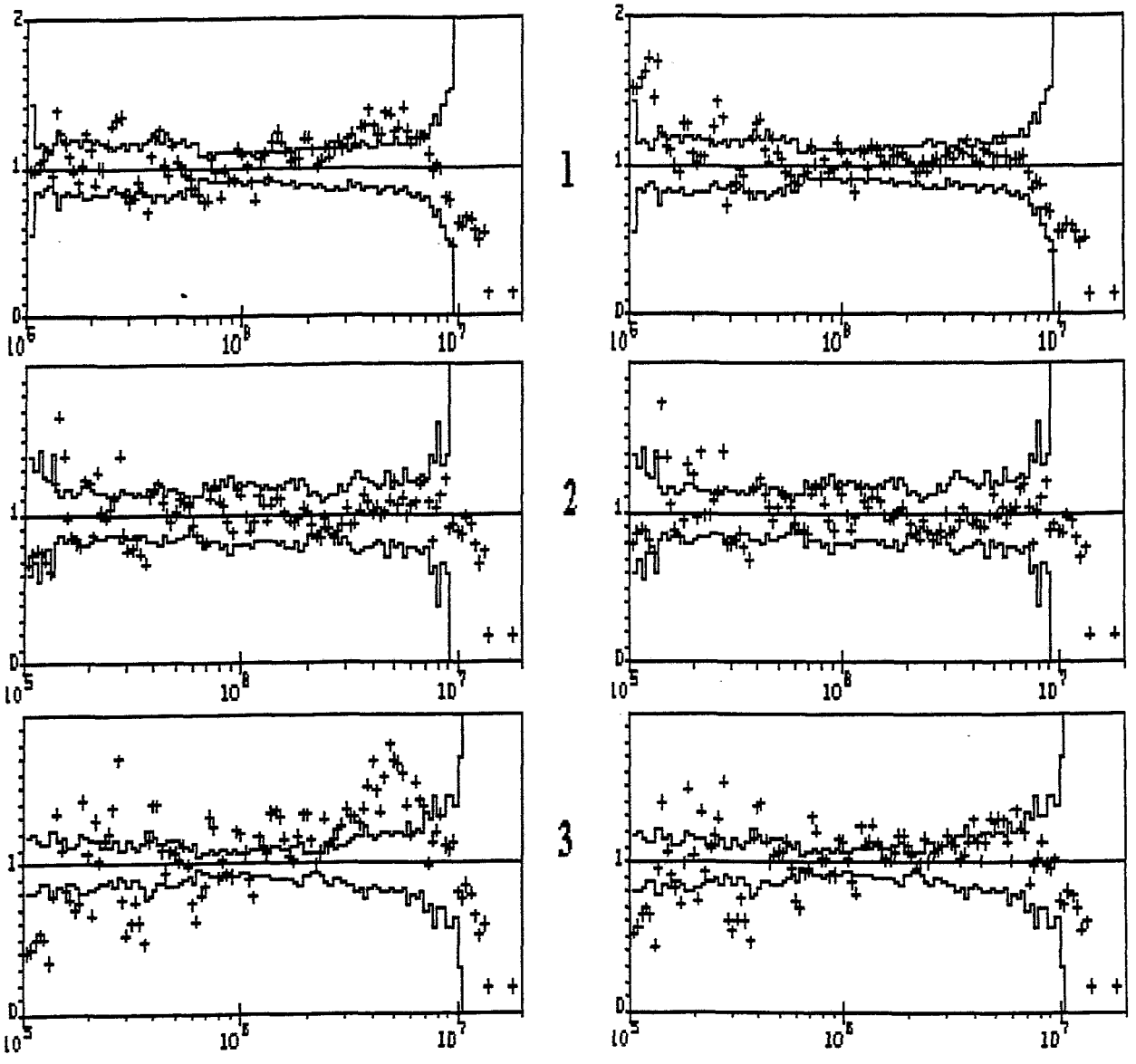

fig.8. Ratios of Measured to Calculated Spectra (+++)

The consistent measurements in the WWER-1000 mock-up and corresponding benchmark formulation are in progress now and we are planning to do the respective calculations. The first attempts were done earlier and the preliminary results are summarized in [2]. In some cases the calculation to experimental ratios were too great.

5. THE EXPERIENCE IN THE NPP TEST CALCULATIONS

The test calculations were carried out for the 4th fuel cycle of Khmelnitsky NPP (Ukraine); during this cycle some measurements on the outer side of PV were carried out.

The main attention was payed to the calculation of the neutron source in the core by the codes BIPR-7 and PERMAK-360. B. The old data library DLC-23/CASK was used in the neutron transport calculations (this data library was used in design calculations of WWER-1000 by general designer).

The preliminary comparison of calculated and measured results showed some discrepancies.

Some other calculations were carried out for South Ukraine NPP and for other NPPs WWER-1000. All these calculations were developed using old data libraries DLC-23/CASK and synthesis of the 2D and 1D neutron flux distributions.

We are going to use modernised data and methods in the calculations, which have been planned in frame of this Project.

It seems to us that these calculations for Balakovo and Rovno NPP, mentioned in p.2 must be carried out for the period, when the activation measurements were created on the outer surface of PVs. In this case we'll have the opportunity for the broad comparisons of experimental and various calculational results.

It would be more convenient if the first calculations will be carried out for the Rovno (but not for the Balakovo) NPP.

The results presented above and some others ones connected with the WWER PV dosimetry problem can be find in the references [2, 5-9].

REFERENCES

1. E.B. Brodkin, A.V. Khrustalev. "Determination of Characteristics of the Neutron Field Affecting the WWER Reactor Vessel", Proc. of the 6th Int. Conf. on Radiation Shielding, 1983, Tokyo, CONF-850538, Vol.2, pp. 1055-1060.
2. S.M. Zaritsky, B. Osmera. Review of Theoretical and Experimental Investigations of VVER Pressure Vessel Radiation Damage in Engineering Benchmarks. Proc. of Int. Conf. on Reactor Physics and Reactor Computations, Tel Aviv, Israel, January 23-26,1994, pp. 757-765.
3. M.L. Williams et al., Transport Calculations of Neutron Transmission Through Steel Using ENDF/B-5, Revised ENDF/B-5, and ENDF/B-6 Iron Evaluations, NUREG/CR-5648, ORNL/TM-11686, Oak Ridge National Laboratory, Louisiana State University Nuclear Science Center, April 1991.
4. B.Osmera, C.Svoboda., The LR-0 Reactor Benchmark - Description and Results. Nuclear Research Institute, Rez, Czech Republic, 1992 (The work was sponsored by International Atomic Energy Agency, Vienna, under contract N^{o} 5964/RB).
5. E.B. Brodkin, A. L. Egorov, S.M. Zaritsky. The PC/AT Software for Multigroup Calculations of Neutron Transport by Discrete Ordinates and ENDF/B Data Files. Proc. of Int. Conf. on Reactor Physics and Reactor Computations, Tel Aviv, Israel, January 23-26, 1994, pp. 657-663.
6. E. B. Brodkin, A. L. Egorov. Calculated Neutron Spectra and Responses in the Pressure Vessel of a WWER-440 Using ENDF/B-4 and ENDF/B-6. Evaluations and Comparison with the Measured Spectra in WWER-440 Mock-up. Proc. of 8th Inter.Conf. on Radiation Shielding, Arlington, Texas, April 24-28, 1994, pp. 694-698.
7. E.B. Brodkin, A. L. Egorov, S.M. Zaritsky, G.I. Borodkin. The Neutron Fluence Monitoring System for VVER-1000 Pressure Vessel and its Validation. Radiation Protection & Shielding Topical Meeting, April 21-25, 1996, No. Falmouth, Mass., USA.
8. E.B. Brodkin, A. L. Egorov, V.I. Vikhrov, S.M. Zaritsky. The Determination of the VVER-1000 Surveillance Neutron Fluence Using the ^{54}Mn Activity Measurements and TORT Neutron Spectra Calculations. Radiation Protection & Shielding Topical Meeting, April 21-25, 1996, No. Falmouth, Mass., USA.
9. A.M. Pavlovichev, S.M.Zaritsky, L.L. Dadakina. Estimation of the Fast Neutron Flux Density Distribution on the Inner Surface of VVER Pressure Vessel in Frame of the Fuel Loading Optimization. Radiation Protection & Shielding Topical Meeting, April 21-25, 1996, No. Falmouth, Mass., USA.

A4

2. Zwischenbericht des RRC KI

"Increasing of the accuracy of the determination of neutron load of WWER-1000 reactor components to get additional information for a safer operation of reactors"

Completion of Transport Calculations for Rovno-3

Interim Report

E.B. Brodkin, A.L. Egorov , S.M. Zaritsky
Nuclear Reactors Institute RRC "Kurchatov Institute"

October 1996

1. INTRODUCTION

The accurate determination of neutron fluence in the WWER pressure vessel (PV) is necessary for the ensuring PV safety. The goal of the Project is carrying out calculations of neutron fluences by codes and data usually used in Russia and comparison of results with alternative calculational results and experimental ones with the aim to increase the accuracy of the determination of neutron load of WWER-1000 reactor components.

This report is the second milestone in frame of the Project.

The total schedule of milestones:

- Preparation of basic data and carrying out of the first test calculations, April 15, 1996
- Completion of transport calculations for Rovno-3, October 15, 1996.
- Completion of transport calculations for Balakovo-3, April 15, 1997.
- Evaluation of results and comparison with other calculations, Oct.15, 1997.

In this 2nd interim report we review the results of transport calculations and comparisons of calculational and experimental reaction rates obtained for Rovno NPP unit 3.

2. THE CALCULATIONAL METHOD

The all WWER-1000 units, operated in Russia, Ukraine and Bulgaria (except Novo-Voronezh unit 5), have the same construction of the core and in-vessel components -see Fig.1.

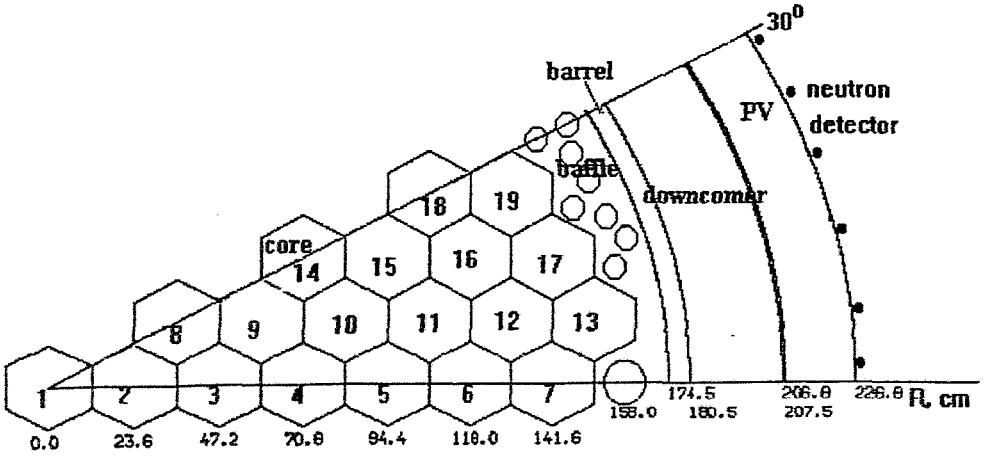

Fig 1. The horizontal section of WWER-1000 30° symmetry sector

The fuel assemblies in the core differ in enrichment and burnup, but the fast neutron transport across the core is independent on the core status. So it can calculate in advance the contribution of each fuel assembly to neutron flux and evaluate the neutron fluence distribution in the PV during the fuel cycle [1,2]:

$$F(r,\theta,z)=k\times\sum_i q_i f_i(r,\theta,z) \qquad (1)$$

where i - assembly index, $f_i(r,\theta,z)$ - neutron flux caused by i-assembly with unity source, q_i - relative source in i-assembly averaged in a one fuel cycle, k - normalisation multiplier, $F(r,\theta,z)$ -neutron fluence in a one cycle. The synthesis procedure is used to obtain 3-D $f_i(r,\theta,z)$ distributions by combining r-θ, r-z (code DOT-3) and r (code ANISN) calculations [3,4]:

$$f(r,\theta,z) = f(r,\theta)\times[f(r,z)/f(r)]. \qquad (2)$$

We propose to use the increment of assembly burn-up in one cycle (obtained from NPP operation data) as a source q_i.

The SAILOR-like cross section library was used in the DOT and ANISN transport calculations. This library was produced using corresponding WWER-1000 zone-wise spectra to collapse cross sections from the 171 group library VITAMIN-C for all nuclides except Fe, Cr and Ni isotopes (the Fe, Cr and Ni cross sections were collapsed from ENDF/B-VI data files).

The contributions of two outer rows of assemblies (assemblies 6, 7, 12, 13, 16, 17, 18, 19, see Fig.1) to fluence was calculated within PV (from inner to outer surface). The contributions of the same assemblies to neutron spectrum was also calculated for inner surface, 1/4 PV thickness and outer surface. The relative contributions of 8 outer assemblies to fluence on the PV inner surface is presented in the Table 1.

Table 1.

The relative contributions of 8 outer assemblies to neutron fluence at inner surface of WWER-1000 PV

θ^o\N^{ass}	6	7	12	13	16	17	18	19	total
0	0.005	0.103	0.039	0.786	0.005	0.053	0.0	0.003	0.994
5	0.005	0.079	0.037	0.789	0.005	0.075	0.001	0.006	0.997
10	0.004	0.045	0.035	0.723	0.009	0.161	0.001	0.018	0.996
15	0.003	0.026	0.035	0.532	0.016	0.311	0.003	0.068	0.994
20	0.002	0.013	0.030	0.275	0.026	0.418	0.010	0.222	0.996
25	0.001	0.005	0.019	0.102	0.035	0.325	0.021	0.490	0.998
30	0.001	0.003	0.012	0.042	0.037	0.221	0.027	0.656	0.999

The contribution of other fuel assemblies (besides of 8 outer assemblies, see Fig.1 and Table 1) is less than 0.6%. Note that using of burn-up increasing as source implies using of average flux in a one cycle for evaluation of neutron fluence.

3. CALCULATIONAL RESULTS AND COMPARISON WITH EXPERIMENTAL DATA

To validate the methodology we used the data obtained from activation experiments [5] performed outside PV on Rovno NPP unit 3 during 6 and 7 fuel cycles separately. The rates of next reactions were measured : $^{54}Fe(n,p)$, $^{58}Ni(n,p)$, $^{63}Cu(n,\alpha)$, $^{60}Ni(n,p)$, $^{237}Np(n,f)$, $^{238}U(n,f)$. The $^{237}Np(n,f)$ and $^{238}U(n,f)$ detectors were covered with Cd. Detectors were located at several azimuthal and axial positions on the outer surface of PV. The angle and the axial positions of detectors were different in two cycles. The power history was used for saturated RR evaluation from measured activations.

Initial and final fuel burn-up (MW•days/kgU) for outer assemblies in 6th and 7th cycles are shown in the Fig. 2, 3.

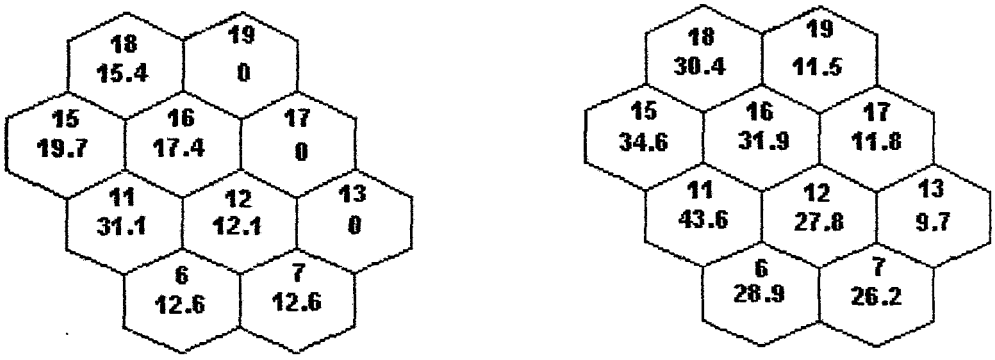

Fig.2. Initial and final fuel burn-up (MW•days/kgU) for outer assemblies in 6th cycle

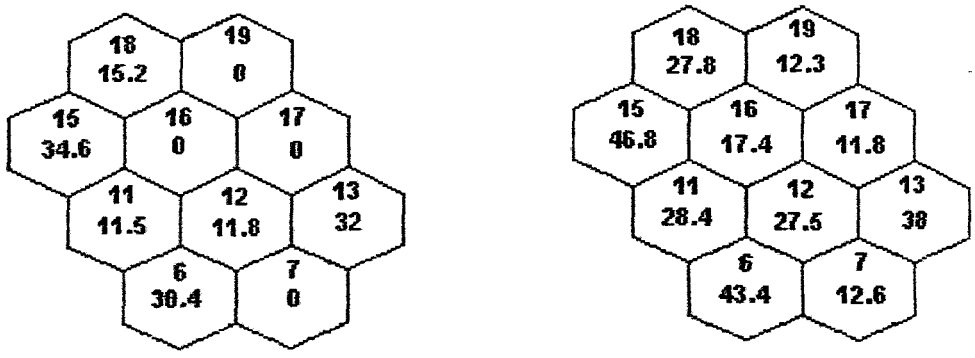

Fig.3. Initial and final fuel burn-up (MW•days/kgU) for outer assemblies in 7th cycle

Calculated reaction rates (RR) were obtained by direct calculation as well as by calculation using assemblies contributions to neutron flux on the outer surface of PV:

$$RR(r_o,\theta,z) = k \times \sum_i q_i \sum_g f_{i,g}(r_o,\theta,z) \times \sigma_g \qquad (3)$$

where r_0 is radius of the PV outer surface, σ_g - cross section of reaction for g energy group (IRDF-90, Rev.1), $f_{i,g}(r_o,\theta,z)$ contribution of i-assembly to flux in g energy group. Calculational RR values, obtained directly and with equation (3), are differed by less than 2%.

The azimuthal distributions of ^{54}Fe(n,p) RR (Bk / atom) in cavity for 6 cycle (z=129 cm from lower core level) and for 7 cycle (z=149 cm) are shown in the Tables 2, 3.

Table 2.

The azimuthal distribution of ^{54}Fe(n,p) reaction rate (Bk / atom) in cavity for 6 cycle (z=129 cm from lower core level , total core height 355 cm).

θ^o	1	4	7	9	12	23	27	28
calc	1.12-16	1.15-16	1.14-16	1.14-16	1.10-16	6.13-17	5.33-17	5.24-17
exp	1.00-16	1.02-16	1.03-16	1.00-16	9.36-17	5.11-17	4.48-17	4.35-17
c/e	1.12	1.13	1.11	1.14	1.18	1.20	1.19	1.20

Table 3.

The azimuthal distribution of ^{54}Fe(n,p) reaction rate (Bk / atom) in cavity for 7th cycle (z=149 cm from lower core level , total core height 355 cm).

θ^o	1	5	6	9	12	23	27	28
calc	8.06-17	8.36-17	8.38-17	8.55-17	8.54-17	5.67-17	5.10-17	5.04-17
exp	7.54-17	7.78-17	7.78-17	7.97-17	7.75-17	4.70-17	4.42-17	4.20-17
c/e	1.07	1.07	1.08	1.07	1.10	1.21	1.15	1.20

Maximum value of ^{54}Fe(n,p) RR in 6 cycle exceeds the same in 7 cycle of 1.33 times as burnup increment in 13 assembly(80% contribution to fluence) differs of 1.62 in these cycles. Maximum fluence (neutrons with energy above 0.5 MeV) on inner surface of PV is 1.25E+18 n/cm^2 in 6th cycle (289. 36 days, average flux 5.0E+10 n/cm^{2}s) and 9.2E+17 n/cm^2 in 7th cycle (294.95 days, average flux 3.6E+10 n/cm^{2}s).

The calculational and experimental axial distributions of ^{54}Fe(n,p) RR are compared in the Tables 4 and 5.

Table 4.

The axial distribution of ^{54}Fe(n,p) reaction rate in cavity (6th cycle, $\theta=4^{o}$).

H,cm	c	e	c/e
39	9.0-17	8.06-17	1.12
99	1.14-16	1.02-16	1.12
129	1.15-16	1.02-16	1.13
143	1.15-16	9.91-17	1.16
164	1.14-16	9.89-17	1.15
339	6.42-17	6.85-17	0.94

Table 5.

The axial distribution of ^{54}Fe(n,p) reaction rate in cavity (7th cycle, $\theta=23^{o}$).

H,cm	c	e	c/e
119	5.68-17	4.56-17	1.25
149	5.67-17	4.70-17	1.21
184	5.63-17	4.77-17	1.18
241	5.51-17	4.69-17	1.17
302	4.75-17	4.14-17	1.15

The azimuthal and axial distributions of this RR are also shown in the Fig. 4 and 5.

The comparison of different calculational and experimental RR in the three detector locations are presented in the Tables 6-8 for 6-th cycle.

Table 6.

Different RR in the cavity
at height 129 cm and $\theta=28^{o}$ for 6th cycle.

RR	c	e	sd(%)	c/e
54Fe(n,p)	5.24-17	4.35-17	5.4	1.20
237Np(n.f)	3.62-15	4.50-15	8.5	0.80
238U(n,f)	2.86-16	2.94-16	7.8	0.97
58Ni(n,p)	7.41-17	6.08-17	5.4	1.22
60Ni(n,p)	2.45-18	2.59-18	6.6	0.95
63Cu(n,α)	6.92-19	5.51-19	6.6	1.26

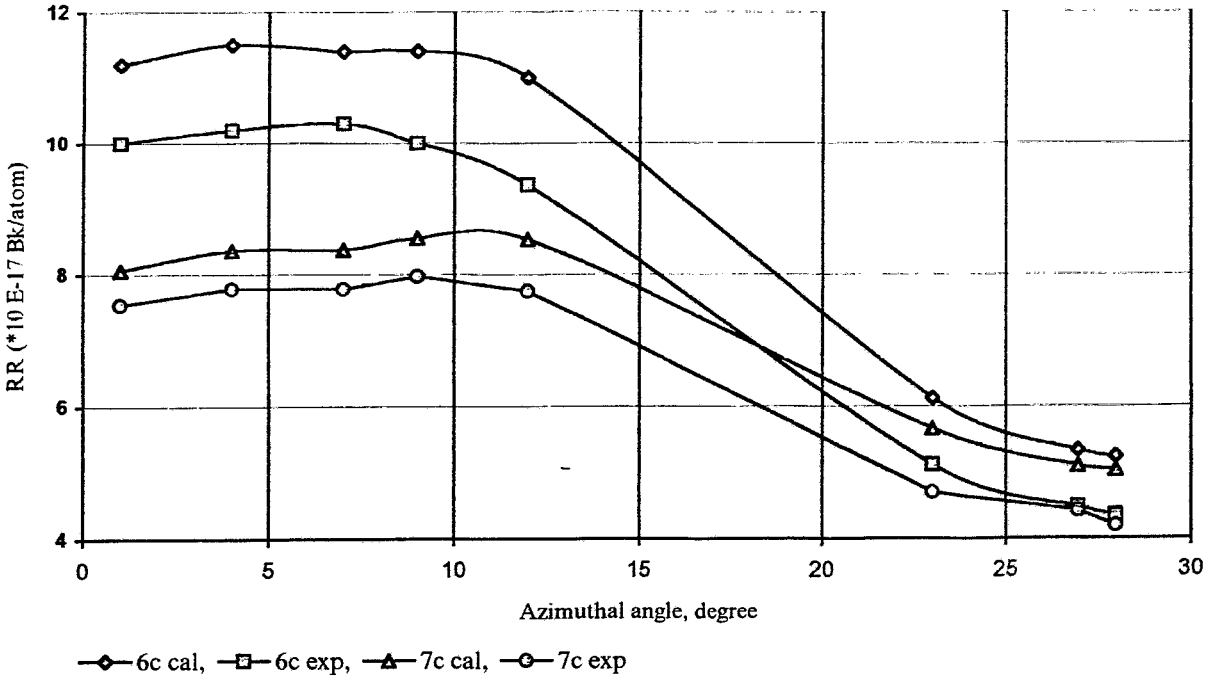

Fig. 4. The azimuthal distribution of ^{54}Fe (n,p) reaction rate

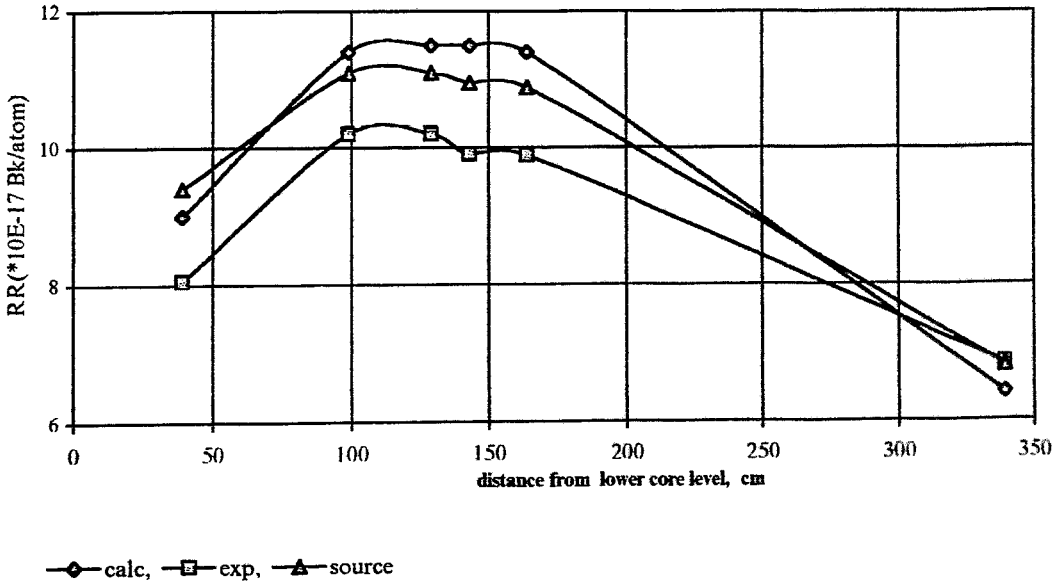

Fig. 5. Axial distribution of ^{54}Fe (n,p) RR in cavity, 6th cycle

Table 7.

Different RR in cavity at height 129 cm and $\theta=4^{o}$ for 6th cycle.

RR	c	e	c/e
54Fe(n,p)	1.15-16	1.02-16	1.13
237Np(n.f)	6.88-15	8.86-15	0.78
238U(n,f)	6.08-16	6.29-16	0.97

Table 8.

Different RR in cavity at height 164 cm and $\theta=4^{o}$ for 6th cycle.

RR	c	e	c/e
54Fe(n,p)	1.14-16	9.89-17	1.15
58Ni(n,p)	1.60-16	1.43-16	1.12
60Ni(n,p)	5.19-18	5.40-18	0.96
63Cu(n,α)	1.46-18	1.20-18	1.22

The comparison of different RR for 7th cycle are presented in the Tables 9-11.

Table 9.

Different RR in cavity at height 149 cm and $\theta=1^{o}$ for 7th cycle.

RR	c	e	c/e
54Fe(n,p)	8.07-17	7.54-17	1.07
58Ni(n,p)	1.13-16	1.02-16	1.12
237Np(n,f)	4.92-15	6.43-15	0.77

Table 10.

Different RR in cavity at height 149 cm and $\theta=5^{o}$ for 7th cycle.

RR	c	e	c/e
54Fe(n,p)	8.36-17	7.78-17	1.07
58Ni(n,p)	1.17-16	1.05-16	1.11
63Cu(n,α)	1.08-18	1.09-18	0.99

Table 11.

Different RR in cavity at height 149 cm and $\theta=28^{O}$ for 7th cycle.

RR	c	e	c/e
54Fe(n,p)	5.04-17	4.20-17	1.20
58Ni(n,p)	7.10-17	5.68-17	1.25
63Cu(n,a)	6.79-19	5.89-19	1.15
237Np(n,f)	3.28-15	4.32-15	0.76

We didn't evaluate the uncertainties of our calculational results, but typically they are equal to 15-25% (standard deviation) for different RR [6], including contributions from the next sources: cross section data, dimensions, material compositions, space distribution of source, fission spectrum, detector location etc. The standard deviations of the experimental data are included in Table 6.

In general the calculated RR for non fissionable detectors are greater than the measured ones up to 25% excluding ^{60} Ni(n,p). Otherwise the RR for both fissionable detectors are under predicted in calculations by a maximum factor of 0.78 for ^{237}Np(n,f). We calculated possible increasing of RR for fissionable detectors due to photofission. Calculation of photofission effect was carried out in 1D geometry using 47 neutron & 20 gamma groups library. Results are in the Table 12.

Table 12.

Gamma spectrum, (γ,f) cross section, neutron and gamma fission RR in cavity from 1D calculation.

Ngr gamma	Eup MeV	flux, γ/cm^2 s	σ(γ,f) ^{237}Np, b	σ(γ,f) ^{238}U, b
1	14	1.96+5	2.06-1	1.11-1
2	10	3.46+8	5.51-2	3.40-2
3	8	9.57+8	3.15-2	1.16-2
4	7	4.29+8	1.65-2	5.87-3
5	6	4.98+8	4.17-3	1.51-3
6	5	6.27+8	6.67-6	2.29-6
RR(γ,f), Bk/atom			5.84-17	2.62-17
RR(n,f), Bk/atom			5.04-15	3.36-16
RR(γ,f)/ RR(n,f)			0.012	0.078

The evaluated increasing of $^{237}Np(n.f)$ and $^{238}U(n,f)$ RR are equal to 1% and 8% respectively. In the case of ^{237}Np the underprediction is not compensated.

4. CONCLUSIONS

There are significant discrepancies between calculational and experimental data.

The over prediction of RR by calculation may be partly caused by using of flat source distribution within each outer fuel assembly. Pin-to-pin source distribution does not access from operation data but such source could be calculated.

In any case the analysis of discrepancies, including the evaluation of uncertainties in calculational results, have to be continued.

REFERENCES

1. E.B.Brodkin, A.L.Egorov, S.M.Zaritsky, G.I.Borodkin. The Neutron Fluence Monitoring System for WWER-1000 Pressure Vessel and its Validation. Radiation Protection and Shielding Topical Meeting, April 21-25, 1996, No. Falmouth, Mass., USA
2. A.M.Pavlovichev, S.M.Zaritsky, L.L.Dadakina. Estimation of the Fast Neutron Flux Density Distribution on the Inner Surface of WWER Pressure Vessel in Frame of the Fuel Loading Optimization. Radiation Protection and Shielding Topical Meeting, April 21-25, 1996, No Falmouth, Mass., USA.
3. E.B.Brodkin, A.V.Khrustalev. Determination of Characteristics of the Neutron Field Affecting the WWER Reactor Vessel. Proc. of the 6th Int. Conf. on Radiation Shielding, 1983, Tokyo, CONF-850538, Vol.2, pp. 1055-1060.
4. Kam et al., Pressure Vessel Analysis and Neutron Dosimetry, ORNL/TM-10651, Oak Ridge National Laboratory (Nov. 1987)
5. G.I.Borodkin et al., Pressure Vessel Fluence Monitoring at NPP with WWER: Routine Technique and New Approaches. Proc. of the 8th ASTM-EURATOM Symposium on Reactor Dosimetry, Vail, Colorado, Aug.29-Sept. 3, 1993, ASTM STP 1228, Philadelphia, 1994, pp. 55-65.
6. Alan Avery et al, Calculations of Pressure Vessel Fluence in PWR's Using ENDF/D-VI Data. Proc. of the 8th Int. Conf. on Radiation Shielding, Arlington, Texas, April 24-28, 1994, ANS, pp. 677-685.

A5

3. Zwischenbericht des RRC KI

"Increasing of the accuracy of the determination of neutron load of WWER-1000 reactor components to get additional information for a safer operation of reactors"

Completion of Transport Calculations for Balakovo-3

Interim Report

E.B. Brodkin, A.L. Egorov , S.M. Zaritsky
Nuclear Reactors Institute RRC "Kurchatov Institute"

April 1997

1. Background and Target

The accuracy determination of neutron fluence in the WWER pressure vessel (PV) is a very actual problem from the point of PV safety guarantee. The goal of the Project is carrying out neutron transport calculations of neutron fluence using Russian data and calculation codes to provide the increasing of the accuracy of the determination of neutron load of WWER-1000 reactor components to get additional information for a safer operation of reactors.

2. Milestones

This work is the third milestone in the Project.
The total schedule of milestones:
2.1 Preparation of Basic Data and Carrying out of First Test Calculations.
2.2 Completion of transport calculations for Rowno-3, 15th October 1996.
2.3 Completion of transport calculations for Balakovo-3, 15th April 1997.
2.4 Evaluation of results and comparison with other calculations 15th Oct. 1997.
In this 3rd interim report we review the results of transport calculations and comparisons with measured reactions rates for Balakovo-3 and the updated results for Rovno-3.

3. INTRODUCTION

The determination of neutron fluence on the inner surface and 1/4 thickness of VVER-1000 PV is performed by calculational method using modern codes and library cross sections. The validation of calculation method is performed by the comparison of ex-vessel measured reaction rates Vs corresponding computed ones because installation of detectors on the inner surface is not possible.

4. THE CALCULATION METHOD

The synthesis procedure is used to obtain 3-D flux distributions by combining r-θ, r-z and r calculating results : $f(r,\theta,z)=f(r,\theta) \times [f(r,z)/f(r)]$.[1,2] The calculation of $f(r,\theta)$, $f(r,z)$, $f(r)$ is conducted by multigroup discrete ordinate codes ANISN (1d) and DOT (2d). The 3d code TORT can be used for calculation directly but it needs too much computer time. To date the method Monte Carlo is used by others scientists also.
The core of VVER-1000 in plane section has 60° sector of rotate symmetry. The reflect symmetry on direction of 30° takes place within 60° sector usually. Therefore 30° sector of core is used in r-θ geometry calculation. The fuel cassettes and pins is arranged in the VVER-1000 core by hexagon lattice with steps 23.6 and 1.275 cm correspondingly. The cassette contains 312 pins. Reactor codes compute cassette and pin power distribution,

which is used as neutron source distribution in the core for calculation of neutron spectra off the core at the various constructions as baffle, barrel and pressure vessel.
The increment of burn-up in one cycle or average power by each assembly from NPP exploitation data are used as neutron source distribution in the core for fluence calculation. The special code was developed for interpolation of reactor power distribution to source distribution in r-θ grid covering 30° sector of core for DOT calculation.

The BUGLE-93 [3] cross section library was used in the DOT and ANISN transport calculations. This library was produced using corresponding PWR zone wise spectra to collapse cross sections from the 199 group library VITAMIN-B6 based on ENDF/B-VI data files.

5. THE COMPARISON WITH EXPERIMENTAL DATA AT THE BALAKOVO-3 NPP

The measurements of neutron activation detectors were carried out in different azimuthal and axial ex-vessel position at the Balakovo NPP Unit 3 during 5th cycle [4]. Location of detectors in plane and assembly power distribution are shown in Figs 1,2.

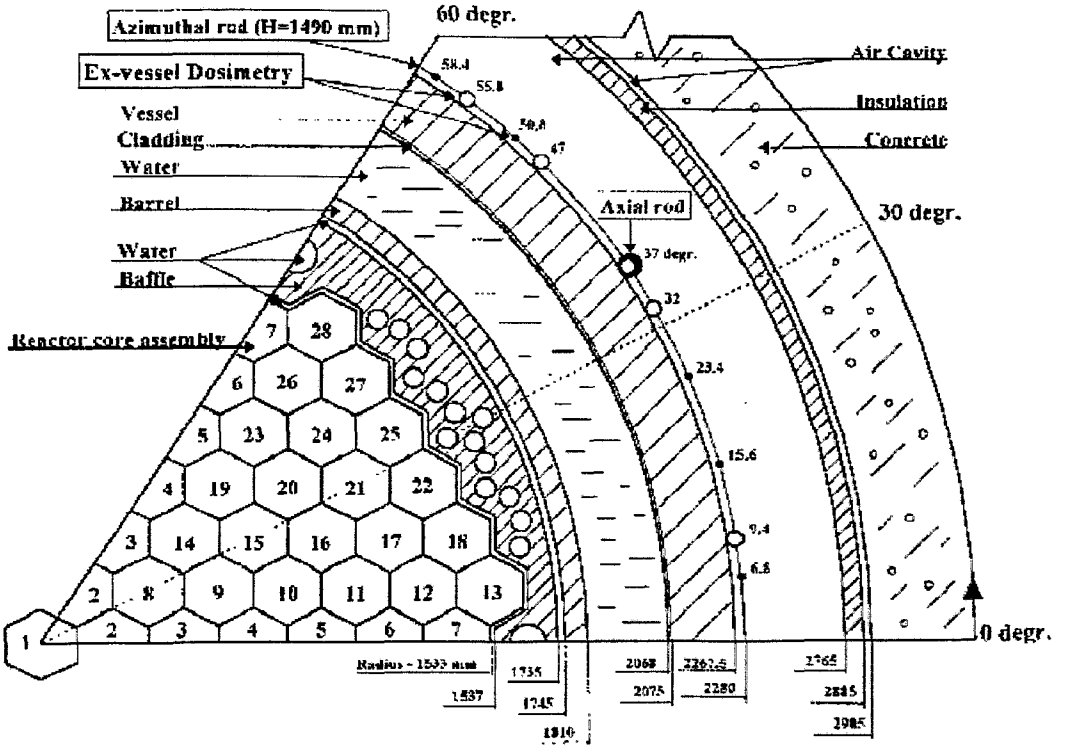

Fig.1. The plane section of 60° sector of VVER-1000 and locations of detectors (o-capsule, • - Fe-54 monitor)

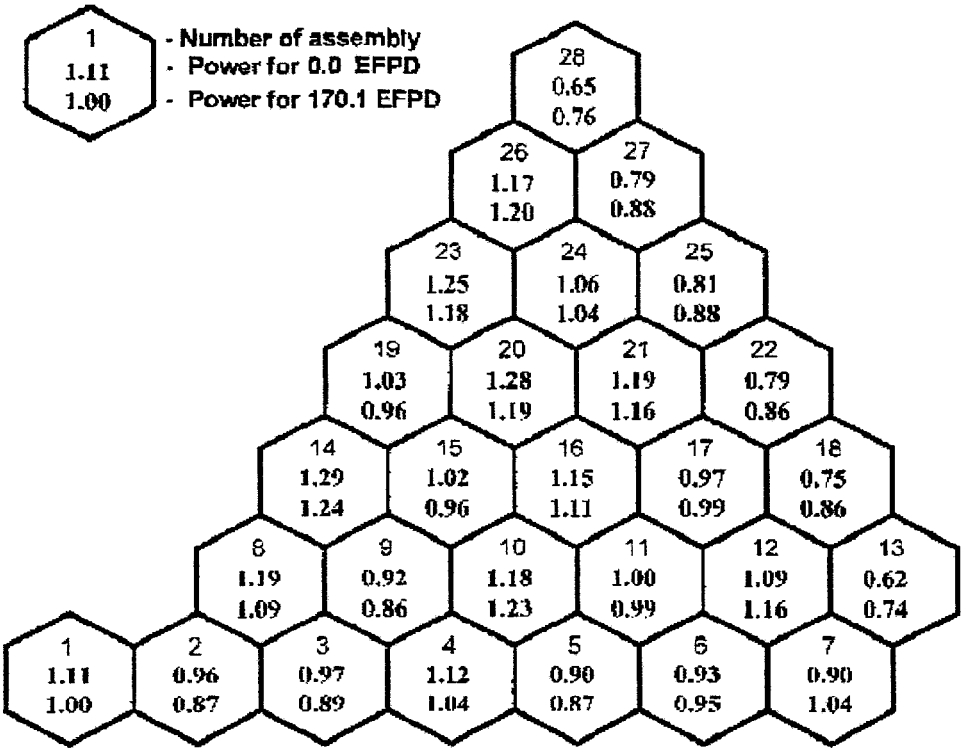

Fig.2. The relative assembly power distribution for begin and end of detector irradiation.

Only relative azimuthal and axial distribution of ^{54}Mn activity are presented in the paper[4]. It was shown in the Interim Report 2 that fast neutron flux at the PV is determined by neutron sources in the two outer arrays of cassettes with numbers 13, 18, 22 (1st array), and 7, 12, 17, 21 (2nd array). Can see in fig.2 that small asymmetry of power (up to 7%) takes place for cassettes located symmetrically about 30° axis.

Calculations of azimuthal and axial distribution of $^{54}Fe(n,p)$ and $^{237}Np(n,f)$ reaction rates were carried out for source distribution within 30°-60°. Calculational grid on θ co-ordinate within 0-30° contains 60 uniform intervals. The computed and measured reaction rates on azimuth at the outer surface of PV and height 129 cm from lower section of core and on height at θ=23° are presented in the Tables 1, 2.

Table 1. The azimuthal distribution of computed and measured reaction rates

	54-Fe(n,p)			237-Np(n,f)
θ, deg	c abs	c rel	e rel	c abs
0.25	1.108E-16	0.977		7.375E-15
1.60			0.983	
1.75	1.118E-16	0.986		7.409E-15
2.25	1.122E-16	0.989		7.428E-15
4.20			0.997	
4.25	1.134E-16	1.000		7.507E-15
5.25	1.129E-16	0.996		7.527E-15

	54-Fe(n,p)			237-Np(n,f)
θ, deg	c abs	c rel	e rel	c abs
6.25	1.118E-16	0.986		7.525E-15
7.25	1.109E-16	0.978		7.500E-15
8.25	1.106E-16	0.975		7.451E-15
9.20			1.000	
9.25	1.104E-16	0.974		7.371E-15
12.75	1.028E-16	0.907		6.766E-15
13.00			0.890	
13.25	1.004E-16	0.885		6.639E-15
22.75	5.976E-17	0.527		4.418E-15
23.00			0.509	
23.25	5.840E-17	0.515		4.345E-15
23.75	5.713E-17	0.504		4.277E-15
27.75	5.130E-17	0.452		3.943E-15
28.00			0.432	
28.25	5.102E-17	0.450		3.925E-15
29.25	5.067E-17	0.447		3.904E-15
29.75	5.061E-17	0.446		3.899E-15

In the Table 1 next reaction rates (RR) are presented:

54-Fe(n,p) **c abs**-computed absolute value (Bq/atom) with the thermal reactor power is equal to 3000 MWt; **c rel** - computed relative value RR(θ)/max {RR}; **e rel** - measured relative value RR(θ)/max {RR}

237-Np(n,f) **c abs**-computed absolute value (Bq/atom) with the thermal reactor power is equal to 3000 MWt

The reaction rates were measured in the interval 0-60°. The reaction rates were computed in the interval 0-30°. The angle of measurement in interval 30°-60° in the table 1 is shown as (60°-θ) where θ is angle in the Fig.1 for θ above 30°.

Can see that azimuthal variation of RR 54-Fe(n,p) in calculation and experiment is very closed. Unfortunately the agreement of the relative RR distribution does not mean the agreement of the absolute RR distribution.

Table 2. The axial distribution of computed and measured reaction rates (θ=23°)

	54-Fe(n,p)			237-Np(n,f)
H, cm	c abs	c rel	e rel	c abs
325.0	3.940E-17	0.675	0.626	3.003E-15
295.0	4.977E-17	0.853	0.951	3.722E-15
265.0	5.522E-17	0.946	0.996	4.112E-15
235.0	5.684E-17	0.974	1.000	4.252E-15
215.0	5.733E-17	0.982	0.996	4.296E-15
192.0	5.774E-17	0.989	0.996	4.331E-15
169.0	5.805E-17	0.995	0.984	4.349E-15
149.0	5.829E-17	0.999	0.954	4.353E-15
116.0	5.837E-17	1.000	0.964	4.321E-15
87.0	5.733E-17	0.982	0.952	4.199E-15

	54-Fe(n,p)			237-Np(n,f)
H, cm	c abs	c rel	e rel	c abs
59.0	5.313E-17	0.910	0.814	3.864E-15
29.0	4.194E-17	0.719	0.558	3.067E-15

The designations in the Table 2 is the same as in Table 1. Height is in cm from lower edge of core. The different positions of RR maximum on core height are observed in calculation and experiment. The typical axial power distribution has maximum as in calculation. The power axial distribution in the core is unknown. Therefore we have used as axial source in core the power axial distribution from Rovno NPP unit 3 during 6 cycle. Possible this is reason of difference between experiment and calculation.

The ratios of RR maximum to minimum in azimuthal distribution at the outer PV surface are presented in paper[4]. We have calculated corresponding distributions of RR 54-Fe(n,p) and 237-Np(n,f) (see table 1). In the table 3 the comparison of these ratios are presented.

Table 3. The comparison of RR ratios (max/min)

RR	c	e
54-Fe (max/min)	2.24	2.30
237-Np (max/min)	1.93	1.94

Results from table 3 is demonstrated excellent agreement between calculation and experiment and some difference of fast neutron spectra (neutron energy >0.5 MeV) on azimuth.

6. THE UPDATED COMPUTED REACTION RATES AND COMPARISON WITH EXPERIMENTAL DATA FOR THE ROVNO-3 NPP

In the interim report 2 and paper[5] the comparison of the computed and measured RR at the outer surface of PV for Rovno-3 NPP was presented. The calculation was carried out by synthesis method described above with cross section library based on ENDF/B-IV files with own correction of Fe, Cr, Ni cross sections based on ENDF/B-VI files. The BUGLE-93 cross section library based on ENDF/B-VI files was used for new calculation.

The section of 30° sector of VVER-1000 core plane section is shown in the Fig.3.

The power distribution in the plane core used in calculation is shown in the Fig. 4 as burn-up of assembly at the beginning and end of fuel cycle. The increment of burn-up by assembly was converted to assembly relative source distribution in core which was used for r-θ DOT calculation.

It is known that account of pin power distribution in the outer array of assemblies can effect to the computed RR distribution at the PV. Therefore the calculation results presented now were obtained with pin-to-pin power distribution in the cassettes number 13, 17, 19 (see Fig.3). The variation of pin power in outer cassettes is equal to 1.5-3 times in radial direction within cassette from inner to outer pin with average cassette power is

equal the same value. The real decreasing of pin power for Rovno outer cassette is unknown. Therefore we used two values of pin power variation: 1.5 and 3 times.

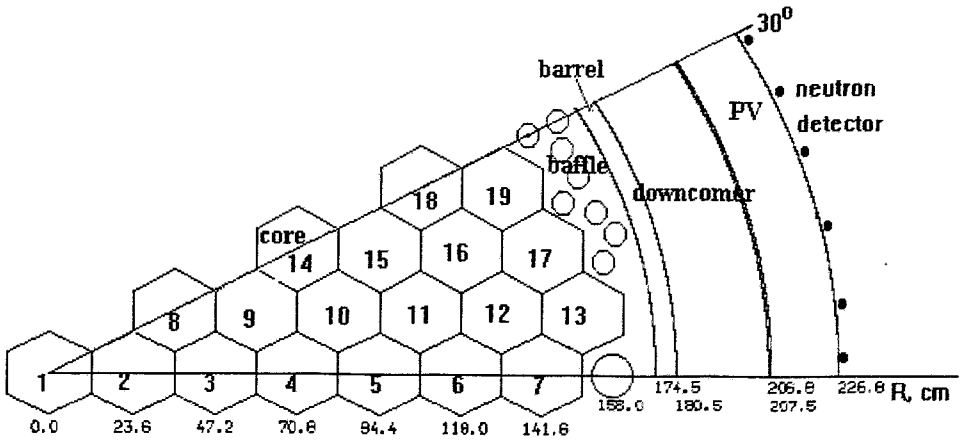

Fig 3. The horizontal section of VVER-1000 30° symmetry sector

The measured data were obtained from activation experiments [5] performed outside PV on Rovenskaya NPP unit 3 during 6 and 7 fuel cycles separately. Several reactions were used : $^{54}Fe(n,p)$, $^{58}Ni(n,p)$, $^{63}Cu(n,\alpha)$, $^{60}Ni(n,p)$, $^{237}Np(n,f)$, $^{238}U(n,f)$. The $^{237}Np(n,f)$ and $^{238}U(n,f)$ detectors were covered by Cd. Detectors were located at several azimuth and axial positions on the outer surface of PV. The comparison of measured and recalculated RR are presented here only for 6th cycle as effect of pin wise power distribution in the outer assemblies to computed RR is the same for the both cycles.

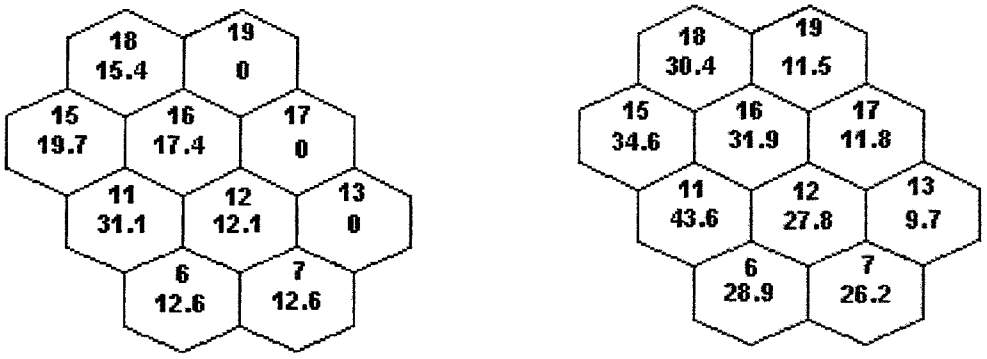

Fig.4. Initial and final fuel burn-up (MW•days/kgU) for outer assemblies in 6th cycle

The recalculated RR is determined by two factors in comparison with old results. The first is the other cross section library and the second is the pin power distribution in the outer cassettes. In the table 4 the ratios (c/e) of azimuthal distribution of $^{54}Fe(n,p)$ reaction rate (dps/atom) in cavity for 6 cycle (z=129 cm from lower core level , total core height 355 cm) are presented for four calculation:

1. Old library (B-IV), assembly wise power distribution in whole core;
2. New library (B-VI), assembly wise power distribution in whole core;
3. New library (B-VI), pin wise power for outer assembly (decreasing of 1.5 times), assembly wise power distribution in rest part of core;
4. New library (B-VI), pin wise power for outer assembly (decreasing of 3 times), assembly wise power distribution in rest part of core;

Table 4. The c/e ratios of RR ^{54}Fe(n,p) (azimuthal distribution) and 58-Ni , 63-Cu.

N \ θ	1	4	5	7	9	12	23	27	28
1fe	1.12	1.13	1.14	1.11	1.14	1.18	1.20	1.19	1.20
2fe	1.19	1.20	1.20	1.16	1.19	1.22	1.25	1.24	1.26
3fe	1.13	1.13	1.13	1.10	1.13	1.14	1.16	1.17	1.18
4fe	0.97	0.98	0.98	0.96	0.98	0.99	1.03	1.03	1.05
4ni									1.06
4cu									1.04

The ^{54}Fe(n,p) reaction have the effective threshold 3 MeV. Can see that second calculation gives greater c/e in average of 5.5%. This is effect of cross section library. It is known that B-VI Fe cross sections increase transmission of fast neutron (above 5 MeV) through Fe layer. The third calculation decreases c/e ratio in average of 7%. This is effect of decreasing (1.5 times) of pin power within outer assembly to baffle direction. And fourth calculation decreases c/e ratio up to 1 in average (±3%). This is effect of greater variation (3 times) of pin power distribution within outer assembly.
The other detectors used in measurements have greater threshold than 3 MeV besides ^{237}Np(n,f) and ^{238}U(n,f) reactions (thresholds are about 0.5 and 1.0 MeV correspondingly). In the table 5 c/e ratios obtained in 4 calculations are presented for positions of detectors located at the same height and at maximum and minimum of azimuthal distribution of fast neutron flux.

Table 5. The c/e ratios of ^{237}Np(n,f) and ^{238}U(n,f) RR (at maximum and minimum of azimuthal distribution in the outer surface of PV)

	1c	2c	3c	4c
^{237}Np(n,f)-max	0.77	0.90	0.86	0.72(0.73)
^{237}Np(n,f)-min	0.80	0.93	0.88	0.76(0.77)
^{238}U(n,f)-max	0.97	1.03	0.97	0.83(0.91)
^{238}U(n,f)-min	0.97	1.02	0.96	0.86(0.94)

It was shown in paper[5] that account of gamma fission reaction in calculation increases RR ^{237}Np(n,f) and ^{238}U(n,f) to 1% and 8% correspondingly. It is presented for only 4th calculation in brackets. Can see from table 5 that under prediction of computed RR

^{237}Np(n,f) for the 4th calculation is practically the same as in the 1st calculation. Above it was shown that c/e ratio of RR ^{54}Fe(n,p) is changed up to 1 during the progress of the 1st to the 4th calculation. The 4th calculation is the most real with respect to neutron source pin distribution in the outer assemblies of core. Besides most modern library cross section based on the ENDF/B-VI files is used here. Uncertainty of calculated RR depends on many factors. The main from ones are adequate neutron source distribution and neutron cross sections.

To eliminate the effect of source distribution to computed RR the spectral indices can compare. The spectral indices as the ratio of RR ^{237}Np(n,f) and others RR to ^{54}Fe(n,p) will be discussed below. The range of neutron spectrum within 0.5-1.0 MeV is most interest. Therefore the spectral indices of ^{103}Rh(n,n') and ^{115}In(n,n') to ^{54}Fe(n,p) will be discussed also.

In the table 6 the spectral indices of ^{237}Np(n,f)/^{54}Fe(n,p) are presented for 4 calculations and experiment.

Table 6. The spectral indices of ^{237}Np(n,f)/^{54}Fe(n,p).

	1c	2c	3c	4c	e	4c/e
Np/Fe-max	60	65.8	66.3	64.5	86.9	0.74
Np/Fe-min	69	76.9	77.2	75.4	103.4	0.73

The spectral index of ^{237}Np(n,f)/^{54}Fe(n,p) determines the ratio of flux above 0.5 MeV to flux above 3.0 MeV with corresponding reaction cross sections and does not depend on source distribution in core. Can see from table 6 that new library (2, 3, 4) increases spectral index of Np/Fe at outer surface VVER-1000 PV of 10% for maximum and minimum of fast neutron flux on azimuth. The measured spectral index of Np/Fe is greater of 25% than computed one. This result correlates with c/e ratio for RR of ^{237}Np(n,f) in 4th calculation where c/e for ^{54}Fe(n,p) is equal to 1. (see tables 4, 5).

In the next table typical uncertainties of measured RR at the outer PV surface and computed RR at the inner and outer surface [6] are presented.

Table 7. The typical uncertainties (sd, %) of computed and measured RR.

RR	c-inner (%)	c-outer (%)	e-sd(%)
^{54}Fe(n,p)	11.4	18.8	5.4
^{237}Np(n,f)	13.8	17.4	8.5
^{238}U(n,f)	10.9	17	7.8

The values of computed uncertainties are from paper [6]. The experimental sd (standard deviation) were put by G. Borodkin.

Can see that difference of c/e (4th calculation) from 1 for ^{54}Fe(n,p) and ^{238}U(n,f) lies within sd of measured RR and for ^{237}Np(n,f) c/e value lies exterior to 1±sd where sd respects to measured RR.

Reaction rates of detectors having threshold within 1-0.5 MeV were measured by G. Borodkin at the outer PV surface of South Ukraine NPP. Besides ^{237}Np(n,f) detector the ^{103}Rh(n,n'), and ^{115}In(n,n') detectors were used also in experiments. The thresolds of two last detectors are 0.7 and 1.1 MeV. For Rovno-3 we have calculated also RR of the ^{103}Rh(n,n'), and ^{115}In(n,n'). In the table 8 spectral indices of these detectors to ^{54}Fe(n,p) are presented. The measured spectral indices are respected to SU NPP and calculated ones are to Rovno NPP. As both reactors have the same construction the comparison of spectral indices are possible.

Table 8. The spectral indices of ^{237}Np(n,f), ^{103}Rh(n,n'), and ^{115}In(n,n') to ^{54}Fe(n,p) (South Ukraine NPP, G. Borodkin's experiment).

	4c	e	4c/e
Np/Fe-max	64.5	92	0.70
Np/Fe-min	75.4	-	-
Rh/Fe-max	30.7	36	0.85
Rh/Fe-min	35.6	38.3	0.93
In/Fe-max	3.7	4.3	0.86
In/Fe-min	3.9	4.3	0.91

Can see that results of table 8 are demonstrated under prediction of computed RR for detectors of ^{103}Rh(n,n'), and ^{115}In(n,n'). This under prediction is less on absolute value than one for ^{237}Np(n,f) and lies within (1-2)σ of measured RR.

We have evaluated effect of steel tube (thickness 3 mm) where detectors are located. The computed spectral index of ^{237}Np(n,f)/^{54}Fe(n,p) is increased to 10% due to decreasing of RR ^{54}Fe(n,p) and not changing of RR ^{237}Np(n,f).

In the paper [7] where calculations were performed by Monte Carlo method the comparison of calculated and measured RR for Rovno-3 during 7th cycle is demonstrated also under prediction of calculated data for ^{237}Np(n,f) (c/e=0.80) and ^{93}Nb(n,n') (c/e=0.78). The effective threshold of ^{93}Nb(n,n') reaction is about 0.5 MeV.

The comparison of measured and calculated RR at the PV outer surface of a PWR H.B. Robinson NPP unit 2 is presented also in the paper [6]. The c/e ratio for ^{237}Np(n,f) reaction in the cavity was obtained there equal to 0.88. The thickness of PWR PV is 22.8cm. The calculation was carried out by MCBEND code using ENDF/B-VI nuclear data. The measured ^{237}Np(n,f) reaction was obtained also at the surveillance position which located at the inner PV surface. The c/e ratio here is equal to 0.97. Let compare the computed and measured spectral index (^{237}Np(n,f)/^{54}Fe(n,p)) at the inner and at the outer surface of PV using corresponding RR which are presented in the paper[6].

Table 9. The comparison of ^{237}Np(n,f)/^{54}Fe(n,p) spectral index at the inner and outer PV surface for PWR Robinson [6].

method	PV inner surface	PV outer surface
c	32	150
e	32	188
c/e	1.0	0.80

Can see from table 9 that the calculated and measured spectral index at the inner surface i.e. in the water is good agreed. Otherwise the calculated spectral index at the outer surface i.e. behind 22.8 cm iron layer is under predicted of 20%. The authors of paper [6] think that this is attributed to the neglect of photo fission effects. Above it was shown that the additional effect of photo fission to ^{237}Np(n,f) reaction is equal about +1% behind 20 cm iron PV. Besides the computed (without photo fission effect) spectral index in water is good agreed with the measured spectral index.
So systematic under prediction of calculated RR with threshold below 1 MeV Vs measured ones is found behind iron layer of thickness 20-23 cm. This is attributed to the transport Fe cross section in the neutron energy range below 1 MeV.

6. The calculation of RR at the outer PV surface using BNAB library.

To evaluate the effect of cross section library we have performed the same calculations using 28 groups BNAB library developed in Obninsk Nuclear Data Center (Russia) [8]. This calculation was carried out for source distribution in core corresponding 4th case (see table 5). The c/e ratios at the outer surface of Rovno-3 PV are presented in the table 10.
Table 10. The c/e ratios of RR with BNAB library.

θ	1	4	5	7	9	12	23	27	28
4fe	0.86	0.87	0.87	0.85	0.87	0.88	0.90	0.90	0.92
4np		0.72			0.73				0.76

Here can see that c/e values for RR of ^{237}Np(n,f) are the same as with BUGLE library and c/e for RR of ^{54}Fe(n,p) is lower than corresponding ones with BUGLE cross sections. Let compare the computed spectral indices for the BNAB library with the corresponding measured ones in the table 11.

Table 11. The spectral indices (Np/Fe) with BNAB

θ	4	9	28
c	72.5	72.6	85.8
e	87.5	86.9	103.4
c/e	0.83	0.84	0.83

The correlation of calculated and measured spectral indices is better with BNAB library (+10%) than with BUGLE-93 library. If to account the effect of steel tube as above mentioned (else +10%) can find a good agreement of calculated spectral index with BNAB library in comparison with measured one.

6. CONCLUSION

The main location where neutron fluence need to evaluate is the inner surface of PV and 1/4 PV thickness. The neutron spectrum is formed here by water. The validation of

calculated neutron spectrum was performed by comparison of RR measured behind PV, i.e. after 20 cm Fe. Uncertainty of calculated fluence on inner surface will be less than the same one on the outer surface as the neutron transport through water is calculated more exactly than through iron (see table 7). Below the comparison of the computed fluxes with BUGLE and BNAB libraries are presented.

Table 12. The computed maximum fluxes above E MeV at inner, at 1/4 thickness, at outer surface of PV with BUGLE and BNAB libraries (Rovno-3, 6th cycle, thermal power 3000 MWt, 4th case of pin power distribution in outer assemblies)

	bugle	bnab	bugle	bnab	bugle	bnab
E MeV	inner		1/4pv		outer	
3	8.28+09	8.18+09	3.29+09	3.23+09	2.22+08	2.10+08
1	2.91+10	2.72+10	1.61+10	1.52+10	1.67+09	1.75+09
0.5	4.41+10	3.95+10	3.10+10	2.73+10	5.03+09	4.67+09
0.1	6.50+10	5.95+10	5.46+10	4.86+10	1.15+10	1.16+10

The ratios of computed flux above 1.0 and flux above 0.5 MeV at the inner, 1/4PV and outer surface can see in the table 13 depending on cross section library.

Table 13. Ratios of BUGLE to BNAB results

	bugle/ bnab	bugle/ bnab	bugle/ bnab
E, MeV	inner	1/4pv	outer
1	1.07	1.06	0.95
0.5	1.12	1.14	1.06

The agreement of computed flux above 1 MeV is better than one is for flux above 0.5 MeV. Behind iron layer (PV) the relation of both fluxes is opposite. It means that accumulation of neutron in the range 1-0.5 MeV with library BNAB is more than with BUGLE in process of neutron transmission through iron.

The spectral indices (ratio of flux above 0.5 MeV to flux above 3 MeV) can see in the table 14.

Table 14. The spectral indices on flux (ratio of flux above 0.5 MeV to flux above 3 MeV)

library	bugle	bnab	bugle	bnab	bugle	bnab
location	inner		1/4pv		outer	
s.i. 0.5/3.0	5.3	4.8	9.4	8.5	22.7	22.3

These results demonstrate that neutron spectrum at inner surface (behind water layer) with BNAB is more hard than one is with BUGLE library and confirm above mentioned conclusion about more accumulation of neutron in the range 1-0.5 MeV with library BNAB behind iron layer.

So the absolute flux above 0.5 MeV and the neutron spectrum at the crucial points of PV is differed in calculations with BUGLE and BNAB libraries. It is needed to remember that the both used libraries are absolute independent. Can suggest that uncertainty of computed flux above 0.5 MeV at the inner and 1/4 PV of VVER-1000 attributed to cross section

library is equal about 12% at other factors being the same. The choice of more adequate library could be done after performing of measurements at the inner surface of PV.

REFERENCES

1. E.B. Brodkin et al., "Determination of Characteristics of the Neutron Field Affecting the WWER Reactor Vessel", *Proc. of the 6th Int. Conf. on Radiation Shielding*, 1983, Tokyo, CONF-850538, Vol.2, pp. 1055-1060.

2. F.B.K. Kam et al., "Pressure Vessel Analysis and Neutron Dosimetry," ORNL/TM-10651, Oak Ridge National Laboratory (Nov. 1987)

3.D.T. Ingersoll et al.,"BUGLE-93 Coupled 47 Neutron, 20 Gamma-Ray Group Cross Section Library Derived from ENDF/B-VI for LWR Shielding and Pressure Vessel Dosimetry Applications, ORNL-6795 August 1994.

4. G.I. Borodkin and .O. Kovalevich, "Interlaboratory VVER-1000 Ex-Vessel Experiment at Balakovo-3 NPP", T*he 9th International Symposium on Reactor Dosimetry*, Prague, Sept. 2-6 1996.

5. E.B. Brodkin, et. al., "The Neutron Fluence Monitoring System for VVER-1000 Pressure Vessel and its Validation", Proc. of Radiation Protection & Shielding Topical Meeting, April 21-25, 1996, No. Falmouth, Mass., USA

6. Alan Avery et al., "Calculations of Pressure Vessel Fluence in PWR's Using ENDF/D-VI Data", *Proc. of the 8th Int. Conf. on Radiation Shielding*, Arlington, Texas, April 24-28, 1994, ANS, pp. 677-685.

7. H.U. Barz et al., "Determination of Pressure Vessel Neutron Fluence Spectra for a Low Leakage Rovno-3 Reactor Core Using Three Dimensional Monte Carlo Neutron Transport Calculations and Ex-Vessel Neutron Activation Data", T*he 9th International Symposium on Reactor Dosimetry*, Prague, Sept. 2-6 1996.

8. L.P. Abagyan et al., Group Constants for Nuclear Reactor Calculations.-N.Y., Consultants Bureau, 1964

A6

Abschlußbericht des RRC KI

Cooperation Agreement on the Project

"Increasing of the Accuracy of the Determination of Neutron Load of WWER-1000 Reactor Components to Get Additional Information for a Safer Operation of Reactors"

Evaluation of Results and Comparison with Other Calculations

Final Report

E.B. Brodkin, A.L. Egorov , S.M. Zaritsky

Nuclear Reactors Institute of RRC "Kurchatov Institute"

October 1997

CONTENTS

INTRODUCTION

The accurate determination of neutron fluence in the WWER pressure vessel (RPV) is necessary for the ensuring RPV safety. This Project is the part of works directed to improving and validating the calculational tools for the evaluation and prediction of the neutron load of WWER-1000 RPV.

The goal of the calculation part of the Project is carrying out calculations of neutron fluences and reaction rates in cavities of WWER-1000 by codes and data usually used in Russia and comparing the results with alternative calculation results and experimental ones to evaluate the accuracy of the calculation methodology.

The schedule of Project milestones:

- Preparation of basic data and carrying out the first test calculations; report [1] was issued on April 1996;
- Completion of transport calculations for Rovno-3 ; report [2] was issued on October 1996;
- Completion of transport calculations for Balakovo-3; report [3] was issued on April 1997; updated results were presented on September 1997 in the workshop "Balakovo-3 Interlaboratory Pressure Vessel Dosimetry Experiment" in FZ Rossendorf [4];
- Evaluation of results and comparison with other calculations, October 1997 - final report of the Project.

This report was prepared as report for the last milestone. The results of the Project are shortly summarized below.

1. METHODOLOGY OF THE WWER-1000 RPV DOSIMETRY CALCULATIONS

The model of the WWER-1000 reactor (the 30° sector of symmetry in the middle plane).is presented on the Fig.1

The main features of the problem of neutron fluence calculation on the RPV are:

- the necessity of 3-dimensional calculations of deep neutron penetration in water-steel compositions, with fast neutron source located in the reactor core,
- the necessity of calculation of detail neutron spectra above 0.1 MeV,
- the necessity of taking into account the detail space distribution of fast neutron source in the core,
- the necessity of taking into account the time dependence of fast neutron source in the core during the fuel cycles.

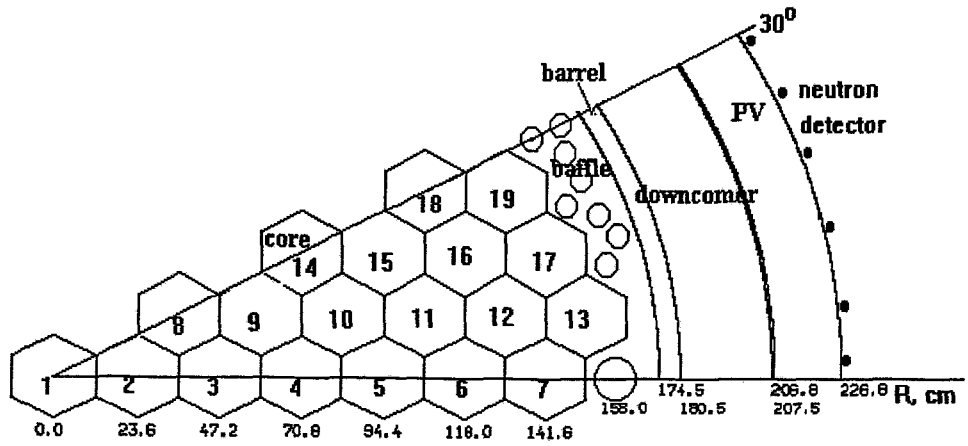

Fig. 1. The horizontal section at 30° symmetry sector of WWER-1000

Commonly the discrete ordinates or Monte Carlo methods are used for such kind of calculations.

We use the first one for solving our problem in three-dimensional RθZ-geometry. The use of Rθ-geometry in plane gives us the opportunity of adequate description of cylindrical surfaces. Other surfaces are described more or less adequate using the fine Rθ-mesh.

As for axial dimensions of model, we consider in this Project only its middle part - opposite to core (in the limits of down and upper core boundaries). It is possible because fluence reaches its maximal value within mentioned boundaries and at the first hand we are interested in calculation of the fluence on the welds located in this region.

The strict calculation of a neutron spectrum in 3-dimensional geometry can be done by the code TORT, but these calculations are very expensive and we use this code only in some cases, e.g. for the calculation of neutron field in surveillance specimens assemblies located on the baffle over the core upper boundary. This task is out of Project.

For calculating the neutron field in the above mentioned region between levels of down and upper core axial boundaries we usually use the synthesis of two - and one - dimensional calculations [5]:

$$\varphi(r,\theta,Z,E) = \varphi(r,\theta,E)\, K(r,z,E) \qquad (1)$$

$$K(r,z,E) = \varphi(r,z,E)/\varphi(r,E) \qquad (2)$$

where

$\varphi(r,\theta,z,E)$ - neutron flux density space and energy distribution with source $q(r,\theta,z,E)$ in core;

$\varphi(r,\theta,E)$ - two-dimensional neutron flux density plane distribution with source $q(r,\theta,E)$ in core; radial and azimuthal dependencies of this source are the same as for $q(r,\theta,z,E)$;

$\varphi(r,z,E)$ - two-dimensional neutron flux density distribution in cylindrical model of reactor with source $q(r,z,E)$ in core; radial and axial dependencies of this source are the same as for $q(r,\theta,z,E)$;

$\varphi(r,E)$ - one-dimensional neutron flux density distribution in cylindrical model of reactor with infinite height and source $q(r,E)$ in core; the radial dependence of $q(r,E)$ is the same as for $q(r,z,E)$ in $\varphi(r,z,E)$ calculation.

Equivalent cylindrical boundary of core is used in (R,Z)- and (R)- calculations.

For neutron transport calculations we use the well known codes developed in ORNL:

TORT - calculations of three-dimensional neutron flux density distributions,
DOT-3 - two-dimensional calculations,
ANISN - one-dimensional calculations.

For source calculations the standard Russian codes BIPR and PERMAK are used (together with data libraries prepared for WWER calculations). BIPR code gives three-dimensional assembly-wise source distribution in core, code PERMAK - two-dimensional pin-to-pin distribution. We developed the special code for transforming the source obtained by these codes to the R-θ grid of transport codes.

Source distribution for neutron transport calculation is specified proportional to average power during fuel cycle or irradiation time.

Also it can use as source in each assembly the increment of burn-up during fuel cycle obtained from NPP operation data.

Usually assembly-wise power distribution in 60° sector of WWER-1000 core is approximately symmetrical relative 30° direction. From this reason the neutron transport calculations in the vicinity of RPV are typically carried out for 30° sector of symmetry of WWER-1000 core - see Fig.1.

Pin-to-pin power distribution is calculated by code PERMAK only for outer assemblies. The pin power within outer assembly changes of 3 times.

The homogenized material of fuel (UO_2), cladding (Zr) and water is used in the core. Detail material specification is used in the out-of-core regions.

For the base calculations we choose the American BUGLE-93 library [6] which is based on the ENDF/B-VI files and contains 47-group data in SAILOR format.

2. FUEL ASSEMBLIES CONTRIBUTION METHOD.

It is convenient in several cases to calculate $\varphi(r,\theta,z,E)$ usig the so called influence functions, i.e. contributions of each fuel assembly to neutron flux density (or fluence) in desirable points of RPV [7,8].

One of the main goal of RPV dosimetry is an evaluation of fluence of neutrons with energy above 0.5 MeV at the inner surface and in the 1/4 of RPV thickness during each fuel sycle.

All the WWER-1000 units operated in Russia, Ukraine and Bulgary (except Novo-Voronezh unit 5) have the same design of core and in-vessel internals.

The fuel assemblies in the core have different enrichment and burnup, but the fast neutron transport across the core is practically independent on the core status. So one can calculate in advance the contribution of each fuel assembly to neutron fluence and calculate distribution of fluence during fuel cycle on and in RPV as:

$$F(r,\theta,z,E) = k \cdot \sum_i q_i f_i(r,\theta,z,E) \qquad (3)$$

where

$F(r,\theta,z,E)$ - neutron fluence distribution in one fuel cycle,

i - assembly index,

$f_i(r,\theta,z,E)$ - neutron fluence caused by i - assembly with unity source,

q_i - relative source in the i - assembly,averaged in one fuel cycle,

k - normalization multiplier.

The contributions $f_i(r,\theta,z,E)$ are calculated as described above - eqs (1), (2).

This approach is convenient e.g. for fuel cycle optimization calculations when it is necessary to evaluate the influence of core loading to fluence on the RPV [7].

This approach can be used in RPV fluence monitoring systems too [2,8].

The contributions of two outer rows of assemblies (assemblies 6, 7, 12, 13, 16, 17, 18, 19, see Fig.1) to fluence within RPV (from inner to outer surface) was calculated. The contributions of the same assemblies to neutron spectrum was also calculated for inner surface, 1/4 RPV thickness and outer surface. The relative contributions of 8 outer assemblies to neutron fluence (E>0.5 MeV) on the RPV inner surface are presented in the Table 1 [2].

The contribution of other fuel assemblies (besides of 8 outer assemblies, see Fig.1 and Table 1) is less than 0.6%.

Table 1

The relative contributions of 8 outer assemblies to neutron fluence (E>0.5 MeV) at inner surface of WWER-1000 RPV

θ°\N^{ass}	6	7	12	13	16	17	18	19	total
0	0.005	0.103	0.039	0.786	0.005	0.053	0.0	0.003	0.994
5	0.005	0.079	0.037	0.789	0.005	0.075	0.001	0.006	0.997
10	0.004	0.045	0.035	0.723	0.009	0.161	0.001	0.018	0.996
15	0.003	0.026	0.035	0.532	0.016	0.311	0.003	0.068	0.994
20	0.002	0.013	0.030	0.275	0.026	0.418	0.010	0.222	0.996
25	0.001	0.005	0.019	0.102	0.035	0.325	0.021	0.490	0.998
30	0.001	0.003	0.012	0.042	0.037	0.221	0.027	0.656	0.999

3. COMPARISON WITH OTHER CALCULATIONS AND EXPERIMENTS

The comparisons of calculated results (reactions rates, neutron spectra, spectral indices) were carried out in frame of this Project with corresponding experimental data obtained at the NPP with WWER-1000, on the WWER mock-ups at LR-0 reactor, and in the benchmark experiments. The results of these comparisons were reviewed in the reports [1,2,3,4]

The comparisons of our calculated results for Balakovo-3 and results of others calculations and experimental data are presented below.

The measurements at NPP Balakovo Unit 3 were carried out on the outer surface of RPV by different dosimetry detectors located in 60° sector and along core height. Locations of detectors are shown in the Fig.2 [9,10].

The assembly-wise core power distribution is presented on the Fig.3 for the beginning and the end of detectors irradiation; these data are obtained from BIPR calculations.

Alternative calculations of fast neutron field behind RPV of Balakovo-3 were carried out by H.-U. Barz and J. Konheiser, FZR, (Monte Carlo method) [11] and by C. Garat, FRAMATOME, (discrete ordinates method, BUGLE-93) [12].

The calculations of FZR have been done using 123 energy groups (VITAMIN-J structure) above 20 KeV accounting different fission sources from ^{235}U, ^{239}Pu and ^{238}U. Neutron data from ENDF/B-VI were used with P_5 -approximation of scattering anizotropy, neutron scattering on the hydrogen was accounted exactly.

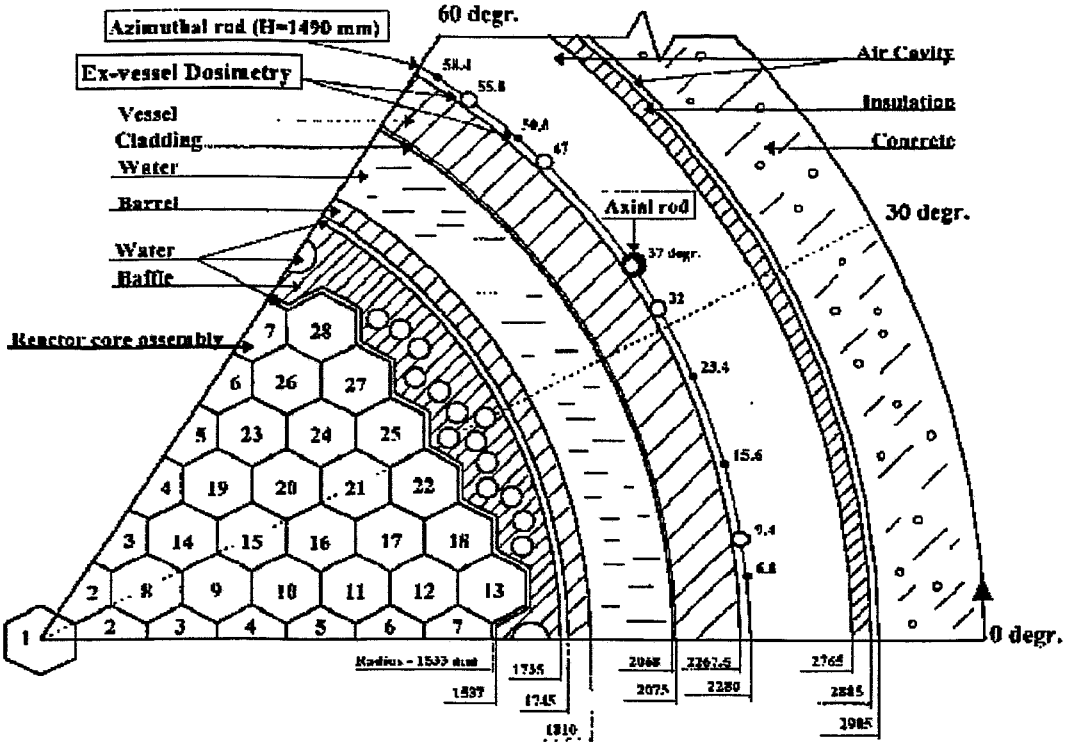

Fig.2. The location of detectors in the plane section of 60° sector of Balakovo-3.
(o-capsule with detector set, •-Fe-54 monitor)

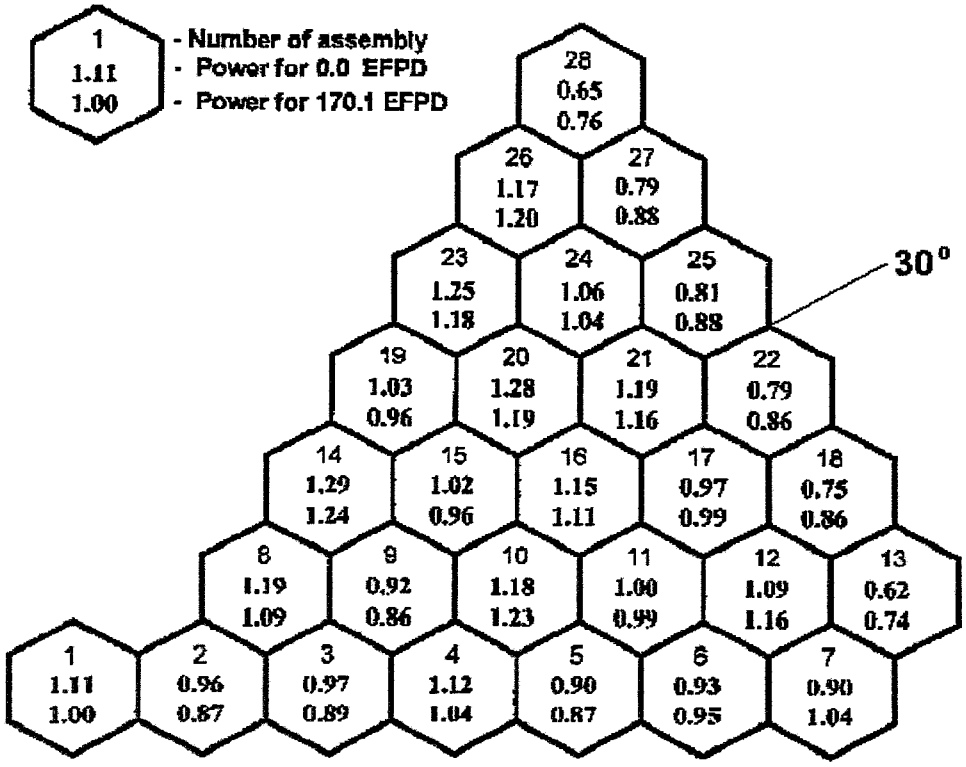

Fig 3. The 60° sector of rotate symmetry of WWER-1000 core
during detectors irradiation on Balakovo-3

Comparison of calculated results is presented in the Table 2.

Table 2

Integral flux above E MeV (n/cm^2 s) and spectral index 0.5/3.0 calculated by RRC KI, FRAMATOME, and FZR.

θ	Data origin	E, MeV				SI
		0.1	0.5	1.0	3.0	0.5/3.0
Max. flux	RRC KI	1.14+10	5.08+9	1.70+9	2.29+8	22.2
	FRAMATOM	1.13+10	4.92+9	1.67+9	-	-
	FZR	1.18+10	4.90+9	1.60+9	2.12+8	23.1
	RRC / FRAM	1.01	1.03	1.02	-	-
	RRC / FZR	0.97	1.04	1.06	1.08	0.96
	FRAM / FZR	0.96	1.00	1.04	-	-
Min. flux	RRC KI	6.72+9	2.68+9	8.26+8	1.06+8	25.3
	FRAMATOM	6.59+9	2.50+9	7.70+8	-	-
	FZR	6.59+9	2.61+9	7.33+8	9.41+7	27.7
	RRC / FRAM	1.02	1.07	1.07	-	-
	RRC / FZR	1.02	1.03	1.13	1.13	0.91
	FRAM / FZR	1.00	0.96	1.05	-	-

The disagreement between our results and other ones is greater in the region of minimal flux caused by features of our calculations methodology based on the calculations in the two adjacent 30° sectors.

The data in the Table 2 illustrate the possible uncertainty of deterministic calculations (comparison RRC KI and FRAMATOME results) and difference of deterministic results from more precise ones.

One can see that deterministic calculations with BUGLE-93 give more "hard" neutron spectrum than Monte Carlo calculations of FZR.

Table 3 illustrates discrepancies between reaction rates calculated by RRC KI, calculated and measured by FZR [10,13] and measured by SEC [10]. Ratios of reaction rates calculated by RRC KI and measured by FZR were obtained as

$$C(RRC) / E(FZR) = \{C(RRC) / C(FZR)\} \cdot \{C(FZR) / E(FZR)\}$$

The 47 group cross sections of dosimetry reactions for calculation of reaction rates were taken from neutron response functions collapsed using 1/4 RPV weighting spectrum (BUGLE-93 library) for all reactions from Table 3 except ^{93}Nb(n,n'). The 47 group cross sections for ^{93}Nb(n,n') reaction were obtained from 171 group cross section (weighted on standard spectra using IRDF90 data) collapsed using ex-vessel WWER-1000 weighting spectrum which was calculated with VITAMIN-C library in 1d radial model of WWER-1000.

Table 3

Comparison of calculated and measured reactions rates
(H=149 cm from level of core bottom)

θ °		Reaction							
	Data origin	$^{237}Np(n,f)$	$^{238}U(n,f)$	$^{93}Nb(n,n^1)$	$^{54}Fe(n,p)$	$^{58}Ni(n,p)$	$^{46}Ti(n,p)$	$^{60}Ni(n,p)$	$^{63}Cu(n,\alpha)$
9.4	C(RRC) / CFZR)	-	-	1.02	1.02	1.02	1.06	-	0.97
	C(FZR) / E(FZR)	-	-	1.01	1.02	1.08	1.00	-	1.02
	C(RRC) / E(FZR)	-	-	1.03	1.04	1.10	1.06	-	0.99
	C(RRC) / E(SEC)	0.87	-	-	1.15	1.13	-	0.88	1.06
32	C(RRC) / CFZR)	-	-	1.09	1.08	1.08	1.12	-	1.00
	C(FZR) / E(FZR)	-	-	0.85	0.97	1.00	0.91	-	0.96
	C(RRC) / E(FZR)	-	-	0.93	1.05	1.08	1.02	-	0.96
	C(RRC) / E(SEC)	0.85	0.99	-	1.14	1.14	-	0.84	1.05
55.8	C(RRC) / E(SEC)	0.83	0.91	-	1.08	1.08	-	0.85	1.04

Reactions rates were calculated by FZR using 29 group fluxes and 29 group cross sections of all dosimetry reactions calculated as for $^{93}Nb(n,n')$ reaction in our case.

The comparison of the azimuth distribution of $^{54}Fe(n,p)$ reaction rate obtained in our calculations and measured by SEC is presented in the Table 4.

Table 4

Comparison of calculated and measured $^{54}Fe(n,p)$ reaction rate
(H = 149 cm from level of the core bottom)

Data origin	θ°										
	6.8	9.4	15.6	23.4	32.0	37.0	47.0	50.8	55.8	58.4	62.1
C(RRC)/E(SEC)	1.14	1.15	1.17	1.18	1.14	1.13	1.08	1.07	1.08	1.10	1.11

The detail analysis of agreement or disagreement between calculations and measurements can be done only after completion of the evaluation of experimental data obtained by all participants of Balakovo-3 Interlaboratory RPV dosimetry experiment.

Today we can see that our calculations agree within 10% with calculations and measurements of FZR.

The discrepancies between our calculated $^{237}Np(n,f)$, $^{54}Fe(n,p)$ and $^{58}Ni(n,p)$ reaction rates and experimental data of SEC are more significant.

The special evaluation [2,3.4] showed that calculated $^{237}Np(n,f)$ reaction rate can be increased by taking into account photofission and using more accurate weighting spectrum for reaction group cross sections preparation; but this increasing of $^{237}Np(n,p)$ reaction rate can reach only approximately 4%, so residual under-prediction will be equal to approximately (10-15)%.

CONCLUSIONS

1. The methodology of calculation of fast neutrons field in WWER-1000 RPV is presented here. This methodology is based on the use of discrete ordinate method, synthesis of 1- and 2-dimensional neutron flux distributions and multigroup cross section library derived from ENDF/B-VI files.
2. The method of assemblies contributions for fluence evaluation is presented. It can be used in fuel cycle optimization and in RPV fluence monitoring system. The contributions of outer assemblies to neutron fluence at inner surface of WWER-1000 RPV were calculated.
3. Validation of calculation methodology was carried out by comparison with alternative calculations and data of different experiments.

4. The comparison with calculation and experimental results of Balakovo-3 Interlaboratory RPV dosimetry experiment have been done in this report, but the analysis can be completed only after finishing the experimental data evaluation. Today's discrepancies between calculation and experimental fast neutron field parameters on the outer RPV surface reach 15%.
5. The comparison of calculated data with experimental ones obtained in cavity experiments is useful for validating the calculation methodology and shows the directions of the following investigations and improvements of methodology.

   But the use of only ex-vessel cavity measurements is insufficient for strong validation of calculation of radiation load on the inner surface and inside RPV. The more informative experiments are necessary. One can solve this problem only using together the simple benchmark experiments (like Fe-spheres with Cf source, and KORPUS facility), the mock-up experiments (like LR-0), the measurements of RPV-material activity (scraps, templetes), and ex-vessel cavity experiments.

REFERENCES

1. Brodkin E.B., Egorov A.L., Zaritsky S.M. Preparation of Basic Data and Carrying out of First Test Calculations. Interim Report of Project, April 1996.
2. Brodkin E.B., Egorov A.L., Zaritsky S.M. Completion of Transport Calculations for Rovno-3. Interim Report of Project, October 1996.
3. Brodkin E.B., Egorov A.L., Zaritsky S.M. Completion of Transport Calculations for Balakovo-3. Interim Report of Project, April 1997.
4. Brodkin E.B., Egorov A.L., Zaritsky S.M. Calculational Results on the Balakovo-3 Cavity Dosimetry Experiment. The Workshop "Balakovo-3 Interlaboratory Pressure Vessel Dosimetry Experiment", FZ Rossendorf, September 1-5, 1997.
5. Brodkin E.B., Kozhevnikov A.N., Khrustalev A.V. Determination of Characteristics of the Neutron Field Affecting the WWER Reactor Vessel, Proc. of the 6th Int. Conf. on Radiation Shielding, 1983, Tokyo, CONF-850538, Vol.2, pp. 1055-1060.
6. Ingersoll D.T. et al.,BUGLE-93 Coupled 47 Neutron, 20 Gamma-Ray Group Cross Section Library Derived from ENDF/B-VI for LWR Shielding and Pressure Vessel Dosimetry Applications, ORNL-6795 August 1994
7. Pavlovichev A.M., Zaritsky S.M., Dadakina L.L. Estimation of the Fast Neutron Flux Density Distribution on the Inner Surface of WWER Pressure Vessel in Frame of the Fuel Loading Optimization. Radiation Protection and Shielding, Topical Meeting, April 21-25, No. Falmouth, Mass., USA, pp. 36-42.

8. Brodkin E.B., Egorov A.L, Zaritsky S.M., Borodkin G.I. The Neutron Flux Monitoring System for WWER-1000 Pressure Vessel and Its Validation. Ibid., pp. 211-216.
9. Borodkin G.I.,Kovalevich O.M. The International Dosimetry Experiment at the Balakovo-3 Pressure Vessel: Status, Description and Realization. The workshop "Balakovo-3 Interlaboratory Pressure Vessel Dosimetry Experiment", FZ Rossendorf, September 1-5, 1997.
10. Borodkin G.I., Overview of the Balakovo-3 Intercomparison Measurements Results and Presentation of SEC Results. Ibid.
11. Barz H.-U., Konheizer J. Rossendorf Monte Carlo Calculations for the Balakovo-3 Experiment and Comparisons to Experimental Results. Ibid.
12. Borodkin G.I., Garat C. Calculation of the Interlaboratory WWER-1000 Ex-Vessel Dosimetry Experiment at the Balakovo-3 NPP with the DORT and DOTSYN Codes. Ibid.
13. Stefan I. Rossendorf Activation Measurements for the Balakovo-3 Experiment. Ibid.

A7

Protokoll und Liste der Beiträge und Teilnehmer des "International Workshop on the Balakovo-3 Interlaboratory Dosimetry Experiment"

Minutes on the International Workshop on the Balakovo-3 Interlaboratory Dosimetry Experiment

The International Workshop on the Balakovo-3 Interlaboratory Dosimetry Experiment was held at September 2-5, 1997 in the Forschungszentrum Rossendorf (FZR). It was organized by the FZR together with the Scientific and Engineering Centre for Nuclear and Radiation Safety of Russian GOSATOMNADZOR (SEC). The Workshop was sponsored by the FZ Rossendorf e.V., the Saxonian Government, the German Federal Ministry BMBF.

The list of the Contributions and participants - see Attachment.

The Workshop was devoted to the first discussion of the results of measurements and calculations in application to the Balakovo-3 Interlaboratory Dosimetry Experiment, which was organized by the SEC GOSATOMNADZOR.

It was concluded that the independent measurement results of different participants agreed well for the $^{54}Fe(n,p)$ monitor reaction and there are greater differences for some other reactions and radiation positions.

Independent neutron transport calculations performed by different centers on the basis of the same reactor model and data presented by SEC have shown reasonable agreement.

The following problems were also discussed: the status of the RPV radiation load predictions, nuclear data files and energy group data preparation, the role of different type of experiments in the RPV dosimetry problem, the general problems of benchmarks formulation, uncertainties of VVER-1000 reactor design parameters.

Recommendations:

- On the basis of the Balakovo-3 Experiment a full-scale 3D ex-vessel fluence benchmark for the standard VVER-1000 RPV should be created.
- A full compilation of experimental results obtained in the frame of the "blind" intercomparison should be completed until the end of October 1997 by G. Borodkin and sent after that to all participants of the measurements in frame of agreements between the SEC and each participant concerning using the results.
- As next step all participants of measurements can analyze and revise their data and uncertainties and send the revised data with an analysis of their uncertainties to G. Borodkin for creating a reference data set.

A summary of the Workshop should be presented to the next meeting of WGRD-VVER in Bulgaria in September 1997 (B.Böhmer and G.Borodkin).

Participants thank FZR for the support and excellent organization of the Workshop.

G.Borodkin
SEC GOSATOMNADZOR

B.Böhmer
Secretary of the Workshop

Attachment to the Minutes of the Interational Workshop on the Balakovo-3 Interlaboratory Pressure Vessel Dosimetry Experiment, Rossendorf, 2. - 5. 9. 1997:

Sessions, Contributions and List of Participants

Opening of the Workshop:
Prof. F.-P. Weiß (FZR Rossendorf)

Session 1 (Experimental Techniques and Results)[1]

Part 1:
Chairman: K. Noack

The International Dosimetry Experiment at the Balakovo-3 Pressure Vessel: Status, Description and Realization
G. Borodkin, O. Kovalevich (SEC GOSATOMNADZOR Moscow, Russia)

Designer Requirements to VVER-1000 Pressure Vessel Dosimetry and the Role of the Balakovo-3 Experiment
V. Tsofin (OKB Gidropress Podolsk, Russia)

Overview of the Balakovo-3 Intercomparison Measurements Results and Presentation of SEC Results
G. Borodkin (SEC GOSATOMNADZOR, Moscow, Russia)

Part 2:
Chairman: G.Borodkin
Rossendorf Activation measurements for the Balakovo-3 Experiment
I. Stephan (FZR)

Neutron Metrology in the Cavity of the Balakovo-3 NPP performed by ECN
W. Voorbraak (ECN Netherlands)

Activation Measurements for the Balakovo-3 Experiment at RRC Kurchatov Institute
A. Borodin (RRC Kurchatov Institute Moscow)

Part 3:
Chairman: W. Voorbraak

Presentation of the Niobium Mass determination by means of the ICP-Spectroscopy
W. Wiesener, I. Stephan (FZR) (in Geb.8)

Activation Measurements for the Balakovo-3 Experiment at Melekes
V. Litchadeev (RIAR Dmitrovgrad)

PV Dosimetry and Surveillance Program on NPP Temelin, Use of Niobium for PV Dosimetry, J. Hogel (SKODA Pilsen, Czech Rep.)

Some Comments to Comparisons of Measured and Calculated Functionals
V. Valenta (SKODA Pilsen, Czech Rep.)

Session 2 (Calculations and Comparison with Experimental Results)

Part1:
Chairman: H.-U. Barz

Calculational Results on the Balakovo-3 and Rovno-3 Cavity Dosimetry Experiments
E. Brodkin, S. Zaritsky (RRC Kurchatov Institute Moscow, Russia)

---

[1]The author named as first presented the contribution

Rossendorf Monte Carlo Calculations for the Balakovo-3 Experiment and Comparisons to Experimental Results
H.-U. Barz, J. Konheiser (FZR)

Calculation of the Interlaboratory VVER-1000 Ex-vessel Dosimetry Experiment at the Balakovo-3 NPP
C. Garat (FRAMATOME, Paris), G. Borodkin (SEC Moscow, Russia)

Part 2:
Chairman: S. Zaritsky

Presentation and Discussion of Differences between Calculational Results and of C/E-values
H.-U. Barz, G. Borodkin, E. Brodkin, C. Garat, ...

NPP Novovoronesh 2 and 3; Comparison of Experimental and Theoretical RPV Fluences
E. Polke (Siemens-KWU Erlangen)

Common Problems of Benchmark Formulation and the Role of the Balakovo Experiment
S. Zaritzki (RRC Kurchatov Institute Moscow, Russia)

Session 3 (Uncertainties, Spectrum Adjustment, Nuclear Data)

Chairman: B. Böhmer

Rossendorf Spectrum Adjustment for the Balakovo-3 Experiment
B. Böhmer (FZR)

Uncertainties of Reactor Design Parameters
V. Tsofin (OKB Gidropress Podolsk, Russia)

Covariance Matrices for the Calculated Spectra at the VVER-1000 Cavity
G. Manturov (IPPE Obninsk, Russia), B.Böhmer (FZR)

Status of the Obninsk BNAB-Libraries
G. Manturow (IPPE Obninsk, Russia)

Session 4 (Discussions about special problems[2])

Niobium Measurements Problems
Chairman: I. Stephan
Contributions by: J. Hogel, V. Litchadeev, I. Stephan, G. Borodkin (SEC proposal for a improvement of interlaboratory comparisons of niobium activation measurements),...

Problems Related to Changes of the Spatial and Energetic Source Distribution During the Irradiation Cycle
Chairman: H.-U. Barz
Contributions by: H.-U. Barz, V. Valenta, G. Borodkin, Voorbraak,...

Fission Detector Measurements Problems
Chairman: G. Borodkin
Contributions by: G. Borodkin, W. Voorbraak, ...

Status and Recommendations for Improvements of Pressure Vessel Dosimetry of VVER type reactors
Chairman: B. Böhmer
Contributions by: S. Zaritsky, E. Brodkin, G.Borodkin, V. Tsofin, ...

---

[2]The named participants gave short contributions as base for the discussion

Excursion to the Preparation and Material Test Laboratories in the Neutron Embrittlement Department

List of the Workshop Participants:

1. A. Borodin	RRC Kurchatov Institute Moscow, Rußland
2. G. Borodkin	SEC NRS GOSATOMNADZOR Moscow, Rußland
3. E. Brodkin	RRC Kurchatov Institute Moscow, Rußland
4. C. Garat	FRAMATOME Paris
5. J. Hogel	Skoda Plzen, Tschechien
6. V. Litchadeev	RIAR Dimitroffgrad, Rußland
7. G.Manturov	IPPE Obninsk, Rußland
8. E. Polke	Siemens KWU Erlangen
9. V. Tsofin	OKB Gidropress
10. V. Valenta	Skoda Plzen, Tschechien
11. W. P. Voorbraak	ECN Petten, Netherland
12. S. Zaritsky	RRC Kurchatov Institute Moscow, Rußland
13. H.-U. Barz	FZ Rossendorf e.V.
14. B. Boehmer	FZ Rossendorf e.V.
15. J. Konheiser	FZ Rossendorf e.V.
16. K. Noack	FZ Rossendorf e.V.
17. I. Stephan	FZ Rossendorf e.V